

**CHARACTERIZATION OF EXPANSIVE SOIL FOR RETAINING
WALL DESIGN**

A Thesis

by

HAKAN SAHIN

Submitted to the Office of Graduate Studies of
Texas A&M University
in partial fulfillment of the requirements for the degree of

MASTER OF SCIENCE

December 2011

Major Subject: Civil Engineering

**CHARACTERIZATION OF EXPANSIVE SOIL FOR RETAINING
WALL DESIGN**

A Thesis

by

HAKAN SAHIN

Submitted to the Office of Graduate Studies of
Texas A&M University
in partial fulfillment of the requirements for the degree of

MASTER OF SCIENCE

Approved by:

Chair of Committee,	Robert L. Lytton
Committee Members,	Charles P. Aubeny
	Giovanna Biscontin
	Ibrahim Karaman
Head of Department,	John M. Niedzwecki

December 2011

Major Subject: Civil Engineering

ABSTRACT

Characterization of Expansive Soil For Retaining Wall Design.

(December 2011)

Hakan Sahin, B.S., Nigde University

Chair of Advisory Committee: Dr. Robert L. Lytton

The current design procedure for cantilever structures on spread footings in the Texas Department of Transportation (TxDOT) is based on horizontal pressure that is calculated by using Rankine's and Coulomb's theory. These are classical Geotechnical Engineering methods. Horizontal earth pressure due to moisture and volume change in high plasticity soil is not determined by these classical methods. However, horizontal pressure on most of the cantilever retaining structures in Texas is determined by following the classical methods. In recent years, a number of consultants have considered the horizontal pressure due to swelling on cantilever retaining structures in Texas. However, the proposed horizontal pressure by consultants is 10-20 times higher than the classical horizontal pressure. This method of cantilever retaining structure design without knowing the real pressure and stress pattern increases the thickness of the wall, and raises the cost of construction.

This study focuses on providing adequate patterns of lateral earth pressure distribution on cantilever retaining structures in expansive soil. These retaining wall

structures are subject to swelling pressures which cause horizontal pressures that are larger than the classical especially near the ground surface.

Beside the prediction of lateral earth pressure distribution, the relations between water content, volume change and suction change are determined. Based on the laboratory testing program conducted, Soil Water Characteristic Curves (SWCC) are determined for a site located at the intersection of I-35 and Walters Street in San Antonio, Texas. Additionally, relations between volume change with confining pressure curve, water content change with the change of confining pressure curve, water content change with change of matric suction and volume change with change of matric suction curves are generated based on laboratory tests.

There are a number of available mass volume measurement methods that use mostly mercury or paraffin to obtain volume measurements. Although these methods are reported in the literature, they are not used in practice due to application limitations like safety, time, and cost. In order to overcome these limitations, a new method was developed to measure the volume of soil mass by using sand displacement. This new method is an inexpensive, safe, and simple way to measure mass volume by Ottawa sand.

DEDICATION

To my adviser Dr. Lytton,
who believed in and supported me in everything that I have ever wanted to do, and for
his love and patience as well.

ACKNOWLEDGEMENTS

I would like to acknowledge all of my professors, friends, colleges and my family because of their friendship, understanding, encouragement, support, and their help during the time of my study.

First of all, the challenge started when this project was given to me to work with. Now we are done with the project and personally, I learned all of the new concepts and methods. Therefore, I would say that sometimes walking on the path might be more interesting than directly arriving to the destination.

Most importantly, I would like to send a sincere appreciation to my advisor and committee chair, Dr. Robert L. Lytton, for not only giving me support during my period of study but also for sharing his immense knowledge with me. In addition to this, I am very thankful for Dr. Lytton's support throughout my study because without his full support, I would not have been able to complete it.

I wish to express sincere gratitude to my committee members, Dr. Giovanna Biscontin, Dr. Charles Aubeny and Dr. Ibrahim Karaman. I am very thankful for all their friendship and assistance because working with them was a learning experience for me.

Also, very special thanks are extended to Dr. Rong Luo who helped me every step of the study with understanding and encouragement whenever I needed it.

Last but not least, to my family whom all of my success is dedicated to because of their encouragement. Finally, this project was conducted in cooperation with Texas A&M University and University of Texas at San Antonio (UTSA). Thus, I am grateful

to Texas Transportation Institute (TTI), University of Texas at San Antonio and Texas A&M University, Dwight Look College of Civil Engineering for giving me this opportunity.

TABLE OF CONTENTS

	Page
ABSTRACT	iii
DEDICATION	v
ACKNOWLEDGEMENTS	vi
TABLE OF CONTENTS	viii
LIST OF FIGURES.....	xi
LIST OF TABLES	xv
NOMENCLATURE.....	xvii
1. INTRODUCTION.....	1
1.1 Background Information	1
1.2 Objectives of Thesis	4
1.3 Organization of Thesis	4
2. LITERATURE REVIEW	6
2.1 Design Criteria for Specific Wall Types	6
2.2 High Plasticity Clays in Texas	6
2.3 Swelling Pressure	7
2.4 Lateral Swelling Pressure.....	8
2.4.1 Factors Affecting Lateral Swelling Pressure.....	10
2.4.2 Effect of Initial Dry Density.....	10
2.4.3 Effect of Initial Moisture Content	10
2.4.4 Effect of Axial Stress	11
2.4.5 Effect of Moisture Content.....	13
2.4.6 Effect of Stiffness of the Support.....	13
2.5 Lateral Earth Pressure Models	14
2.5.1 Lateral Earth Pressure on Flexible Retaining Wall.....	15
2.5.2 Lateral Earth Pressure on Stationary Retaining Wall.....	16
2.6 Suction Profile at Different Sites	18
2.7 Scope of This Thesis	18
2.7.1 Information Search.....	19
2.7.2 Laboratory Procedure for Clay Soil Characterization.....	19
2.7.3 Field Instrumentation and Data Collection	22

	Page
2.7.4 Computation of Lateral Earth Pressures against Retaining Walls ..	22
2.8 Soil Water Characteristic Curve.....	23
2.9 Conclusion.....	24
3. LABORATORY TEST METHODS.....	25
3.1 Introduction	25
3.2 Construction Site.....	25
3.3 Collected Samples	27
3.4 Soil Characterization in Laboratory	28
3.5 Plasticity Properties.....	29
3.6 Liquid Limit Test	29
3.7 Plastic Limit Test	30
3.8 Hydrometer Analysis Test.....	31
3.8.1 Introduction	31
3.9 Wet Sieve Analysis Test	33
3.9.1 Introduction	33
3.10 One Dimensional Consolidation Test	34
3.10.1 Introduction	34
3.11 Filter Paper Test Method.....	35
3.11.1 Introduction	35
3.12 Pressure Plate Test	39
3.12.1 Introduction	39
3.13 Volume Measurement of Soil Sample by a New Method.....	45
3.13.1 Test Apparatus.....	45
3.13.2 Test Procedure.....	46
3.14 Unconfined Compression Test	49
3.14.1 Introduction	49
4. UNSATURATED SOIL MECHANICS	51
4.1 Introduction	51
4.2 Concept of Soil Suction.....	51
4.3 Soil Water Characteristic Curve (SWCC).....	53
4.4 Determining the SWCC through Mathematical Models	55
4.5 Volume Change in Expansive Soils	59
4.6 Swelling Pressure in Expansive Soils	65
4.7 Horizontal Earth Pressure in Retaining Walls Due to Suction.....	66
4.8 Swelling Lateral Earth Pressure on Stationary Walls	67
4.9 Retaining Wall in Expansive Soils.....	71

	Page
5. RESULTS AND DISCUSSION	73
5.1 Introduction	73
5.2 Volume Change Versus Change of Confining Pressure Curve.....	73
5.3 Water Content Change Versus Change of Matric Suction Curve.....	76
5.4 Volume Change Versus Change of Matric Suction Curve.....	78
5.5 Soil Water Characteristic Curve Fitting Parameters	83
5.6 Optimization Nonlinear Relationship of the Fitting Parameter	83
5.7 Formulation of the Optimized Fitting Parameter	85
5.8 Plotting of the Soil Water Characteristic Curves	89
5.9 Matric Suction-Confining Pressure-Shear Strength Curves.....	92
5.10 Prediction of Lateral Earth Pressure against the Retaining Wall	95
5.10.1 Moisture Content Variation.....	95
5.10.2 Suction Profile.....	97
5.10.3 Horizontal Pressure on the Retaining Wall	98
6. SUMMARY AND CONCLUSION	101
REFERENCES.....	103
APPENDIX.....	111
VITA	157

LIST OF FIGURES

	Page
Figure 2-1: Schematic diagram of the lateral pressure on wall at dry condition (After Brackley and Sanders 1992).	11
Figure 2-2: Swelling tests performed (a) at lower of stiffness of 850 MPa ring and (b) at higher stiffness of 3045 MPa ring (after Windal et al. 2002).	12
Figure 2-3: Constitutive relation between moisture content and state of stress (After Fredlund and Rahardjo, 1993).	13
Figure 2-4: Lateral earth pressure on flexible retaining wall (After Ertekin 1991).	16
Figure 2-5: Lateral earth pressure on a stationary retaining wall in expansive soils with proposed three earth pressure zones (Hong 2008).....	17
Figure 2-6: The minimum and maximum suction profile (Bryant et al., 2008).....	18
Figure 3-1: Location view of the construction site on map (Google Maps)	26
Figure 3-2: (a) Boreholes location on the ramp (b) boreholes drilling and soil sample collection of the samples behind the wall.	27
Figure 3-3: Extracted and wrapped soil sample from boreholes.....	28
Figure 3-4: Liquid limit device and other tools.....	30
Figure 3-5: Plastic limit tools	31
Figure 3-6: Hydrometer suspended in water in which the soil is dispersed.....	32
Figure 3-7: Shows consolidation tools like the ring, porous stones put separately and assembled.....	35
Figure 3-8: Geometric configuration of a filter paper test jar with filter papers inside and a sample.	36
Figure 3-9: Soil samples, filter papers for matric and total suction. (Report No: TX-05/ 0-4518-1)	37
Figure 3-10: Filter paper, tins, tweezers, latex gloves, PVC ring, and electrical tape are shown in the picture. (Report No: TX-05/0-4518-1)	37

	Page
Figure 3-11: Filter paper calibration curve (from Bulut et al., 2001).	38
Figure 3-12: A pictorial view of the pressure plate apparatus with internal apparatus and soil samples (online source from New Mexico State University)	39
Figure 3-13: An illustration of water films coated soil particles on a ceramic plate magnified by air pressure. (Soil Moisture Equipment Corporation, CA, USA).	41
Figure 3-14: An illustration of a ceramic plate pore and air-water, interface curvature diameter changes under different level air pressure. (Soil Moisture Equipment Corporation, CA, USA).....	42
Figure 3-15: Pressure plate set in the laboratory and A 15 bar (1500 kPa) ceramic plate in the vessel is shown after the distilled water was submerged (Soil Moisture Equipment Corporation, CA, USA)	43
Figure 3-16: (a) Sample is placed vertically in the jar, (b) Ottawa sand is dumped onto the sample.	47
Figure 3-17: (a) Sand on top of the filled jar is trimmed level with the top of the jar, (b) sample is gently cleaned	49
Figure 3-18: Unconfined compression test instrumental in geotechnical laboratory.....	50
Figure 4-1: A typical wetting and drying soil water characteristic curves (Sillers, et al. 2001)	54
Figure 4-2: Volume change process in unsaturated soils within natural limits (Hong 2008)	59
Figure 4-3: The volume–mean principle stress-suction surface curve (Hong 2008).	61
Figure 4-4: The regression equation based on the relation on the empirical correlation between ϕ' and PI. (after Holtz and Kovacs 1981).	62
Figure 4-5 : Suction vs. volumetric water content curve and ‘S’ parameter (Lytton 1994).	63
Figure 4-6: Montmorillonite particle adsorbed water	66
Figure 4-7: Lateral pressure due to suction change (Hong, 2008).	68

	Page
Figure 4-8: Typical distribution of lateral earth pressure (Hong, 2008).	68
Figure 4-9: Three earth pressure zones (Zone I is shear failure state, Zone II swelling passive state and Zone III is at rest state) are shown.	69
Figure 4-10: Behavior of expansive soils with horizontal pressure distribution on the left and right side of the retaining wall system (Hong, 2008).	72
Figure 5-1: Volume change and confining pressure, (σ -ua) relation for an unsaturated sample of B1-13.	74
Figure 5-2: Matric suction versus water content curve based on laboratory sample of Boring No. 2 and depth of 17-18 ft.	77
Figure 5-3: Volume change points are shown by changing suction in the sample of B2-8	79
Figure 5-4: Volume change points are shown by changing suction in the sample of B1-20	79
Figure 5-5: Change in a_f with pfc percent passing fine content.	87
Figure 5-6: Change in b_f with pfc percent passing fine content.....	88
Figure 5-7: Change in c_f with pfc percent passing fine content.....	88
Figure 5-8: Change in h_r with pfc percent passing fine content.	89
Figure 5-9: A generated soil water characteristic curve.....	90
Figure 5-10: Minimum and maximum slope of SWCC, and change of the slope by pfc	91
Figure 5-11: Measured suction values are fitting the SWCC.....	92
Figure 5-12: Mohr's failure circle and Mohr's envelope are shown with stresses acting on it.	93
Figure 5-13: Three dimensional matric suction, shear strength and confining pressure constitutive surfaces for a soil sample on boring no.2.....	94

	Page
Figure 5-14: Determined moisture content profile change rate with depth	96
Figure 5-15: Estimated volumetric water content profile based on the moisture content.....	96
Figure 5-16: Generated suction profile that shows change in suction with depth.....	97
Figure 5-17: Calculated horizontal swelling pressure behind the retaining wall	99
Figure A-1: Hydrometer test results of boring no1 all depths are together.....	124
Figure A-2: Hydrometer test results of boring no2 all depths are together.....	125
Figure A-3: An determined SWCC curve by using the pressure plate extractor	149
Figure A-4: Shows pictures of PVC cylinders that used for calibration.	150
Figure A-5: Relation change in mass and volume is shown.	153

LIST OF TABLES

	Page
Table 4-1: Proposed mathematical equations used to fit the soil-water characteristic curve (Zapata, 1999).....	57
Table 4-2: Range of saturated volumetric water content by unified soil class (Mason, Ollayos et al. 1986).....	65
Table 5-1: Volume indexes for two borings of boring no.1 and boring no.2 are given.....	76
Table 5-2: Measured volume data and calculated (γ_h)Swelling and (γ_h)Shrinkage based on the volume change measurement.....	82
Table 5-3: Measured volume data and calculated (γ_h)Swelling and (γ_h)Shrinkage based on the volume change measurement.....	82
Table 5-4: Percent fine content (pfc) values are shown with depth for boring no. 1 and boring no. 2	86
Table A-1: Liquid limit test results for boring no 1	115
Table A-2: Liquid limit test results for boring no 2	115
Table A-3: Plastic limit, liquid limit, plasticity index and related test results for boring no 1	118
Table A-4: Plastic limit, liquid limit, plasticity index and related test results for boring no 2	119
Table A-5: A full set of sieves includes the following sieves	121
Table A-6: A set of wet sieves analysis results for boring no 1	129
Table A-7: A set of wet sieves analysis results for boring no2	129
Table A-8: Consolidation test results of void ratio, compression index, recompression index and volume compression index for boring no1	134
Table A-9: Consolidation test results of void ratio, compression index ,recompression index and volume compression index for boring no 2	134
Table A-10: Matric, total and osmotic suction are estimated by the filter paper test for boring no 1.	139

	Page
Table A-11: Matric, total and osmotic suction are estimated by the filter paper test for boring no 2.	140
Table A-12: Pressure plate is used to determine soil sample suction change. An example pressure plate spreadsheet is given for boring no 2, depth of 17-18 ft.....	148
Table A-13: Unconfined compression strength and effective cohesion are determined for boring no 1.	150
Table A-14: Unconfined compression strength and effective cohesion are determined for boring no 2..	151
Table A-15: Determined volume is shown for each cylinder PVC.....	152
Table A-16: Unconfined compression strength and effective cohesion are determined for boring no 1	156
Table A-17: Unconfined compression strength and effective cohesion are determined for boring no 2	156

NOMENCLATURE

ABBREVIATIONS

AASHTO	American Association of State Highway and Transportation Officials
ASTM	American Society for Testing Materials
TxDOT	Texas Department of Transportation

SYMBOLS

pF	A unit of soil suction
$SWCC$	Soil Water Characteristic Curve
h	Soil matric suction, in psi
a_f	The air entry value of the soil.
b_f	The rate of water extraction of the soil.
c_f	The residual water content of the soil
h_r	The suction value at which the residual water content occurs
pfc	Percent fine content

1. INTRODUCTION

1.1 Background Information

For a number of years, the retaining walls which were built in Texas were primarily cantilever structures on spread footings. On soft clays, the footings were placed on pilings of various configurations. Closely separated drilled shafts were used to accommodate the absence of site access space in the 1970s. Later on, to reduce the number and size of the drilled shafts, pre-stressed ground anchors were added. The reinforced earth walls used with soil nails were introduced in the late 1970s.

The most frequently used retaining wall types are drilled shafts, tie-backs or soil nails in roadway cuts. The up-to-date design procedure endorsed by TxDOT for designing such walls depends on lateral pressure calculations from the classical Rankine and on the Coulomb methods. These contemplate the drained shear strength parameters of soil. The current design procedure does not carry any guidelines to measure the lateral pressure from high plasticity expansive soils, where extra lateral pressure due to swelling from the moisture changes may be valid. TxDOT has been using these methods for designing cut type walls in expansive soils for the last 20 years. As reported by TxDOT, these designs have performed well, but they likely result in smaller than necessary structures that are inexpensive but unconservative.

This thesis follows the style and format of the *Journal of Geotechnical and Geoenvironmental Engineering*.

Lately, in the swelling pressure on retaining structures from expansive soils there has been a renewed interest. Some of the design work for such retaining walls was conducted by consultants. Such designs predicted that the lateral pressure due to swelling of the high plasticity expansive soil is as high as 8000 psf. As a result, the retaining walls designed by this method are very thick and costly. The estimated lateral pressure due to the swelling is commonly based on one-dimensional soil swell tests, where the change in suction was recognized between extreme conditions. Because of the very small hydraulic conductivity of high plasticity expansive soils, such ultimate moisture changes are fairly limited in practical situations. The question is if these additional pressures are realistic and under what circumstances they materialize in the field. If indeed such high pressures are possible, accordingly they need to be considered in the design of retaining structures. This would be a radical departure from the current design method used by TxDOT. However, there is a necessity to evaluate the problem in an analytical way, by utilizing the realistic moisture changes encountered in the field.

Due to changes in their moisture content, there are a considerable number of references in the literature dealing with swelling pressure by unsaturated high plasticity clay soils. Even though significant research has been reported out on how to measure these swelling pressures, especially for reinforced walls, such as soil nailed and tied-back walls, virtually no systematic research has yet been carried out on how to account for these pressures exerted on soil retaining structures. In response to this need, this study was undertaken. This work deals with the most important elements of the problem including:

- The in-situ measurements of the moisture content profile during construction
- Collection of data on the seasonal variation of the moisture content profile
- Prediction of the swelling characteristics of the soils based on the state of stress in the field
- The analysis of the effect of wall rigidity on lateral swelling pressure.

The approach of the research includes laboratory testing to characterize the swelling properties of high plasticity clays and the numerical simulation of the cooperation between the retaining structure and soil due to the maximum modifications in pore water pressure/suction measured at the field site.

The main objective of this study is to evaluate the lateral pressure on cut-types retaining walls such as drilled shaft, tied-back, and soil nailed retaining walls due to the change in the moisture content of high plasticity expansive soil. Several tasks are performed in order to achieve this objective. These include:

- Literature review
- Characterization of high plasticity expansive soil in-terms of volume change and swelling pressure.
- Recording the seasonal variation of moisture content at a field site.
- Evaluating the lateral pressure on cut-type retaining structures constructed on high plasticity expansive soil.

This study serves the ability to design economical and safe structures in expansive soil. The prospect of instability in failure due to swelling soils cannot be

neglected, so the estimation of the durability of the lateral earth pressure due to high plastic soils on the retaining structure is significantly important.

1.2 Objectives of Thesis

This thesis presents the full set of tests that are required to characterize the properties of expansive soil that are needed to predict realistic lateral earth pressure against retaining walls. A prediction of such lateral pressure will be made based on the suction changes measured in the field behind a retaining wall. The resulting lateral earth pressure will demonstrate the realistic range of pressures that should be used for design.

1.3 Organization of Thesis

This thesis is organized into the following sections:

Section 1 presents the description of the research problem and the scope of the research.

Section 2 provides a concise overview of swelling and lateral earth pressure for expansive soil. The effect of lateral pressure on the retaining wall structures and the experience gained with different methods are discussed. Also, a comprehensive literature review is presented for swelling, volume change and pressure in expansive soils.

Section 3 presents the construction site and a series of laboratory tests to determine characteristics of soil samples.

Section 4 explores the fundamental properties of unsaturated soil mechanics, and compiles the theoretical information about volume change, the soil water characteristic curve (SWCC), and lateral earth pressure in soil.

Section 5 discusses findings of laboratory tests and characterization of soils samples. In addition, this part combines the laboratory results to obtain a relation between water content, confining pressure, matric suction and volume change curves. In addition, SWCC parameters based on Fredlund and Xing model are determined in this chapter. Further, the lateral earth pressure is investigated for optimum design parameters due to swelling in near the ground surface.

Section 6 presents conclusions along with recommendations for the use of the parameters of the SWCC, volume change, and lateral pressure based on the findings of this study.

Appendices are provided which describe the testing procedures used in this thesis and give typical results of those test.

2. LITERATURE REVIEW

2.1 Design Criteria for Specific Wall Types

The analysis and design of retaining walls are based on the guidelines in the 17th edition of the AASHTO Standard Specifications for Highway Bridges. The soil strengths are estimated from the correlations of Texas Cone Penetrometer (TCP) test values. In general, a friction angle of 30 degrees and cohesion of zero apply for most soil conditions. A standard value of 20° of the friction angle is applied in all retaining wall structures (TxDOT 2006).

The lateral earth pressure applied by the soil to the wall in retaining structures depends on the type of structure and assumptions that are made. The pressure distribution is recognized to be in an active state and it is assumed to have a triangular distribution with depth with the maximum pressure developing at the base of the wall. Primarily, the assumption is that the lateral soil pressure increases linearly with depth along the wall at a rate of 40 psf per ft (TxDOT 2006). The design of the retaining walls as an infinitely long beam on nonlinear support is a simplified assumption. The retaining walls are mostly fixed in the soil and, therefore, the lateral pressure distribution is calculated depending on at rest conditions.

2.2 High Plasticity Clays in Texas

Clay-rich soils which shrink and swell with changes in the moisture content are named Vertisols and considered the dominant soil orders of Texas. The soil shrinks and forms deep wide cracks during dry periods. As the soil gets wet the volume expands.

Serious engineering problems take place when shrink/swell action occurs. Extending from north of Dallas to south of San Antonio, Vertisols cover nearly 1.5 million acres in Texas. Water is known to enter the soil rapidly when the soil is dry and very slowly when the soil is moist.

2.3 Swelling Pressure

Due to changes in the moisture content the expansive soil exhibits significant changes in volume. Structures which are constructed on this soil are subjected to large forces due to swelling, which could result in damage and cracks on structures. A number of reports on expansive soil problems and related damages have been published (Ruwaih, 1987; Chen, 1988; Nelson and Miller, 1992). Problems associated with the soil heave in the foundations of diverse infrastructure elements account for more economic losses than those of all other soil problems. Due to expansive soil problems, the cost of damages in the United States alone is about \$2.3 billion annually (Dhowian et al., 1987). Due to change in the moisture content (Hudak, 1998), the damage is especially severe in montmorillonitic clay which significantly changes its volume.

A complex phenomenon is the swelling in expansive clays which are rooted in electrochemical that affect the internal stress distribution between soil particles (Kehew, 1995). In most cases, the clay particles are platelets with a negative surface electrical charge in the pore-water solution and the polar water molecules are attracted to these particle surfaces. The double diffuse layer is the combination of the negative charges on the surface of the clay and the attracted cations and water molecules. The negative

surface charges and the electrochemistry of the pore water are the electrical inter-particle force fields. Influenced by the van der Waals surface forces and the adsorptive forces between the clay crystals and water molecules is the inter-particle force field. With the externally applied stress and the capillary tension in the soil water the internal electrochemical system should be in equilibrium. Cations that are attracted to the clay surfaces present another factor in swelling behavior.

Small pores between or within clay particles may contain a higher concentration of cations than larger pores within the soil due to the attraction of negatively charged clay-particle surfaces to cations. An osmotic potential is caused by this condition between the pore fluids and the clay-mineral surfaces (Mitchell 1993). In order to evenly distribute the ions throughout the solution usually cations diffuse from a higher to a lower concentration. Because ions are held by clay particles in expansive soils, water from areas of low ionic concentration move to areas of high ionic concentration inside the clay aggregates. This movement of water exerts pressure and as a result the clay swells.

2.4 Lateral Swelling Pressure

The problem of swelling pressure generated by expansive soil has received a significant amount of attention over the past three decades. However, most of the previous research activities focused more on vertical swelling pressures. It is well known and thought that the soil shows anisotropic behavior and generally their lateral swelling pressure differs compared to their vertical swelling pressure. Saturated expansive soil

behaves unconventionally in applying lateral pressures under both at rest conditions and active conditions (Katti et al. 1987).

Predictions of vertical swelling pressures can be made by using conventional laboratory test by a PVC meter, oedometer tests, or by soil suction methods. Furthermore, the prediction of lateral swelling pressure in this test requires the use of a lateral swelling pressure ring (Ofer 1980), a thin wall oedometer ring (Ertekin 1991), or a modified hydraulic triaxial apparatus (Fourie 1989). All of these laboratory techniques do not necessarily reflect on the in-situ vertical and lateral swelling pressures. Actually, research studies have shown that these laboratory tests tend to overestimate the actual in-situ earth pressures (Nelson and Miller, 1992).

The lateral swell pressure of a series of expansive soils are measured by Sapaz (2004) using a thin wall oedometer set-up containing strain gauges at the midpoint of the thin wall. Also, the strain was converted to lateral pressure through a calibration process. The vertical swell pressure was measured as well. The magnitude of the lateral swell pressure was always found to be smaller than the vertical swelling pressure. The ratios of the swell pressures varied between 0.59 and 0.86. The definite reason for the relatively lower lateral pressure was examined. However, it was concluded that clay minerals are usually sheets with a flakey texture and orient themselves parallel to each other when the water is added. It was also found that the top and bottom of the surface of the flaky sheet attracts more water than the sides of the clay sheet.

2.4.1 Factors Affecting Lateral Swelling Pressure

Various studies have been conducted on lateral swell pressure and it was concluded that the initial dry density, initial water content, moisture content, rigidity of the wall, surcharge load, and lateral earth pressure condition are the main factors of affecting the lateral swell pressure of high plasticity expansive soils (Nelson and Miller, 1992, Sapaz, 2004).

2.4.2 Effect of Initial Dry Density

With increasing initial dry density, the lateral swelling pressure increases. Initial lower dry density means a higher porosity, which may accommodate additional adsorbed water by driving air out from the pore space without a significant change of volume (Chen 1988, Ofer 1980). The lateral swell pressure depends on the potential of volume change as a result (Ofer 1980).

2.4.3 Effect of Initial Moisture Content

Erol and Ergun (1994) indicated that both the lateral and vertical swell pressures decrease with increasing initial moisture. To some extent, high moisture content indicates that the soil is already swollen, whereas, the moisture content below the shrinkage limit indicates that the potential for volume change is maximum. If the moisture content during construction or the initial moisture content is quite high, the chance of further swelling will decrease and the lateral pressure diagram would be totally different than if it were constructed under dry conditions. Figure 2-1 shows a schematic diagram of the lateral pressure on a wall when the in-situ moisture content is lower than the moisture content during construction. It can be seen from in Figure 2-1

that under these circumstances, there would not be any additional lateral pressure (Lytton 1994).

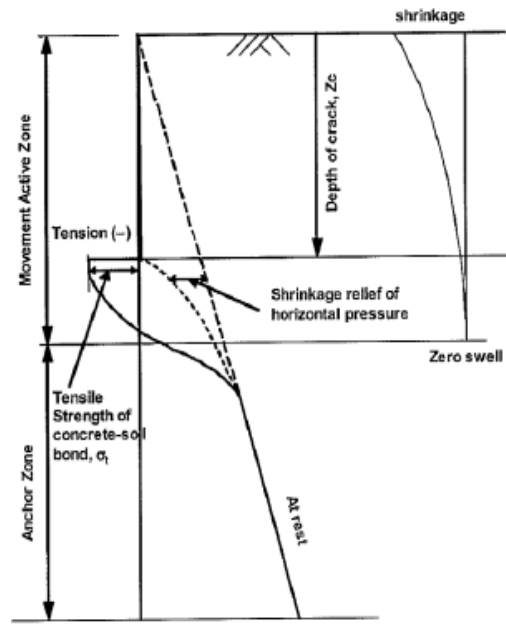


Figure 2-1: Schematic Diagram of the Lateral Pressure on Wall at Dry Condition (After Brackley and Sanders 1992).

2.4.4 Effect of Axial Stress

The effect of the surcharge load on lateral swelling pressure is significant as well. The lateral swelling pressure increases with increasing surcharge load (Joshi and Katti 1984; Lytton 1995). However, the rate of the lateral swelling pressure increases with increasing surcharge. The surcharge tends to prevent the vertical swelling. This constraint in volume change of the soil may result in increased lateral pressure.

Shahrour et al. (2002) studied the effect of axial stress on lateral stress. The lateral pressure was measured by varying the axial stress in a flexible ring oedometer in their

study. Tests were performed by using two ring stiffnesses (850 MPa and 3045 MPa). The lateral pressure increased with increasing axial stress. However, the ratio of the maximum lateral stress to the axial stress decreased at higher axial stress levels, which shows that the lateral stress is usually higher than the axial stress in shallow depth levels. Effect of axial stress and stiffness on lateral pressure can be seen in Figure 2-2 that the increasing lateral pressure period was shorter when the axial stress increased.

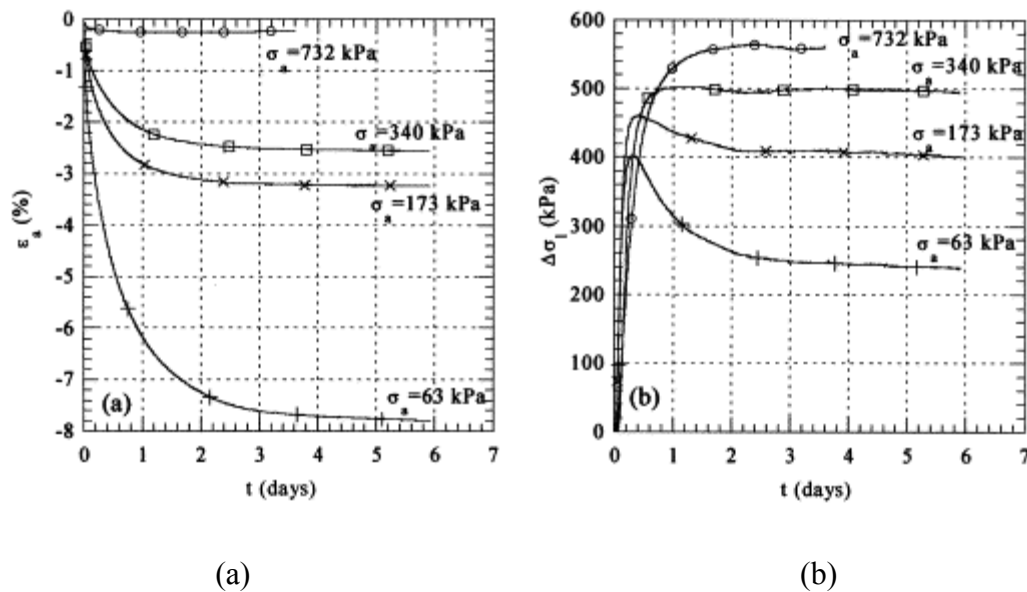


Figure 2-2 Swelling tests performed (a) at lower of stiffness of 850 MPa ring and (b) at higher stiffness of 3045 MPa ring (after Windal et al. 2002).

The lateral pressure reached a peak value at lower axial stress levels, then decreased and finally leveled off at a lateral pressure limit that seems to be a function of the applied axial stress. In addition, the peak value of the lateral pressure was less pronounced as the axial stress increased and disappeared at high axial stress levels. This

reduction in lateral pressure from the peak value was due to the gradual changes in the soil structure and the clay particle orientation associated with the saturation process according to Chen and Huang (1987).

2.4.5 Effect of Moisture Content

The constitutive relationship between the logarithm of the stress state and the moisture content is shown in Figure 2-3. The soil pore water pressure/suction increases with a decreasing of moisture content and the swelling pressure increases with an decrease in moisture content (Fredlund and Rahardjo, 1993).

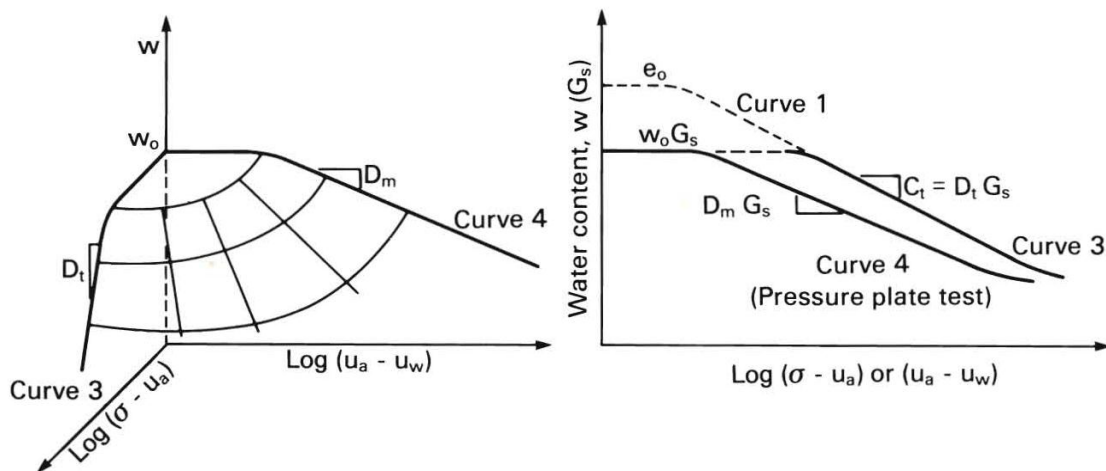


Figure 2-3: Constitutive Relation between Moisture Content and State of Stress (After Fredlund and Rahardjo, 1993).

2.4.6 Effect of Stiffness of the Support

In general, the characterization of expansive soil is carried out by using classical oedometer testing, which permits the measurement of axial pressure and swelling deformation. This method imposes a zero lateral deformation during the swelling of soil,

which is not necessarily representative of the in-situ condition, especially in the case of flexible structures, such as a drilled shaft or cantilever retaining walls, where the soils behind the walls are free to deflect or move in response to the applied loads. Several studies have shown that the swelling pressure decreases significantly, if a small deformation is allowed during swelling (Ofer 1980). According to Chen and Huang (1987), the swelling pressures measured in laboratories are generally higher than those observed in-situ. This observation can be partially attributed to the fairly high stiffness of the conventional oedometer tests performed using rings with two different stiffnesses (850 MPa and 3045 MPa), which clearly shows that the maximum lateral pressure at a given axial stress is significantly smaller for a lower stiffness support. For flexible structures such as a drilled shaft or cantilever retaining walls, laboratory tests usually overestimate the actual lateral swelling pressure.

2.5 Lateral Earth Pressure Models

Two models are presented here for the lateral earth pressure on retaining walls. Both of the models consider lateral earth pressure from the soil, and the lateral swelling pressure due to moisture changes in expansive soils. One of the models exhibits a condition where the structure at the top is flexible and the soils behind the walls are free to deflect or move in response to the applied loads. The other model is developed for a situation when the structure is very rigid and the lateral expansion of the soil causes a lateral passive shear failure.

2.5.1 Lateral Earth Pressure on Flexible Retaining Wall

A lateral pressure distribution on a flexible retaining wall was proposed by Ertekin (1991). According to this situation shown in Figure 2-4, it was assumed that when the earth pressure is applied the retaining structure may deflect slightly. The lateral earth pressure increased linearly with depth. Also, the earth pressure was recommended to be calculated by the use of the active earth pressure coefficient. The lateral pressure from the surcharge was linear, which decreases slightly with depth. This phenomenon can be explained with Boussinesq's equation. As depth increases, areas that tend to resist load increase. Hence, the ratio of the vertical stress to the surcharge decreases. The lateral pressure that is computed as multiplying the vertical pressure by the lateral earth pressures coefficient decreases. Ertekin (1991) proposed two different slopes for the increase in lateral swelling pressure. The lateral swelling pressure increases with increasing axial stress, while the ratio of the lateral swell pressure to the axial stress decreases for greater depths.

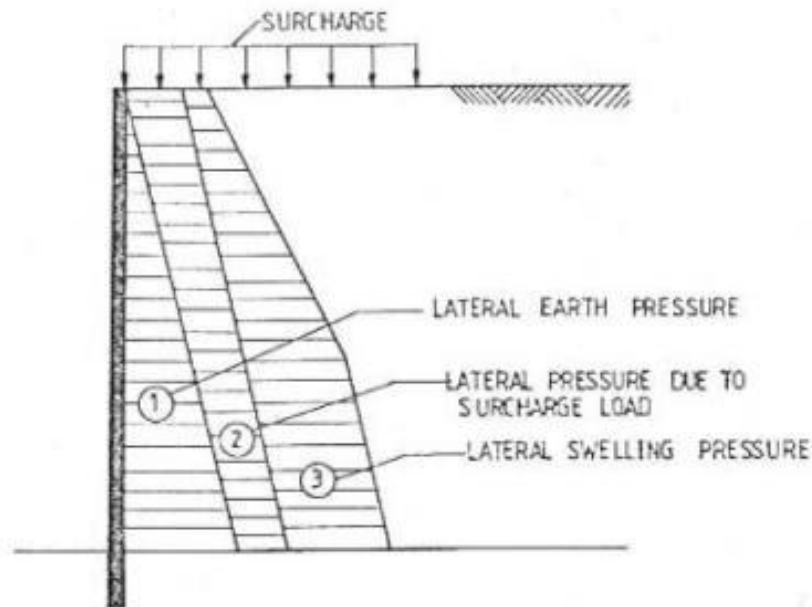


Figure 2-4: Lateral Earth Pressure on Flexible Retaining Wall (After Ertekin 1991).

2.5.2 *Lateral Earth Pressure on Stationary Retaining Wall*

A number of studies have been conducted to estimate the lateral earth pressure opposed to retaining walls in expansive soils. The common pattern of lateral swelling pressures on the stationary wall proposed by Hong (2008) consists of three zones, which are shown in Figure 2-5. The concepts of effective stress of unsaturated soil and the volume change equation were used to formulate the lateral swelling pressure equations in pressure zones I, II and III. The prediction of the lateral pressures due to changes in the soil moisture content was compared with the in-situ measurement of natural lateral pressures observed by Brackley and Sanders (1992) and with the measurements from the large scale tests (Katti et al. 1979; Komornik 1962).

In Figure 2-5, Zone I is the upper zone where a passive failure state of stress exists to a depth where the maximum lateral swelling pressure occurs. The maximum lateral pressures near the ground surface have been measured within a depth of 2 to 4 ft. The maximum horizontal pressure near a depth of 3 ft was found by Joshi and Katti (1980). It was taken into account that the maximum lateral pressure occurs at the depth of 2.5 ft in a model pile test by Komornik (1962). Yet, all those lateral swelling pressures were estimated from the vertical swelling pressure. Zone II represents the lateral passive pressure state and Zone III which is in the anchor zone is the at rest position.

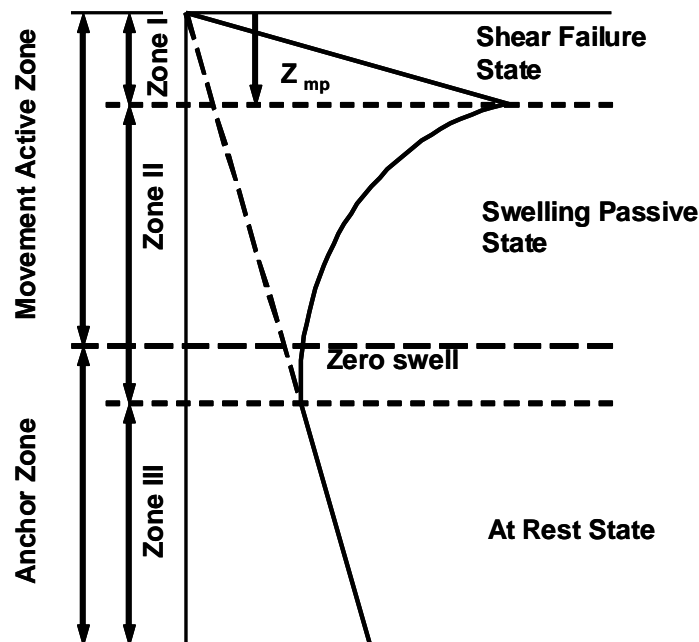


Figure 2-5: Lateral Earth Pressure on a Stationary Retaining Wall in Expansive Soils with Proposed Three Earth Pressure Zones (Hong 2008).

2.6 Suction Profile at Different Sites

Bryant et al. (2008) measured 26,000 values of soil suction at different depths. The maximum and minimum suction values versus depth are shown in Figure 2-6, which shows that the maximum measured suction in the field could be as high as 4.5 pF.

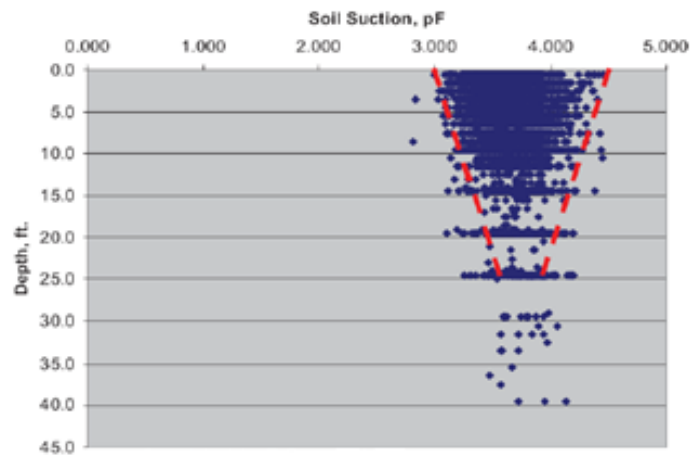


Figure 2-6 : The Minimum and Maximum Suction Profile (Bryant et al., 2008).

2.7 Scope of This Thesis

The support conditions of the soil nailed or tied back retaining wall are fixed at the two ends and the lateral earth pressure is calculated based on the at-rest condition. The support conditions of the drilled shaft retaining wall are fixed at the bottom and free at the top. The lateral earth pressure is calculated based on the active condition. For characterization, soil samples will be collected from the field sites . Suction data measured with psychrometer probes at these field sites will be obtained from UT San Antonio and reports by TxDOT/FHWA . Accessed and determined information will be used to compute realistic lateral earth pressure distributions.

2.7.1 Information Search

A comprehensive literature from past studies was reviewed. As the body of literature is fairly extensive with studies pertaining to retaining structures, the literature review focused more on studies that are related to the problem associated with expansive soils, which includes:

- The laboratory measurement techniques of the lateral swelling pressure to simulate the lateral pressure on retaining structures.
- The field measurement techniques of lateral swelling pressure on retaining structures.
- Measurement techniques of the moisture profile at the field.
- The relationship of the moisture profile with the lateral swelling pressure at different depths.
- The effect of vertical stress (from overburden pressure) on lateral swelling pressure
- The effect of the stiffness of the retaining wall on lateral swelling pressure.
- How the support conditions of the retaining structure affect the design procedure
- Design criteria for nailed soil, drilled shafts and tie-back retaining walls on expansive soils.

2.7.2 Laboratory Procedure for Clay Soil Characterization

The additional lateral pressure recommended by the TxDOT consultants was estimated based on a one-dimensional swell test (ASTM 1990). Even though a variety of parameters can be ascertained from this type of an index test, the findings of these

tests are inadequate to predict the lateral pressure on retaining structures for many cases.

The quantitative interpretation of the index test data may not be used to estimate the lateral pressure on walls due to the lack of correspondence between test conditions and conditions encountered in the field. Some of the more rigorous 3-D test procedures may be adapted to simulate the field conditions, such as boundary conditions and state of stress.

To perform the analyses of retaining walls with commercially available software, it will be necessary to measure the required soils input data. This includes the following:

- a. The Volume change characteristic as it varies with confining pressure and soil suction level
- b. The soil stiffness as it varies with confining pressure and the soil suction level
- c. Moisture diffusivity of in-situ soil
- d. The initial moisture conditions in-situ
- e. The moisture boundary conditions in-situ.

There are two approaches to obtain this information:

1. Determine items (a) through (d) by direct measurement on the soil samples in the laboratory. Estimate item (e) from item (d).
2. Estimate items (a) through (e) by using the properties generated from Atterberg limits and #200 and – 2 micron sizes, as provided in Reports FHWA/TX-05/0-4518-1, Volumes 1, 2 and 3.

The complete determination of the soils mechanical properties is summarized. There are a total of four curves that have been measured to characterize the volume change properties of the soil. These are given as

Curve 1: Volume change versus change of confining pressure;

Curve 2: Volume change versus change of matric suction;

Curve 3: Water content change versus change of confining pressure;

Curve 4: Water content change versus change of matric suction.

These four curves in the laboratory, tests No. 6, 7 and 8, are indicated below. The remaining tests are for determining the soil indexes, initial conditions, and moisture diffusivity.

The laboratory tests to run on the soil samples are listed below:

I. Initial Condition Tests

1. Total and matric suction tests using filter paper as in the FHWA/TX-05/0-4518-1 reports.
2. Water content and dry unit weight tests.

II. Index Tests

3. Atterberg limits
4. Sieve analysis (especially the -#200 size)
5. Hydrometer analysis (especially the – 2 micron size)

III. Moisture Property Tests

6. Matric suction-water content characteristic curve using pressure plate equipment according to the ASTM D2435 (2001 d) protocol. This will produce Curve No. 4.

IV. Mechanical Property Tests

7. Matric suction versus volume change test using pressure plate equipment. This will produce Curve No. 2
8. Triaxial confining pressure versus volume test using triaxial test equipment equipped to monitor both volume change and water content change at different levels of total suction. This will produce Curves No. 1 and 3.

2.7.3 Field Instrumentation and Data Collection

Thermocouple pcyhrometers placed in bore holes will acquire the field data of suction changes measured behind retaining walls located at San Antonio by UT San Antonio. This will be used to compute the lateral earth pressure.

2.7.4 Computation of Lateral Earth Pressures against Retaining Walls

Determined the laboratory characteristics will be applied to Hong's (2008) procedure to calculate the lateral earth pressure against a rigid retaining wall. This will be the maximum lateral pressure and the suction change that will be used to calculate the volume change and lateral pressure will be taken from field measurements behind a retaining wall by UT San Antonio. These measurements are published by Bin-Shafique, et al. (2010) in a TxDOT/FHWA reports of No. 0-6375.

2.8 Soil Water Characteristic Curve

The soil-water characteristic curve (SWCC) represents the relationship between water content and matric suction for a particular soil. The matric suction is a very important soil property. It is fundamental when solving engineering problems associated with unsaturated soil mechanics in the three (3) standard areas: compressibility, fluid flow, and shear strength (Perera, Y.Y., Zapata, C.E., Houston, W.N., Houston, S.L., 2005). For example, when modeling the unsaturated moisture flow beneath a highway pavement, the subgrade materials and hydraulic conductivity of the base course as a function of the water content must be known. This function can be estimated based on the SWCC.

The fine grain-size-distribution of a soil is related to its pore size distribution and hence, the fines percent in a soil matrix has a close relation with the soil-water characteristic curve (SWCC). The data obtained in the laboratory are on samples that are representative of the field. The samples are subjected to SWCC testing using the filter paper method and a pressure plate device.

SWCCs were determined by using the pressure plate device capable of measurements of the moisture content. In addition to these suction tests, a soil index property such as a fine grain-size-distribution of the soil and SWCCs was incorporated into the analysis. Each set of SWCC data was fitted with a Xing and Fredlund curve, which provided an S-shaped curve with four parameters a_f , b_f , c_f and h_r . Using the multiple regression analysis, the fines content equations were derived for these four

parameters. The equations presented in this study are useful for predicting the SWCC of any given soil, without carrying out the actual SWCC testing.

2.9 Conclusion

This thesis presents the full set of tests required to characterize the properties of expansive soil that are needed to predict realistic lateral earth pressure against retaining walls. A prediction of such lateral pressure will be made based on the suction changes measured in the field behind a retaining wall. The resulting lateral earth pressure will demonstrate the realistic range of pressures that should be used for design.

3. LABORATORY TEST METHODS

3.1 Introduction

The retaining wall design on high plasticity soil is described in Section 2. From the literature search, a procedure to determine the swelling pressure of high plasticity soil is identified. The objective of this study is to determine the lateral swelling pressure on the retaining wall by using the soil characteristics. In this section, general information about the construction site, collected samples, and the methodology used to conduct laboratory testing are described. The laboratory tests are described which determine the soil characteristics and engineering properties. A series of detailed laboratory tests are carried out on high plasticity collected soil samples. The experimental tests were completed in the Texas A&M University geotechnical engineering laboratory. The ASTM standards, AASHTO standards, or previous TxDOT reports are followed to conduct the tests. All of the tests, test methods, apparatus, and test process are described in detail in this section.

3.2 Construction Site

The location of the construction site is at the intersection of Walter's street and I-35 in San Antonio, Texas. The construction site is shown in Figure 3-1.



Figure 3-1: Location view of the construction site on map (Google Maps)

A 20 ft high retaining wall is built in very high plasticity expansive clay. This is an implementation task of the project to study the design of cut-type retaining walls in high plasticity soils.

As it is shown in Figure 3-1, both sides of the retaining wall are open to the traffic. On the backside of the retaining wall is a ramp that connects the traffic with the travel lanes of IH-35. Soil samples are collected from two boreholes behind the retaining wall. The two boreholes are shown in Figure 3-2 as boring no.1 and boring no.2. These borings were drilled and samples were extracted within the depth of 20 ft. The boring no. 1 is the closer borehole to the retaining wall and boring no.2 is further from the retaining wall.

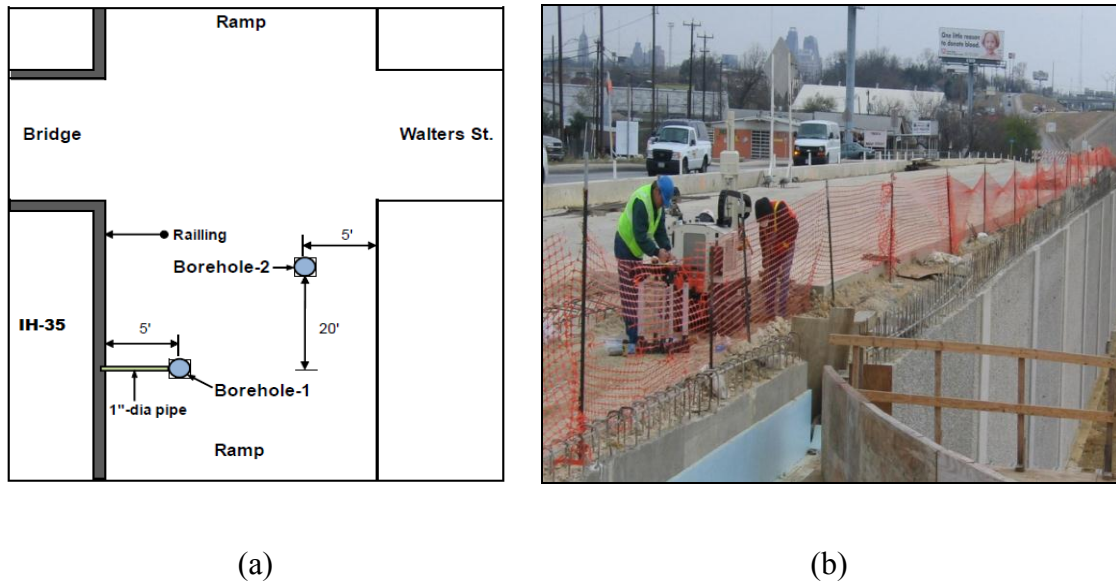


Figure 3-2: (a) Boreholes location on the ramp (b) boreholes drilling and soil sample collection of the samples behind the wall.

3.3 Collected Samples

Soil samples are collected from drilled boreholes, and one sample is collected every foot within each of the bore holes. The undisturbed samples are wrapped in aluminum foil and put in plastic bags in San Antonio. A total of twenty samples are brought to College Station for laboratory testing. Figure 3-3 shows soil samples 3 inches in diameter and usually 7 to 8 inches in length.



Figure 3-3: Extracted and wrapped soil sample from boreholes

3.4 Soil Characterization in Laboratory

The SWCC, the density, initial and final void ratio, the friction angle, compression and swelling index are some of the most important soil properties. To determine the soil characterization of the collected samples, the following laboratory tests were conducted on the samples.

- a. Atterberg Limit
- b. Hydrometer
- c. Sieve Analysis
- d. Wet Sieve Analysis
- e. Consolidation Test
- f. Filter Paper Test
- g. Pressure Plate Test
- h. Triaxial Test

The results of the tests are presented in this section. All laboratory tests have been conducted successfully and significant test results have been obtained. Some tests, like the water content and dry unit weight tests are not discussed below as an entitled subsection, but they were conducted many times as a component of a test.

3.5 Plasticity Properties

Liquid limits, plastic limits, and the plasticity index, are used as a fundamental part of the engineering classification such as compressibility, hydraulic conductivity, compatibility, the shear strength and the shrinkage-swelling. Liquid limits, plastic limits, and the plasticity index are utilized comprehensively either individually or with other soil properties relate to engineering behavior.

3.6 Liquid Limit Test

A liquid limit is a stage where soil changes from a plastic to a liquid by changing moisture content of the soil. Liquid limit is expressed as percent moisture by weight of the soil. The standard liquid limit test procedure is given in ASTM 4318.

Liquid limit test devices at the Texas A&M University Geotechnical Engineering graduate student laboratory are used. The tools used for the experiment are shown Figure 3-4 below.



Figure 3-4: Liquid limit device and other tools

3.7 Plastic Limit Test

The plastic limit is defined as the moisture content at which a soil thread of a 3.2 mm diameter which breaks into pieces when rolled on a glass plate. To determine the plastic limit, the soil is rolled by hand on a plastic surface until the soil starts to break at a diameter of 3.2 mm. The standard plastic limit test procedure is given in ASTM 4318.

Liquid limit test devices at the Texas A&M University Geotechnical Engineering graduate student laboratory are used for the test and Figure 3-5 shows the tools.



Figure 3-5: Plastic limit tools

3.8 Hydrometer Analysis Test

3.8.1 Introduction

The primary purpose of using the hydrometer test is to determine the particle size gradation curve for soil particles smaller than sieve No. 200 or 0.0075 mm. The gradation curve for particle sizes larger than the No. 200 sieve, is determined by the sieve analysis. For the hydrometer test a soil and water suspension is prepared. In the suspension all soil particles are assumed to have a spherical shape, and larger particles settle with a higher velocity. This phenomenon is explained by the Stokes' law. The hydrometer is shown in Figure 3-6. Standard test method for particle size analysis is given in ASTM D 422-63.

$$v = \frac{\rho_s - \rho_w}{18\eta} D^2 \quad (3-1)$$

where: v , velocity of soil particles; ρ_w , density of particles; ρ_s , density of water ; η , viscosity of water; D , diameter of soil particles.

The diameter of soil particles D can be calculated from above equation as

$$D = \sqrt{\frac{18\eta v}{\rho_s - \rho_w}} = \sqrt{\frac{18\eta}{\rho_s - \rho_w}} \sqrt{\frac{L}{t}} \quad (3-2)$$

where: L : distance from the center of the hydrometer to the surface of the suspension mixture; t : elapsed time during the test.

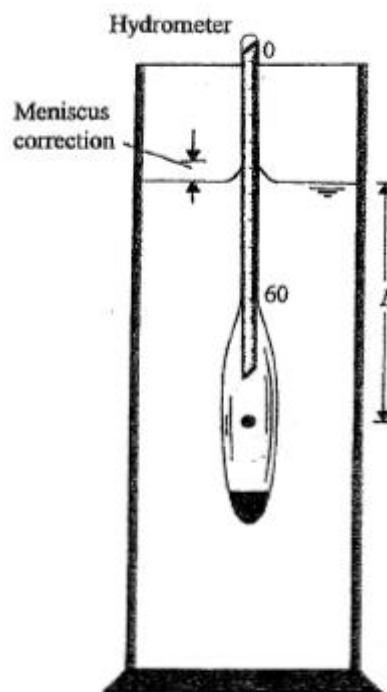


Figure 3-6: Hydrometer suspended in water in which the soil is dispersed.

3.9 Wet Sieve Analysis Test

3.9.1 Introduction

The wet sieve analysis method covers the determination of the soil gradation curve, and an estimation of finer than No. 200 sieve for adhesive material by means of washing. Some soils are not tested under some dry conditions. If the soil materials are finer grained or finer than a 75- μm sieve plastic clay particle, they have tendency to adhere together, even subjected to breaking, grinding, and crushing. Therefore, applying the dry sieve analysis for plastic clays is difficult, and results in experimental mistakes. At this point the wet sieve analysis is used to overcome these mistakes. Samples are taken out for the sieve analyses and are soaked for hours in the deflocculating agent solution. The solution with the sample is then washed through a number No.200 (75- μm) sieve, and the mass of the dry retained particles are determined as the mass percentage of material larger than 75- μm . The wet sieve analysis test procedure is described in ASTM D 1140-00. The calculation of the percentage retained at each sieve can be estimated by using

$$PR = \frac{M_r}{M_t} \quad (3-3)$$

where: PR : Percentage of retained soil; M_r : Mass soil retained at each sieve; M_t : Mass of dry soil after washing,

3.10 One Dimensional Consolidation Test

3.10.1 Introduction

When a surface load is increased by any kind of construction such as a building, road retaining wall, the stress on the surface and underneath the surface will increase. Due to the increase in load and stress, it will cause settlement and also decrease the volume of the soil. The loading, first, is carried by the pore water in the soil and then the excess pore pressure slowly decreases over time.

The consolidation test measures the rate of settlement of the soil. The soil is placed in a metal ring, and a loading is applied to the soil. The soil stays under the same loading for 24 hours. Then the loading is doubled, and the loading stage is repeated usually 5 or 6 times, and then the loading is decreased by the same process. Basically, the aim of the consolidation test is to obtain the height change of a confined sample by loading since the height will decrease during the loading. From the measured empirical data the pressure, usually in kPa, versus the void ratio rate can be plotted. The compression index, the recompression index and the pre-consolidation pressure can be obtained from this test. These consolidation properties are significantly important in the design of any engineering construction, and maintain the construction without deformation in the future.

The one dimensional consolidation test apparatus is shown in Figure 3-7 and the test method is given in ASTM D 2435 (2001 f.) as the standard test method for one-dimensional consolidation test.



Figure 3-7: Shows consolidation tools like the ring, porous stones put separately and assembled.

3.11 Filter Paper Test Method

3.11.1 Introduction

This test method covers the measurement of the soil suction by filter paper which is a method that has been used in unsaturated soil mechanics, and currently is suitable for suction measurements. Measurements of suction outputs are matric, osmotic and total suction, which are free energy parameters of pore-water between soil particles and moisture. This well-known free energy of the soil matrix is determined in the laboratory by using the filter paper method. According to the filter paper test, the soil specimen and filter paper are placed in an airtight container where they are kept for a sufficient time for the pore-water in the specimen and water vapor to reach the equilibrium in Figure 3-8. The measured mass of the filter paper and the water content at equilibrium from the filter paper gives the magnitude of free energy of the soil specimen as the suction.

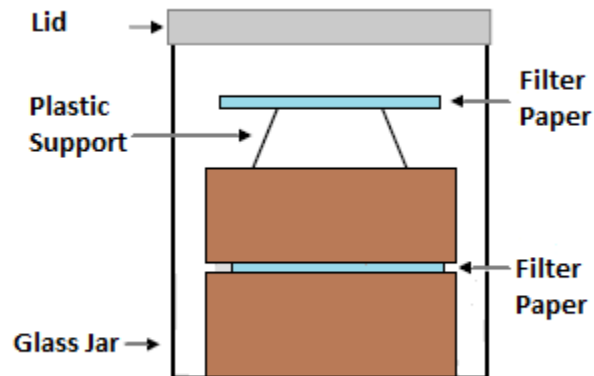


Figure 3-8 Geometric configuration of a filter paper test jar with filter papers inside and a sample.

Both total and matric suction can be determined by means of the filter paper method. In the matric suction measurement, the filter paper is placed between two samples in Figure 3-9. Water flows between the samples which is in liquid form and thus at equilibrium the water that was absorbed by the paper is in liquid form. Two filter papers are placed on top of and out of contact with the samples; the papers absorb water in vapor form. When the samples reach the equilibrium, the suction in the sample and filter papers will be equal. After the equilibrium, the water content of the filter paper gives both total and matric suction measurements. The procedure for using the wetting filter paper calibration curve is developed in Bulut et. al.(2001).

The standard method for the measurement suction using the filter paper method is given in the ASTM D 5298-94. The tools used for the filter paper test are shown in Figure 3-10 and described below.

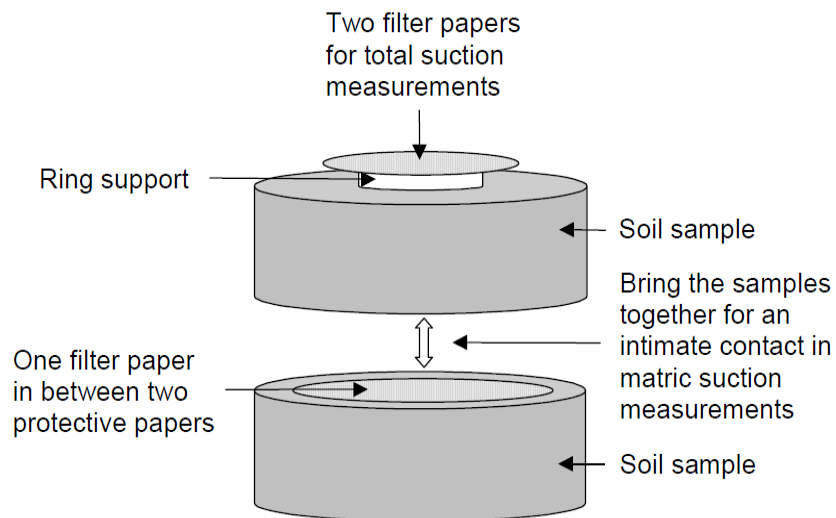


Figure 3-9 Soil samples, filter papers for matric and total suction. (Report No: TX-05/0-4518-1)



Figure 3-10: Filter paper, tins, tweezers, latex gloves, PVC ring, and electrical tape are shown in the picture. [Report No:TX-05/0-4518-1]

In order to get a soil suction value based on the water content which is determined above, the filter paper calibration curve shown in Figure 3-11 is used. Equation (3-4) and (3-4) shows suction calculations.

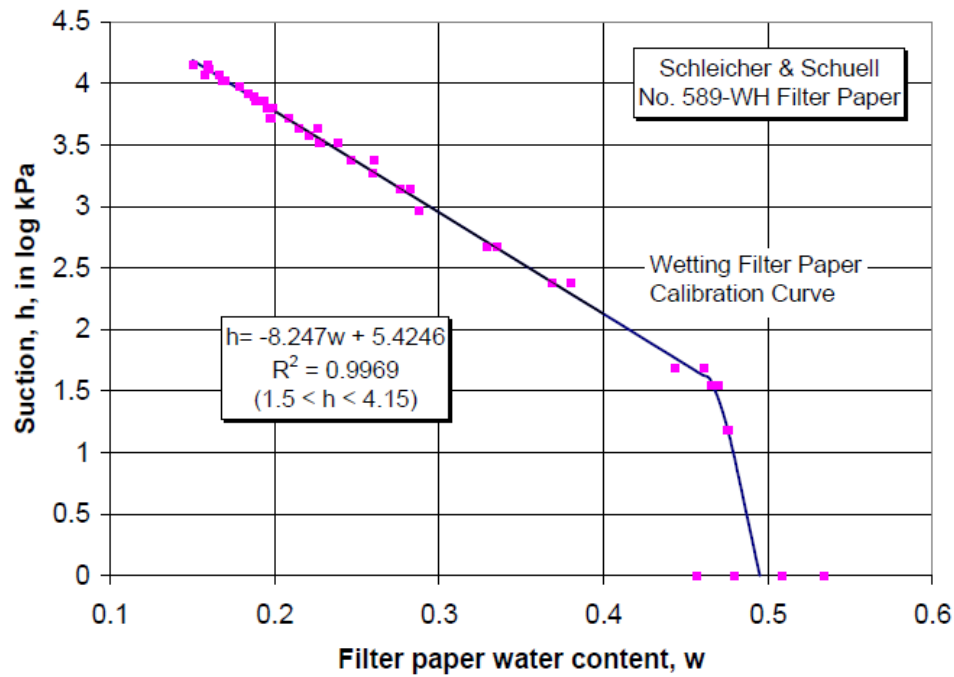


Figure 3-11: Filter paper calibration curve (from Bulut et al., 2001).

$$h_1 = -8.247W_f + 5.426 \quad (3-4)$$

$$h_2 = -8.247W_f + 6.426 \quad (3-5)$$

where:

h_1 : suction ($h_1 > 1.5$ log kPa),

h_2 : suction ($h_2 > 2.5$ PF)

Both the soil matric and the total suction test can be applied to the same soil sample at the same time. And then the determinations of the methods of the soils total suctions are very similar and they can be determined after getting the water content of the papers for all. The unit of suction is usually stated as pF . Based on the filter paper

calibration curve, the gathered suction values need to be larger than 1.5 kPa and smaller than 4.15 kPa.

3.12 Pressure Plate Test

3.12.1 Introduction

This test determines the characteristic moisture content for different air pressure levels or PF suction values by using a pressure plate extractor which is shown in Figure 3-12. One of the important phenomena for geotechnical engineering is to determine the interaction between water and soil particles. In laboratory studies, the physical properties of soils can be determined by using pressure plate extractors which is the most useful experimental tool for researchers in the unsaturated soil mechanics laboratory.

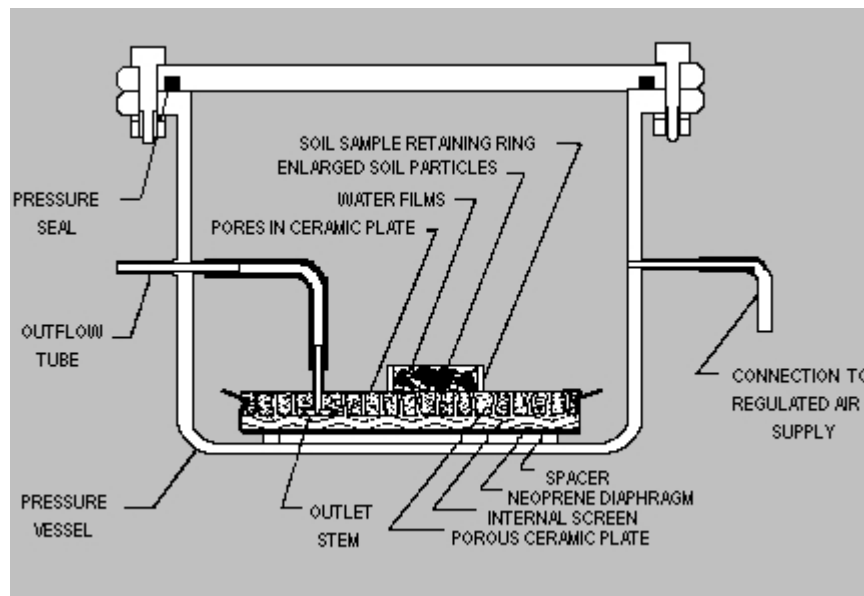


Figure 3-12: A pictorial view of the pressure plate apparatus with internal apparatus and soil samples (online source from New Mexico State University)

There are some other methods available to determine the physical characteristics of soils including suction like centrifugation compaction, and displacement, but each of these methods has a limited range of applications. In some cases soil samples are destroyed in the extraction process of soils (Thakur, 2005). However, pressure plate extractors give reliable and precise physical characteristics of both disturbed and undisturbed soil core samples, through extracting the soil moisture and without disturbing the sample.

The pressure plate extraction, Figure 3-12, is a well-known method for removing water from soil by maintaining different levels of air pressure, thus overcoming the suction pressure of the soil particles on water and draining the water through the porous ceramic plate. Under air pressure, liquid water in the soil moves through the porous ceramic in this phase of the extraction process by using positive pressure. At the equilibrium phase, the water or moisture content remains constant in the soil due to a suction (negative) pressure; therefore negative pressure is related to the moisture content.

Figure 3-13 indicates that water coats soil particles under air pressure on the ceramic plate inside the pressure plate vessel to create a thin film. Soil samples are directly set on the saturated ceramic plate which supports soil samples and provides a passageway for the water to transfer out of the vessel.

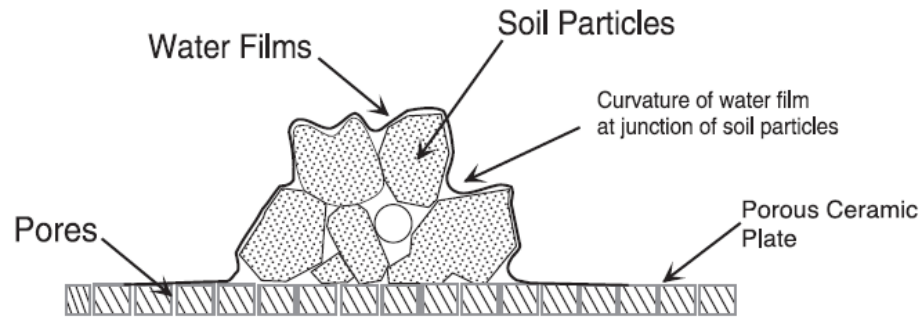


Figure 3-13: An illustration of water films coated soil particles on a ceramic plate magnified by air pressure. (Soil Moisture Equipment Corporation, CA, USA).

When the air pressure is applied on the samples inside the extractor, the force starts pushing excess water towards the ceramic plate. The pores in the plate are filled with water so that in even in higher air pressure, air cannot pass easily through these pores and exit the vessel. Because of surface tension, a water diaphragm exists between soil particles. In order for air to leave the extractor, air must first break this water diaphragm. The radius of the diaphragm decreases with increasing air pressure Figure 3-14.

When the air pressure is increased in the chamber, soil moisture will start to flow in the chamber and between soil particles until the water film curve is the same for all particles. When this happens, water flows through the outside of the chamber and terminates. This occurs at the end of every step of an air pressure that is increased.

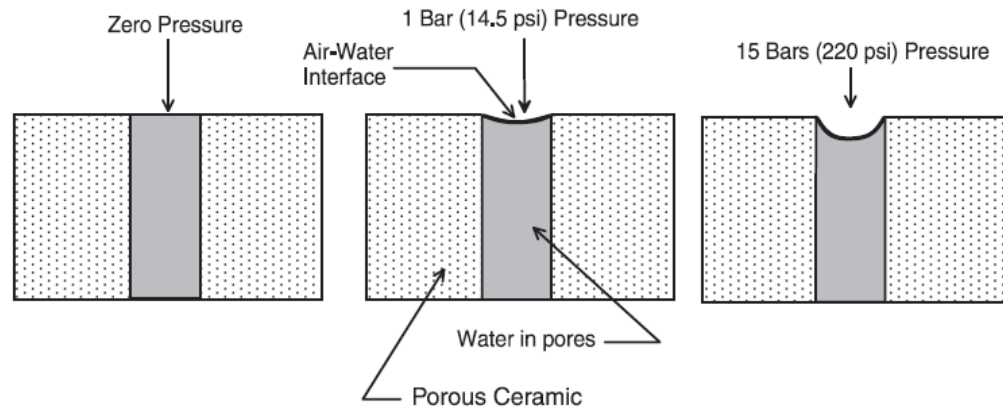


Figure 3-14: An illustration of a ceramic plate pore and air-water, interface curvature diameter changes under different level air pressure. (Soil Moisture Equipment Corporation, CA, USA).

At equilibrium, the water content of the samples in the chamber can be determined by weight or by volume. There is an equal, but opposite relationship between positive air pressure (+) and negative soil suction (-). By determining the water content at the known equilibrium pressure, a water content versus a suction curve can be plotted at the end of each pressure increment or decrement. For example; at 1 atmosphere (1 bar =14.5 psi) of air pressure, the soil suction will be 1 atmosphere (1 bar), or at 15 atmospheres (15 bar=220 psi) of air pressure, the soil suction will equal to 15 atmospheres (15 bar) which is known as the wilting point for some vegetation.

When the air is applied, the air pressure will increase in the chamber. However, a 15 bar ceramic plate is quite strong in Figure 3-15. To avoid damage or breaking of the ceramic plate due to different air pressure, keep the ceramic plate off of the bottom of the extractor. A metal triangular support is used for this purpose.



Figure 3-15: Pressure Plate Set in the Laboratory and A 15 bar (1500 kPa) ceramic plate in the vessel is shown after the distilled water was submerged (Soil Moisture Equipment Corporation, CA, USA) .

Also, in order to avoid apparatus errors, check the ceramic plate to make sure it does not have any damages before making a run. Leave the pressure plate cell in a box, which has approximately 150 ml of distilled water, let the excess water stand on the surface for several hours. Place the ceramic plate on the triangular support in the pressure plate and connect the plate at the lowest outlet port by a passage way to the outflow tube assembly. Before closing the lid, apply a thin coat of heavy grease to the bolts, and close the lid and insert the bolts, one on each side. Tighten the first two wing nuts, and then insert the other six bolts and wing nuts . Snug them back and forth, one side then the other side.

At 15 bar (=220 psi), the flow rate of air is ideally 1/10 ml of atmospheric air pressure per minute. If the rate is larger than this, there might be leaking due to either a damaged cell or a crack in the “O” ring seal.

As a gas pressure source an electrical compressor can be used to generate pressure levels from 10 to 1500 kPa. However, if the compressor is used, an air filter should be used which can be installed somewhere on the pipe where air flows into the pressure plate extractor.

An air pressure gauge is required between the pressure plate and the compressor to manage the amount of obtained and regulated air to the flow chamber. In order to reach the equilibrium in a shorter time, a soil sample should be limited to a height of 1 cm. Ideally soil samples should be 1 cm high by 5-1/2 cm in diameter. Connect a burette (cup) to the out flow tube, so air bubbles and water flow can be seen, and hence this can give an idea by looking at them whether the samples are reaching equilibrium or not. Quite a few samples come to equilibrium within 18 to 20 hours (Soil Moisture Equipment Corporation, CA, USA).

Air pressure in the pressure plate extractor, where water moisture is higher, forces moisture out through microscopic pores in the ceramic plate. The air pressure cannot go through to the outside since the pores are full of water. Therefore, the air pressure has to break the surface tension of the water between particles by pushing the curvature of the gas –liquid curvature. At any given pressure this whole process will occur, until the effective curvature of gas water films throughout the sample and air pressure in the chamber reach equilibrium.

3.13 Volume Measurement of Soil Sample by a New Method

One of the physical soil properties is the volume change under different pressures. Numerous test methods have been used by researchers to determine the volume of samples laboratories. Even though these test methods generally are used in for volume determination, they carried with them some unexpected problems for researchers and samples. The Mercury method, for instance, is a well-known volume measurement method, but the method includes a health hazard for researchers. Paraffin, for example, is another volume determination method. There is a negative side to this method as well, because trimming the paraffin from a surface of a sample always damages some of the samples surface. Current test methods are very useful for researchers conceptually. However researchers meet some implementation problems during the test process. Therefore, a new test method has been developed for the determination of volume measurements and also volume changes of samples in the laboratory. This new improved method is based on measuring the mass of the displaced Ottawa sand. The first application of the method was proposed for irregular shaped small stones by Yeager and Slowey (1996).

3.13.1 Test Apparatus

1. Ottawa sand; needs to be sieved and needs to be smaller than No.200 sieve and should not be taken for the test.
2. Test Jar; can be a glass, plastic or metal jar which is rigid enough, and must not be flexible. The upper edge of the jar needs to have the same geometric shape.

3. Ruler; a hard plastic ruler, which does not bend.
4. Brush; a very soft and small brush for cleaning the surface of the samples.
5. Desiccators; a large enough volume size desiccator to store samples during the volume measurements and must be kept in constant moisture content.
6. Scale; with a minimum capacity of 2000 g and 0.01 g of a sensitive scale.
7. Jar container; needs to hold ottawa sand and needs to supply the sand during the test.
8. Plastic Container; a big rectangular container that can contain the test jar and that can hold the displaced sand from the test jar. Even if the plastic container has enough volume to hold the jar, it should not be deep so that the researcher has to run the test in side of the plastic container.

3.13.2 Test Procedure

1. The volume measurement needs to be made after 0.5 bars, maximum 15 bars and last 0.5 bars.
2. The soil sample needs to be taken out from the pressure plate and the readings of the weight need to be taken, and then the sample needs to be placed into the desiccators.
3. Place all the apparatus on a big table. Mix the Ottawa sand thoroughly inside of the jar container.
4. Repeat couple empty runs which means take the empty jar and Ottawa sand. Then pour the Ottawa sand in the test jar until it becomes full and then empty

out the test jar. Repeat this process a couple times with and without the sample in the test jar.

5. Take the sample from the desiccators and place it in to the jar very carefully in a vertical position illustrated in Figure 3-16 (a). In order to surround the sample by the Ottawa sand, the sample must stay in the jar in a vertical position.
6. Pour the Ottawa sand slowly into the jar illustrated in Figure 3-16 (b). The Ottawa sand needs to fall in to the jar from one point with a constant speed. Be careful to not dump the sand on the sample because the Ottawa sand can stick to the sample.
7. Pour the Ottawa sand until the jar becomes completely full and keep pouring the sand until it becomes a small hill on top of the jar.
8. At this point do not move or shake the jar.



(a)



(b)

Figure 3-16: (a) Sample is placed vertically in the jar, (b) Ottawa sand is dumped onto the sample.

9. Take the ruler and trim out the surface of the jar in (a). This needs to be done only one time. Also while trimming the Ottawa sand, the ruler must be held in a perpendicular position to the surface of the jar.
10. Hold the jar and clean the surface of it from the Ottawa sand around the jar. While doing this, do not drop the sand inside of the jar.
11. Weigh the jar and take a reading of the full jar.
12. Pour the sand out of the jar and into the container. Once the sample is seen in Figure 3-17 (a) the jar, the sample needs to be taken out and then the rest of the sand needs to be poured.
13. Repeat steps (5) to (12) for the same sample for at least five times.
14. After the last repetition clean the surface of the sample with a soft brush in Figure 3-17 (b).

Place the sample back into the desiccators. If one sample is tested the desiccators are not needed. Thus, the sample can be placed directly in to the pressure plate extractor.

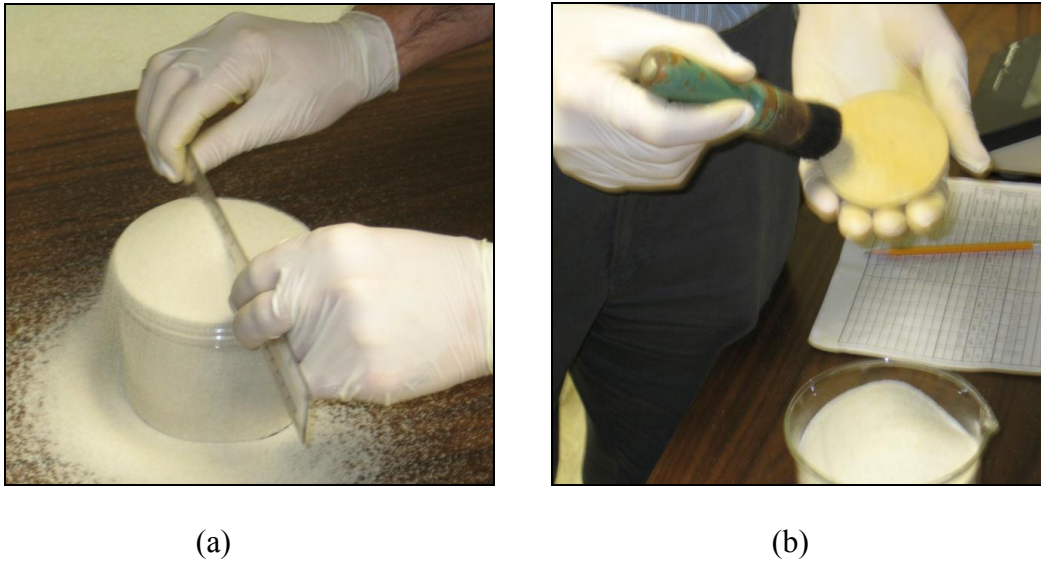


Figure 3-17: (a) Sand on top of the filled jar is trimmed level with the top of the jar, (b) sample is gently cleaned

3.14 Unconfined Compression Test

3.14.1 Introduction

The objective of the test is to quickly determine the undrained shear strength of cohesive soils. In this test, only the load on the sample (vertical) axial stress (σ_1) will increase. Since there is no (horizontal) radial stress ($\sigma_3=0$), it will not increase. The sample is sheared in a constant volume because the load is applied rapidly, and the pore water pressure is not drained. This test is only applied for the sample which has been obtained and in the undistributed state which has no cracks or fractures. The sample is trimmed in a cylindrical shape which has a ratio of $2 < \text{Length/Diameter} < 3$ before placing the sample into the unconfined compression testing device in Figure 3-18.

The following equation shows the determination of the undrained shear strength

$$\tau_f = \frac{\sigma_1}{2} = \frac{q_u}{2} = c_u \quad (3-6)$$

where: τ_f = undrained shear strength, σ_1 = total major principal stress, q_u =
unconfined compression strength, c_u = unconfined compression strength

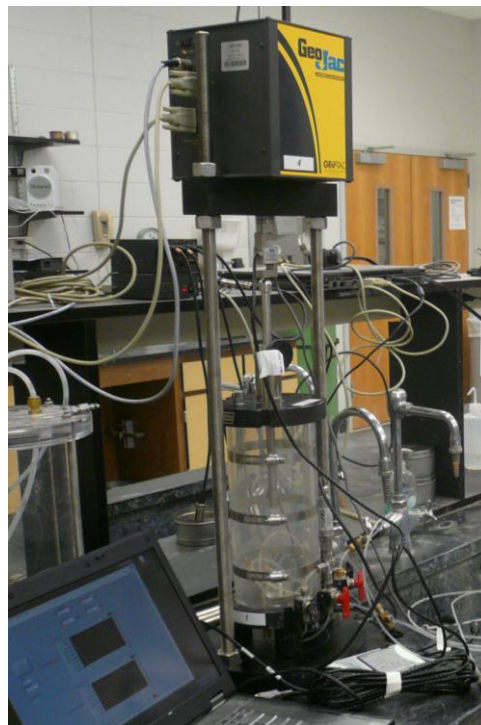


Figure 3-18: Unconfined compression test instrumental in geotechnical laboratory

4. UNSATURATED SOIL MECHANICS

4.1 Introduction

The soil water characteristic curve (SWCC) represents a relation between soil and the suction of particular soil. This relation presents a very important key role for determining fundamental engineering soil properties such as shear strength, hydraulic conductivity, and compressibility. A fundamental concept of soil suction in unsaturated soil mechanics and horizontal earth pressure based on the suction are briefly summarized in this chapter.

4.2 Concept of Soil Suction

Soil suction is a free energy state of water and this free energy is determined in terms of vapor pressure of soil water (Edlefsen and Anderson 1943). Suction is free energy per unit volume applied to the water which is absorbed by the soil. Soil suction has two components which are matric and osmotic suction. The sum of these suctions is total suction (Fredlund and Rahardjo 1993). The components of soil suction are defined by Aitchison (1965).

The total suction is defined as “measurement of the partial pressure of the water vapor in equilibrium with a solution identical in composition with the soil water, relative to the partial pressure of water in equilibrium”. Total suction is a phase of free energy of water having no external force, but gravity. The total suction is determined by the Kelvin equation which is given below:

$$h_t = \frac{RT}{V} \ln \left(\frac{P}{P_o} \right) \quad (4-1)$$

where:

h_t : total suction, V : molecular volume of water, R : universal gas constant, T : absolute temperature degrees K, and P/P_o : vapor pressure or relative humidity.

Matric suction is measurement of partially saturated water vapor in equilibrium with the soil, relative to the partial pressure of the soil water in equilibrium. In addition, matric suction is expressed in terms of $h_m = - (u_a - u_w)$, the difference of pore-air pressure, u_a , and the pore-water pressure, u_w , which is a function of the relative humidity or water vapor pressure at ambient temperature.

Osmotic suction is the measurement of the partial pressure of the water vapor in equilibrium with a solution identical in composition with the soil water, relative to the partial pressure of water vapor in equilibrium with distilled water. In addition, Osmotic suction is caused by salt dissolving a solution.

The mathematical relationship of this phenomenon for the total of matric and osmotic suction is given below.

$$h_t = h_m + h_\pi \quad (4-2)$$

where:

h_t : total suction (kPa),

h_m : matric suction (kPa),

h_π : osmotic suction (kPa)

The unit of free energy of the soil suction is gm-cm/gm. However; in the international system the unit of suction expressed as kPa. For the engineering unit of soil suction and which is currently very common in practice is defined as pF (Schofield, 1935). An alternative and practical unit presentation of pF has been expressed as log kPa (Fredlund and Raharjdo, 1993). Relations between units are approximately as the following.

$PF = \log_{10}(\text{suction for water as cm or gm-cm/gm})$ and $\log \text{ kPa} = PF - 1$ and $\log \text{ kPa} = \log_{10}(\text{suction in kPa})$.

4.3 Soil Water Characteristic Curve (SWCC)

The relation between the soil matric suction and the moisture content is represented by the soil water characteristic curve (SWCC). This relationship is important for unsaturated soil mechanics and provides fundamental soil and engineering properties. The relation between the soil matric suction and the gravimetric water content, or the soil matric suction and the volumetric water content, or the soil matric suction and the degree of saturation is defined as the Soil Water Characteristic Curve. The SWCC represents the characteristic properties of a soil so that every soil has a unique SWCC curve. The SWCC varies with soil parameters such as the type of the soil, the type of mineral in the soil, the gradation of the soil, the percent of fines in the soil, and the percent passing the No 200 sieve. A typical SWCC is shown in Figure 4-1 which shows the descriptive soil parameters.

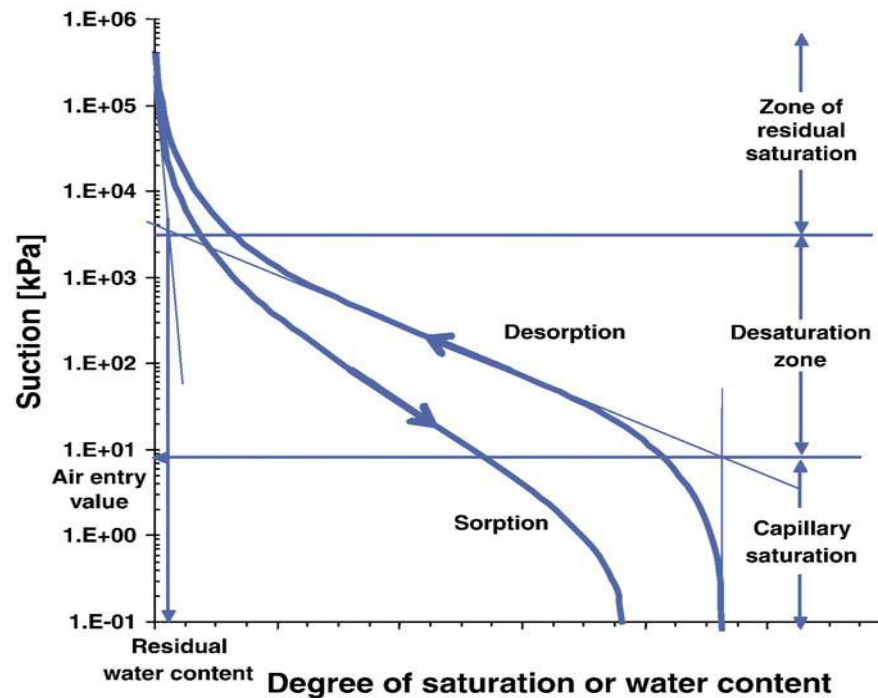


Figure 4-1: A typical wetting and drying soil water characteristic curves (Sillers, et al. 2001)

The unsaturated soil degree of the suction and water content gives a fundamental relationship which provides a framework to understand the behavior of the soil. The thermodynamic potential in a soil system is a state which pore water is expressed as a function of the amount of observed water (Lu and Likos, 2004). This fundamental relationship between the soil moisture content and the magnitude of the suction is defined as the Soil Water Characteristic Curve (Williams 1983).

Figure 4-1 illustrates descriptive parameters which are the air entry value ($u_a - u_w$)_b, residual volumetric water content θ_r and the saturated volumetric water content θ_s . The air entry value ($u_a - u_w$)_b is commonly defined as a matric suction value which the

differential pressure between the air and soil that will de-saturate the largest soil pores (Vanapalli, Fredlund, Pufahl, & Clifton, 1996). The residual volumetric water content θ_r is defined as a limiting water content state at which an increase in matric suction does not make any change in the water content. The saturated volumetric water content θ_s is defined as the porosity of the soil, or it is a water content state in the saturated condition of the soil.

4.4 Determining the SWCC through Mathematical Models

Many effective laboratory devices such as the pressure plate extractor is utilized to generate a relationship between the water content and the matric suction of soil by determining the moisture content of the soil. All experimental tests aim to determine several pairs of suction moisture data to generate a complete Soil Water Characteristic Curve. These experimental procedures may take several days or a longer time period to obtain these suction moisture pairs. A number of mathematical models have been proposed to determine the SWCC base on a few limited points to overcome this time problem. These models are used so that fewer empirical parameters are needed to generate a complete SWCC in a shorter time. The lists of common mathematical models that are used to fit a SWCC are given in Table 4-1.

Based on experimental observations most of the models define the shape of the SWCC as a sigmoidal or an S-shaped curve. Several studies have shown that the sigmoidal curve is the best shape for the soil moisture retention curve among the other models. A study conducted by Zapata (1999) showed that the Fredlund and Xing (1994)

model fits very well for a number of different soils. According to Zapata (1999) the best fitting model for sandy and clay soil is proposed by Fredlund and Xing (1994). When the models are grouped based on the unknown parameters Fredlund and Xing (1994) and van Genuchten (1980) have four unknown parameters. The Fredlund and Xing equation includes a correction factor of $C(h)$. This correction factor is used to push volumetric water content to minimum when suction reaches the maximum.

The second group includes the models developed by McKee and Bumb (1987), van Genuchten and Mualem (1980), Gardner (1958), and Brooks and Corey (1964) which have three unknown parameters. The last group is the models of Williams et al. (1983), Farrel and Larson (1972), and Assouline et al. (1998) that have two unknown parameters.

A list of all most common mathematical models, references for equations and parameters for each equations are given in Table 4-1.

Table 4-1: Proposed mathematical equations used to fit the soil-water characteristic curve (Zapata, 1999)

Reference	Equation	Unknowns
Fredlund and Xing (1994)	$\theta_w = C(h) \times \left[\frac{\theta_s}{\left[\ln \left[\exp(1) + \left(\frac{h}{a} \right)^b \right] \right]^c} \right] \dots\dots(11)$ $C(h) = \left[1 - \frac{\ln \left(1 + \frac{h}{h_r} \right)}{\ln \left(1 + \frac{10^6}{h_r} \right)} \right] \dots\dots\dots(12)$	<p>a = a soil parameter and it is a function of the air entry value of the soil in kPa.</p> <p>b = a soil parameter and it is a function of the rate of water extraction from the soil, once the air entry value exceeded.</p> <p>c = a soil parameter and it is a function of the residual water content.</p> <p>h_r = a soil parameter and it is a function of the suction at the residual water content in kPa.</p>
van Genuchten (1980)	$\theta_w = \theta_r + \frac{\theta_s - \theta_r}{\left[1 + \left(\frac{h}{a} \right)^b \right]^c} \dots\dots\dots(13)$	<p>θ_r = residual volumetric water content.</p> <p>a = a soil parameter and it is a function of the air entry value of the soil in kPa.</p> <p>b = a soil parameter and it is a function of the rate of water extraction from the soil, once the air entry value has been exceeded.</p> <p>c = a soil parameter and it is primarily a function of the residual water content.</p>
McKee and Bumb (1987)	$\theta_w = \theta_r + \frac{\theta_s - \theta_r}{1 + \exp(1) \left[\frac{(h-a)}{b} \right]} \dots\dots\dots(14)$	<p>θ_r = residual volumetric water content</p> <p>a = curve-fitting parameter</p> <p>b = curve-fitting parameter</p>
van Genuchten and Mualem (1980)	$\theta_w = \theta_r + \frac{\theta_s - \theta_r}{\left[1 + \left(\frac{h}{a} \right)^{bm} \right]^{\left(1 - \frac{1}{bm} \right)}} \dots\dots\dots(15)$	<p>θ_r = residual volumetric water content.</p> <p>a = a soil parameter and it is a function of the air entry value of the soil in kPa.</p> <p>b_m = a soil parameter and it controls the slope of SWCC at the inflection poin.</p>

Table 4-1:Cont.

Reference	Equation	Unknowns
van Genuchten and Burdine (1980)	$\theta_w = \theta_r + \frac{\theta_s - \theta_r}{\left[1 + \left(\frac{h}{a}\right)^b\right]^{\frac{1-2}{b}}} \dots\dots\dots(16)$	θ_r = residual volumetric water content. a = a soil parameter and it is a function of the air entry value of the soil in kPa. b = a soil parameter and it is a function of the rate of water extraction from the soil, once the air entry value exceeded.
Gardner (1958)	$\theta_w = \theta_r + \frac{\theta_s - \theta_r}{1 + \left(\frac{h}{a}\right)^b} \dots\dots\dots(17)$	θ_r = residual volumetric water content. a = a soil parameter and it is a function of the air entry value of the soil in kPa. b = a soil parameter and it is a function of the rate of water extraction from the soil, once the air entry value exceeded.
Brooks and Corey (1964)	$\theta_w = \theta_r + (\theta_s - \theta_r) \left(\frac{ab}{h}\right)^{b_b} \dots\dots\dots(18)$	θ_r = residual volumetric water content a_b = bubbling pressure in kPa b_b = pore size index
Williams et al. (1983)	$\ln \Theta_e = A + B \ln h \dots\dots\dots(19)$	A = fitting parameter B = fitting parameter
Farrel and Larson (1972)	$h = (u_a - u_w)_b \exp[\alpha(\theta_s - \theta_w)] \dots\dots\dots(20)$	α = empirical constant $(u_a - u_w)_b$ = air-entry value
Assouline et al. (1998)	$\theta_w = \theta_L + (\theta_s - \theta_L) \left[1 - \exp\left[-\xi \left(\frac{1}{\Psi} - \frac{1}{\Psi_L}\right)^\eta\right]\right] \dots\dots\dots(21)$	Ψ = capillary head Ψ_L = capillary head that corresponds to a very low water content, at which the hydraulic conductivity is negligible. θ_L = volumetric water content at capillary head Ψ_L . η = fitting parameter ξ = fitting parameter

4.5 Volume Change in Expansive Soils

The prediction of volume change in expansive soils is highly important for the purpose of the design procedure of ground supported structural elements. The rate of the movement due to the maximum heave or shrinkage behind the structure is important because it affects the principal priority of making an accurate estimation in the design.

The prediction of the movement in expansive soils based on change of the suction was developed at Texas A&M University. A prior study was carried out by Juarez-Badillo (1986, 1987). The theory of natural limits was proposed by Juarez-Badillo to predict expansion and the settlement of high plasticity Mexico City clays.

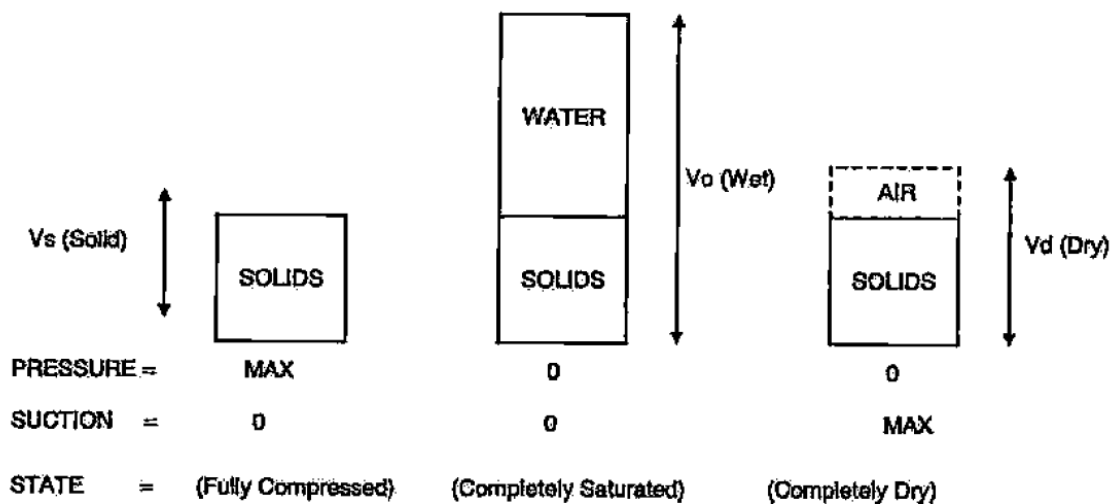


Figure 4-2: Volume Change Process in Unsaturated Soils within Natural Limits (Hong 2008)

Figure 4-2 shows that the expansion and settlement characteristics process of the natural limits are mean principal stress, suction and volume change. Figure 4-2

illustrates that the soil reaches the maximum volume, V_o , under conditions of zero mechanical pressure and suction. The soil volume compresses to the volume of the solids mass, V_s , under conditions of zero suction and infinite mechanical mean principal stress. The soil volume compresses to the dry volume, V_d , under condition of zero mean principle stress and infinite suction.

Figure 4-3 shows that volume change of $\Delta V/V$ on the volume-mean principal stress-suction surface is related to the logarithm of mechanical pressure and logarithmic suction components.

$$\frac{\Delta V}{V} = -\gamma_h \log_{10} \left(\frac{h_f}{h_i} \right) - \gamma_\sigma \log_{10} \left(\frac{\sigma_f}{\sigma_i} \right) - \gamma_\pi \log_{10} \left(\frac{\pi_f}{\pi_i} \right) \quad (4-3)$$

where:

$\frac{\Delta V}{V}$ = the volume strain,

h_i, h_f = the initial and the final values of matric suction,

σ_i, σ_f = the initial and the final values of mean principal stress,

π_i, π_f = the initial and the final values of osmotic suction,

γ_h = the matric suction compression index,

γ_σ = the mean principal stress compression index,

γ_π = the osmotic suction compression index,

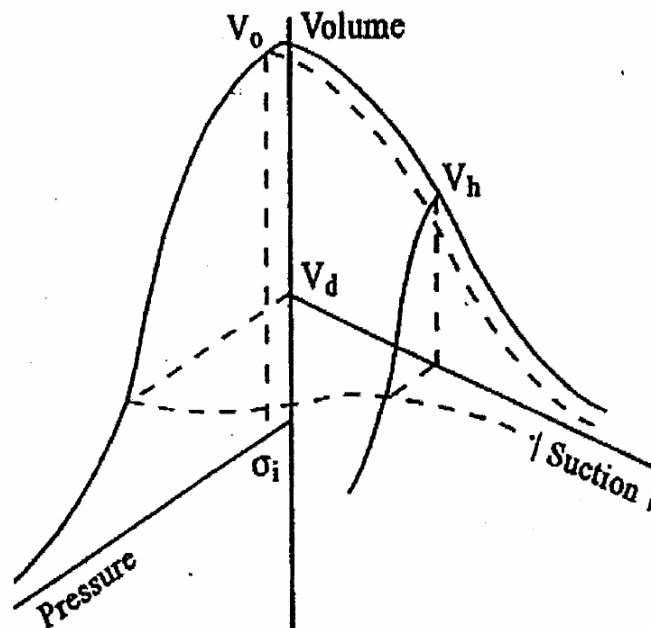


Figure 4-3: The Volume–Mean Principle Stress-Suction Surface Curve (Hong 2008).

The mean principle stress compression index, γ_σ , is related to the commonly used compression index, C_c , by:

$$\gamma_\sigma = \frac{C_c}{1 + e_o} \quad (4-4)$$

where:

e_o = the void ratio,

Initial and final values of the matric suction, osmotic suction and mean principle stress profile change with depth therefore the suction values must be known to predict either movement or volume change in the soil.

The effective friction angle, ϕ' , is determined by the regression equation which is based on the plasticity index. The empirical correlation is given in Figure 4-4. The equation is given as follows:

$$\phi' = 0.0016PI^2 - 0.302PI + 36.208 \quad (4-5)$$

where:

PI = Plasticity Index,

ϕ' = effective friction angle,

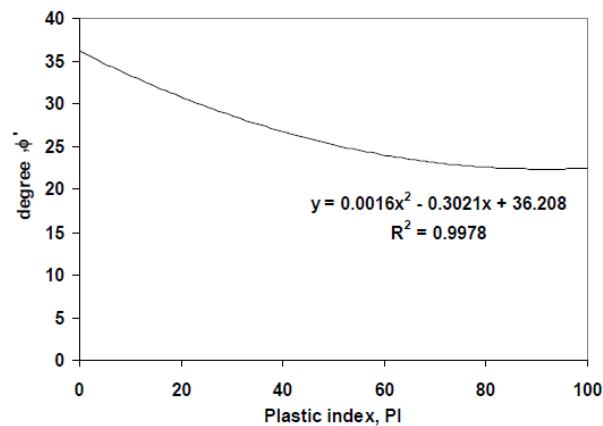


Figure 4-4: The Regression Equation Based on the Relation on the Empirical Correlation Between ϕ' and PI. (after Holtz and Kovacs 1981).

Figure 4-5 illustrates that the parameter ‘S’ is obtained from the slope of the suction vs. the gravimetric water content curve. The Texas Transportation Institute (TTI) gives an equation to obtain the slope “S” based on a completed research study in Project Report 4518. The equation for the “S” is presented as follows:

$$\left[\frac{\partial h}{\partial \theta} \right] = \frac{1}{0.4343} \frac{S \gamma_w}{\gamma_d} \quad (4-6)$$

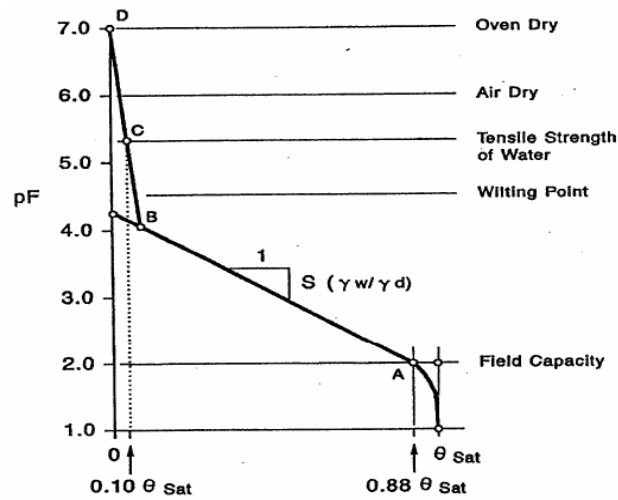


Figure 4-5 : Suction vs. Volumetric Water Content Curve and 'S' Parameter (Lytton 1994).

Both h and S values are given in the equation and are negative thus the slope of the curve is positive. The slope function for the suction volumetric water content curve is given as follows.

$$\left(\frac{\partial h}{\partial \theta} \right) = \frac{1}{0.4343} \frac{S \gamma_w}{\gamma_d} \quad (4-7)$$

$$\left(\frac{h}{\theta \left(\frac{\partial h}{\partial \theta} \right)} \right) = \frac{0.4343}{S_w} \quad (4-8)$$

where:

w = the gravimetric water content,

h = suction a negative value,

θ =volumetric water content,

The S value is estimated based on the Atterberg limits and sieve analysis results of passing No. 200 sieve. The S -value equation is given by:

$$S = -20.29 + 0.1555(LL) - 0.177(PI) + 0.0684(\#200) \quad (4-9)$$

where:

LL = the liquid limit in percent,

PI = the plasticity index in percent,

$\#200$ = the percent of soil passing the No. 200 sieve,

γ_w = the unit weight of water,

γ_d = the dry unit weight of the soil,

The suction as pF-versus volumetric water content, θ , can be estimated based on the empirical equation (4-8) given above. This relation uses volumetric water content and Table 4-2 which includes the saturated volumetric water content.

Table 4-2: Range of Saturated Volumetric Water Content by Unified Soil Class (Mason, Ollayos et al. 1986).

Unified Class	Range of θ_{sat} *
GW	0.31-0.42
GP	0.20
GM	0.21-0.38
GM-GC	0.30
SW	0.28-0.40
SP	0.37-0.45
SM	0.28-0.68
SW-SP	0.30
SP-SM	0.37
SM-SC	0.40
ML	0.38-0.68
CL	0.29-0.54
ML-CL	0.39-0.41
ML-OL	0.47-0.63
CH	0.50
* $\theta_{sat} = n$ (porosity)	

4.6 Swelling Pressure in Expansive Soils

Many studies show that expansive soils have a high potential of volume change due to changes in the moisture content. Moisture changes are caused by changes of suction in the soil and also causes the soil to swell or shrink. The swelling pressure and volume change problem arises on high plasticity soil by changes in moisture. The swelling pressure occurs when the high plasticity soil gets in contact. Also expansive soils the only soil that has a high plasticity potential that can damage the structures. These types of clay minerals are generally classified as high plasticity soils which are kaolinite, illite, and montmorillonite. A typical Montmorillonite particle is shown in Figure 4-6 with absorbed water.

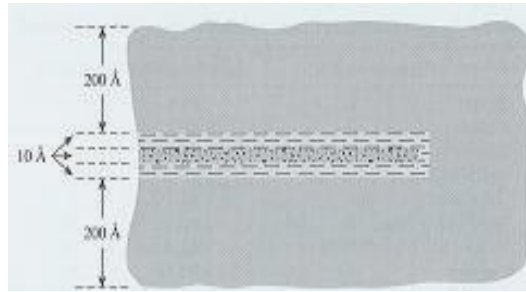


Figure 4-6: Montmorillonite particle adsorbed water

The greatest volume change occurs in montmorillonite then in kaolinite and illite, respectively. Therefore montmorillonites have a more severe potential damage capacity when they are subject to significant moisture content changes (Hudak, 1998). Additionally the magnitude of volume change for high plasticity expansive clays cannot be predicted by classical soil mechanics principles.

4.7 Horizontal Earth Pressure in Retaining Walls Due to Suction

A number of research activities have focused on vertical swelling pressure which is generated by expansive soil. However the lateral pressure is different than the vertical swelling pressure due to expansive soils which have an anisotropic structure and behavior. All common buried retaining structures in cuts, such as soil nailing, tied-back, and drill shaft walls are subjected to swelling and shrinkage force due to moisture changes in the soil. These structures are not only subjected to uplift forces but also they are subjected to horizontal swelling pressure which tends to cause lateral deformation.

Several research efforts have been undertaken to estimate lateral earth pressure against retaining walls. Based on the research typically three zones are proposed by

Hong (2008) to estimate the lateral swelling pressure. To formulate the lateral pressure equation in three zones, the effective stress concept and the volume change concept equation in unsaturated soil are used.

The concept of volume change and effective stress equations are formulated for horizontal swelling pressure in these three zones. Comparison of horizontal pressure for a predicted soil with in situ natural soils was observed by Brackley and Sanders (1992). The significance of the prediction of horizontal pressure is clarified for expansive soils.

4.8 Swelling Lateral Earth Pressure on Stationary Walls

The typical pattern of lateral swelling pressures on a stationary wall in the three zones is shown in Figure 4-7 and Figure 4-8 and this pattern is proposed by (Hong, 2008). Suction change from the initial to the final suction within the profile is shown in Figure 4-7. The figure also shows that the suction change increases from the bottom to the surface. The typical lateral earth pressure distribution is shown in Figure 4-8.

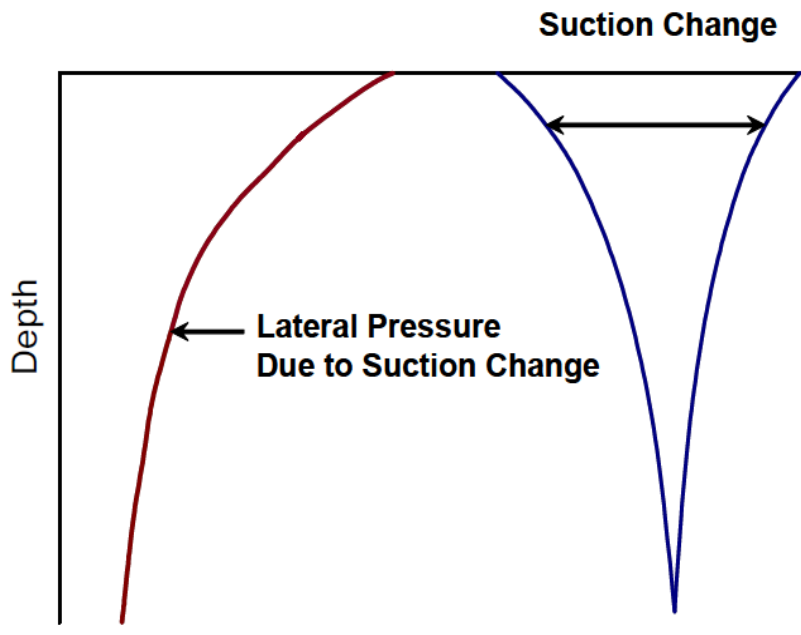


Figure 4-7 : Lateral Pressure due to Suction Change (Hong, 2008).

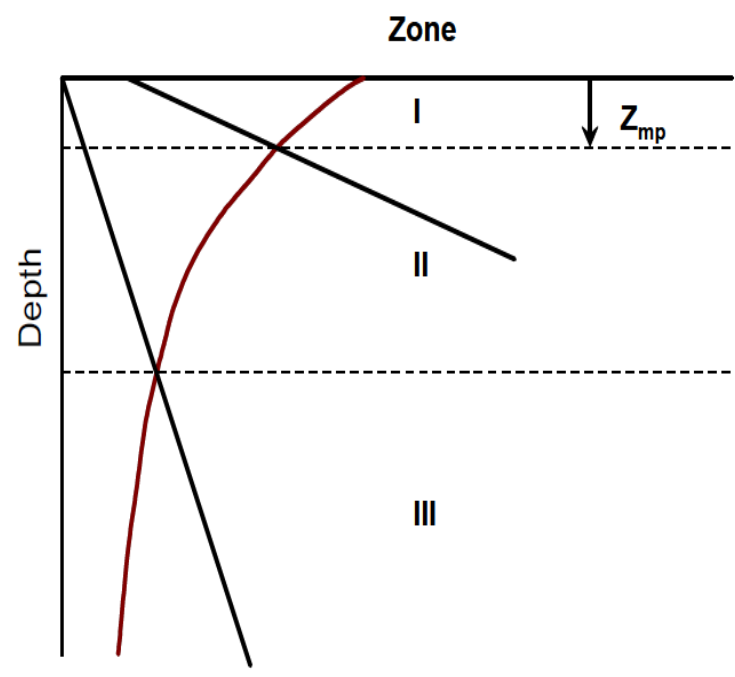


Figure 4-8 : Typical Distribution of Lateral Earth Pressure (Hong, 2008).

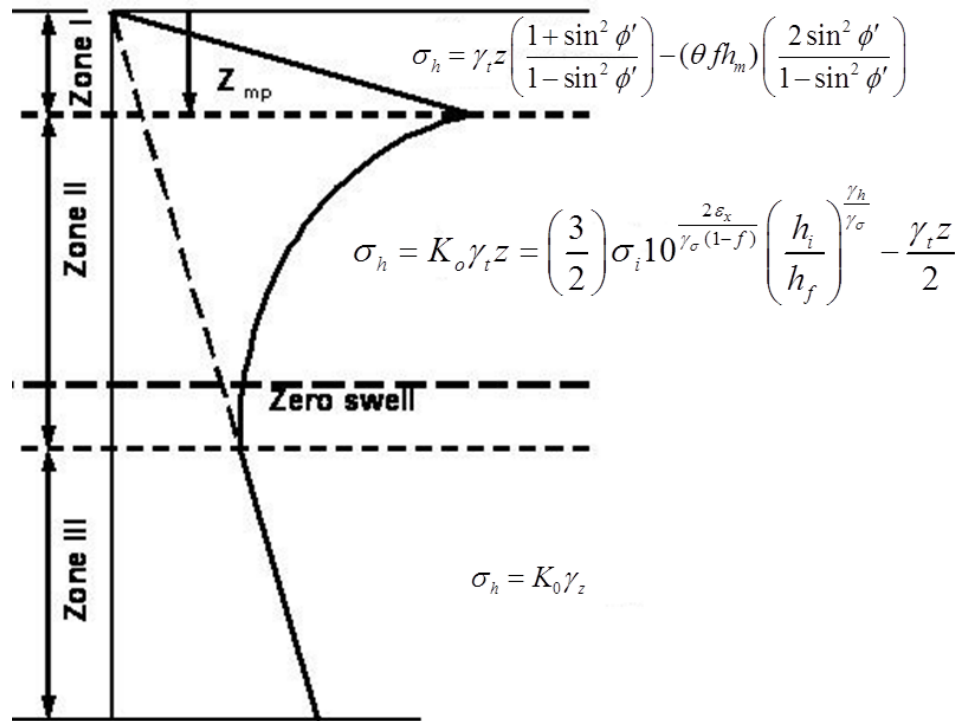


Figure 4-9: Three earth pressure zones (Zone I is shear failure state, Zone II swelling passive state and Zone III is at rest state) are shown.

Figure 4-9 shows the lateral earth pressure distribution and illustrates the three pressure zones. The upper zone is zone I and the depth of maximum lateral swelling pressure is z_{mp} . A passive failure state of stress occurs in the upper zone to a depth of z_{mp} which is usually within a depth of 2 or 4 ft. A measure of the lateral pressure is found at a depth of 3 ft by Joshi and Katti (1980). The lateral passive pressure state is presented in zone II. Zone III represents the classical at rest state condition..

The passive earth pressure equation is used in zone I and the formulation of the equation is given by:

$$\sigma_h = \gamma_t z \left(\frac{1 + \sin^2 \phi'}{1 - \sin^2 \phi'} \right) - (\theta f h_m) \left(\frac{2 \sin^2 \phi'}{1 - \sin^2 \phi'} \right) \quad (4-10)$$

In zone II the soil is in passive state and the lateral pressure is due to swelling.

The lateral earth pressure is calculated as follows:

$$\sigma_h = K_o \gamma_t z = \left(\frac{3}{2} \right) \sigma_i 10^{\frac{2\varepsilon_x}{\gamma_\sigma (1-f)}} \left(\frac{h_i}{h_f} \right)^{\frac{\gamma_h}{\gamma_\sigma}} - \frac{\gamma_t z}{2} \quad (4-11)$$

For a soil the horizontal strain is given by:

$$\varepsilon_h = \left(\frac{1 - f_c}{2} \right) \left(\frac{\Delta V}{V} \right) \quad (4-12)$$

Horizontal strain is formulated as follows:

$$\varepsilon_h = \left(\frac{1 - f_c}{2} \right) \left[-\gamma_h \log_{10} \left(\frac{h_f}{h_i} \right) - \log_{10} \left(\frac{\sigma_f}{\sigma_i} \right) \right] \quad (4-13)$$

The at-rest earth pressure coefficient and equation are used in zone III and the formulation of the equation is given by:

$$K_0 = 1 - \sin \phi' \quad (4-14)$$

$$\sigma_h = K_0 \gamma_z \quad (4-15)$$

where $\Delta V/V$ = volumetric strain, f_c = crack fabric factor, σ_h = horizontal pressure, K_o = earth pressure coefficient, γ_t = unit weight of the soil, z = depth of the soil, σ_h = lateral earth pressure, σ_i = mean principal stress which occurs at around 80 cm depth, h_i = equilibrium suction at the initial condition, h_f = equilibrium suction at the final condition (dry side), γ_h = shrink-swell index (suction), γ_σ = volume change index (confining pressure), ε_h = horizontal strain, σ_f = final principal stress, ϕ' = effective friction angle, θ = volumetric water content.

4.9 Retaining Wall in Expansive Soils

Retaining wall systems are affected by lateral pressure due to annual suction change. Seasonal moisture change creates a lateral earth pressure at or near the ground surface. Both the hot summer moisture evaporation and seasonal rainfall ratio changes in the active zone of soil at the top near the ground surface. Even the ground water level may vary depending upon the seasonal weather.

The soil expansion in the active zone causes stress and deformation to the soil-retaining wall system. High lateral pressure causes not only stress and pressure but also causes bending moments and shear forces in the retaining wall.

Figure 4-10 shows configuration of lateral expansion pressure behind the retaining wall system, and shows the resisting pressure distribution of the wall on the left side. Figure 4-10 illustrates a simplified soil retaining wall pressure model. In the figure,

the transition of stress from neutral to the equilibrium stress state is presented on both sides of the wall.

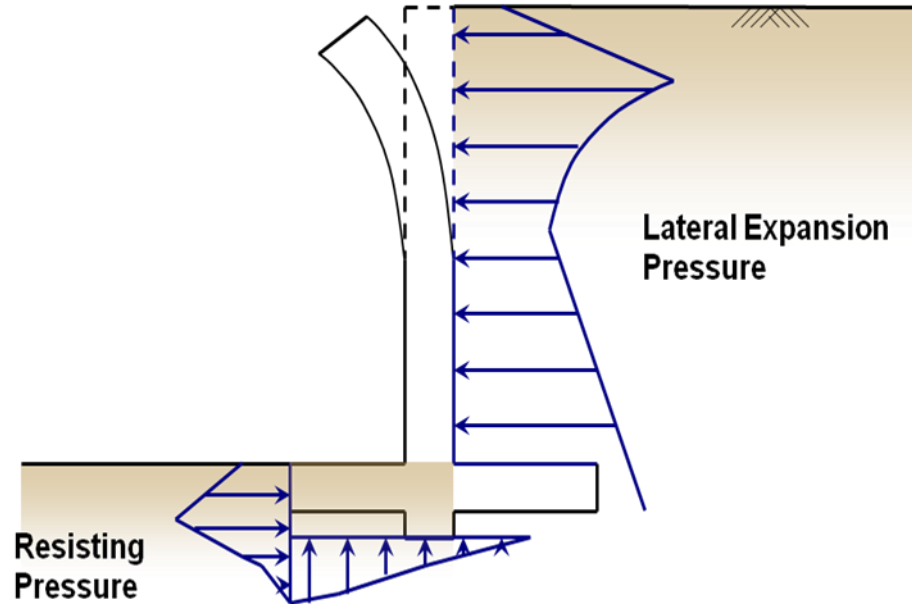


Figure 4-10: Behavior of expansive soils with horizontal pressure distribution on the left and right side of the retaining wall system (Hong, 2008).

5. RESULTS AND DISCUSSION

5.1 Introduction

The laboratory test results are compiled to characterize the soil. These test results are used to determine the volume change characteristics, soil water characteristic curve (SWCC), and horizontal pressure in expansive clay based on the constitutive equation. A new method is proposed to determine the SWCC curve parameters. Therefore the soil water characteristic curve and its parameter are described to show the estimated new method in detail. Several important curves are presented to show the relation between volume change, confining pressure, water content and the suction. These curves are volume change with confining pressure curve, water content change with change of confining pressure curve, water content change with change of matric suction curve and volume change with change of matric suction curve. The constitutive surfaces of confining pressure, matric suction and shear strength are illustrated in a three dimensional model. The last part of the section, the horizontal pressure on a stationary retaining wall is determined based on the three zones method. In addition, University of Texas at San Antonio provided data of the seasonal water content measurements in the field behind the retaining wall are presented.

5.2 Volume Change Versus Change of Confining Pressure Curve

The volume change of the soil, and volume change coefficient indexes were determined experimentally for both boring no.1 and boring no.2. Test results the illustrate the relation between the volume change and the confining pressure which are

presented in semi logarithmic form. The volume change with pressure relation for the soils is shown in Figure 5-1.

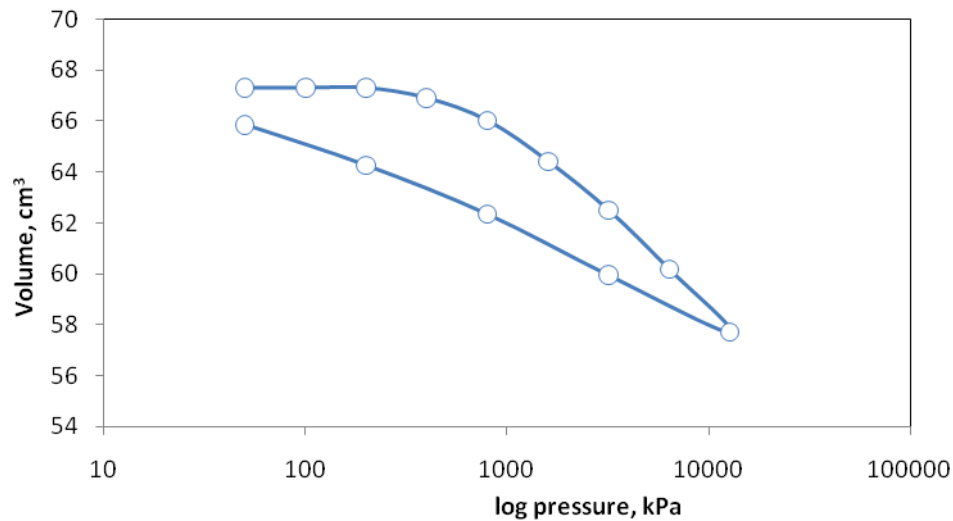


Figure 5-1 Volume change and confining pressure, $(\sigma-u_a)$ relation for an unsaturated sample of B1-13.

Figure 5-1 shows that under the condition of zero mechanical pressure, the soil sample is at the maximum volume or initial volume. The soil volume compresses to the volume of the solid alone by increasing the pressure. The soil volume includes a volume of solid, water, and air-filled voids, so increasing pressure decreases the volumes of water and air-filled voids. This volume change phenomenon continues until a stage where the confining pressure reaches a maximum. A subsequent decrease in the pressure on the soil sample increases volume of the sample. In return, an increase in the absorbing water increases the volume of absorbed water.

The relation between the volume change and the confining pressure of the sample provides data to generate two curves. The first curve shows a volume decreasing

process by increasing pressure, and the second one shows the volume increases by decreasing the pressure. The slopes of the two curves are compression index C_c and recompression index C_r . These indices are utilized to determine the volume compression index, γ_{σ_c} , and the volume recompression index, γ_{σ_r} . The formulations of these indexes are given in equation (5-1) and equation (5-2). All of the index values, C_r , C_c , γ_{σ_r} and γ_{σ_c} are compiled and presented in Table 5-1. Test results show that the tested soil samples have very high volume compression and volume recompression indexes.

$$\gamma_{\sigma_r} = \frac{C_r}{1 + e_o} \quad (5-1)$$

$$\gamma_{\sigma_c} = \frac{C_c}{1 + e_o} \quad (5-2)$$

where: γ_{σ_c} = volume compression index, γ_{σ_r} = volume recompression index, C_c = compression index C_r = recompression index, e_o = initial void ratio.

Table 5-1: Volume indexes for two borings of boring no.1 and boring no.2 are given

Boring	Depth (ft)	e_o	C_c	C_r	Volume Recompression Index, γ_{σ_r}	Volume Compression Index, γ_{σ_c}
B1-11	10-11	0.8100	0.2200	0.1300	0.0718	0.1215
B1-12	11-12	0.8000	0.2008	0.1100	0.0611	0.1115
B1-13	12-13	0.8800	0.2750	0.1250	0.0665	0.1462
B1-14	13-14	0.9000	0.2345	0.1373	0.0723	0.1234
B1-15	14-15	0.9400	0.2006	0.1089	0.0562	0.1033
B1-16	15-16	0.8400	0.2917	0.1599	0.0869	0.1585
B1-17	16-17	0.7600	0.2400	0.1316	0.0748	0.1363
B1-18	17-18	0.8500	0.2414	0.1224	0.0662	0.1305
B1-19	18-19	0.7900	0.2289	0.1114	0.0622	0.1278
B1-20	19-20	0.7200	0.1717	0.0920	0.0535	0.0998
B2-7	10-11	0.7783	0.2677	0.1173	0.066	0.1505
B2-8	11-12	0.6006	0.2003	0.1001	0.063	0.1251
B2-9	12-13	0.6593	0.2146	0.1260	0.076	0.1293
B2-10	13-14	0.6702	0.2295	0.1118	0.067	0.1374
B2-11	14-15	0.8163	0.1912	0.1118	0.062	0.1052
B2-12	15-16	0.6194	0.2146	0.1200	0.074	0.1325
B2-13	16-17	0.6783	0.2432	0.1295	0.077	0.1449
B2-14	17-18	0.6058	0.2146	0.1130	0.070	0.1336
B2-15	18-19	0.6647	0.2432	0.1260	0.076	0.1461
B2-16	19-20	0.6728	0.2289	0.1299	0.078	0.1368

5.3 Water Content Change Versus Change of Matric Suction Curve

The water content change versus change of matric suction shows a relation between the change in gravimetric water content and matric suction of the soil. This empirical relation is determined by means of the pressure plate apparatus in the laboratory. The water content is taken after an equilibrium period; therefore, the water

content depends on the air pressure that was applied to the soils. Thus, the water content will vary based on the applied air pressure. Each pressure and water content pairs are compiled to generate the matric suction-water content curve from the test. In addition, the curve can be generated either in a drying or wetting water retention curve by means of the pressure plate extractor. In this study, the drying process is applied to the samples by increasing the air pressure. Furthermore, a partial wetting process is applied at the end of the test.

The water content of the sample is determined when the sample moisture reaches equilibrium at the end of each air pressure increment. Figure 5-2 illustrates the variation of matric suction with water content. Each water content value or point at the plot corresponds to a suction level. The unit of suction is given as pF.

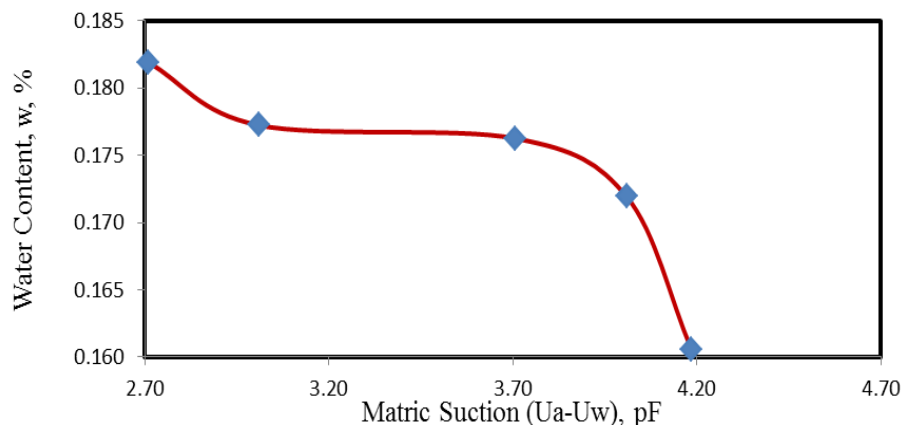


Figure 5-2: Matric suction versus water content curve based on laboratory sample of Boring No. 2 and depth of 17-18 ft.

Figure 5-2 is a plot of the results of a laboratory pressure plate test. The water content is decreased regularly by increasing the air pressure. At lower suction level, the soil has more water, but in a higher suction level the sample has less water. In other words, suction is higher in dry samples and the suction level is lower in wet samples. The curve gives a line between suction pF 4.0 and 4.20, which verifies the “Suction vs. Gravimetric Water Content Curve as seen in Figure 5-2.

5.4 Volume Change Versus Change of Matric Suction Curve

The pressure plate is a test apparatus to determine suction change compressibility of expansive soil. A newly developed volumetric measurement method is used to measure the volume of the soil sample. Thus the pressure plate test and volume measurement method are used to determine the relation between the volume change and the suction change of the soil. The change of suction imposed on the soil is between 0.5 bar (50 kPa) as the initial pressure and 15 bar (1500 kPa) as the maximum pressure. The volume of the soil sample is measured at the initial pressure level and at the maximum pressure level. The volume change of the soil sample is determined between 0.5 bar and 15 bar. The initial pressure and the maximum pressure are used as limit pressures to determine the initial and final volume of the soil samples. Volume and suction measurements on two samples are shown for the two borings in Figure 5-3 and Figure 5-4. Figure 5-3 shows the volume change for a sample from boring no. 2, and the Figure 5-4 shows the volume change for a sample from boring no. 1.

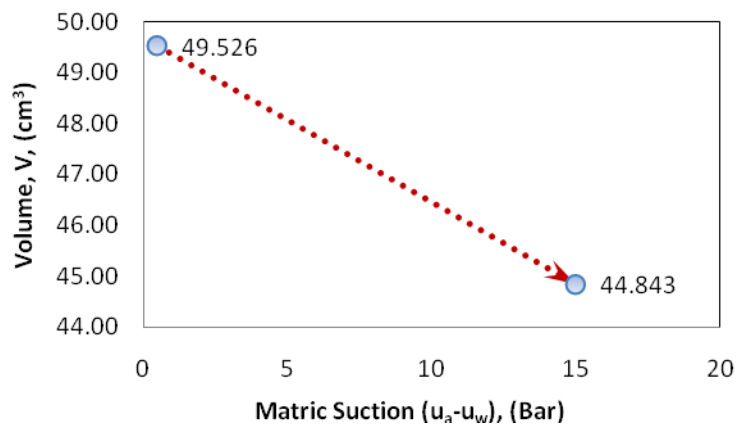


Figure 5-3: Volume change points are shown by changing suction in the sample of B2-8

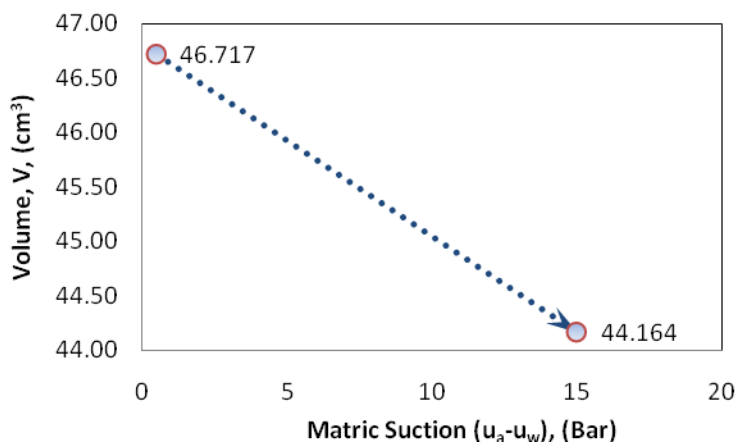


Figure 5-4: Volume change points are shown by changing suction in the sample of B1-20

To determine the volume of a soil sample, a new test method that allows the soil volume to be measured using by Ottawa sand is proposed. The new method uses Ottawa sand for volume measurement because it gives more accurate and precise test results in a shorter time than the volume measurement methods that are currently used. The volume

change results show that an increase in air pressure on the soil samples cause a loss of water content of the samples. Thus, air pressure and change in water content leads the change in volume of the soil samples. The initial and final volume measurement readings are used to determine the suction compression index γ_h . For swelling (wetting) and shrinkage (drying) cases the suction compression index is determined as $(\gamma_h)_{Swelling}$ and $(\gamma_h)_{Shrinkage}$ respectively. The formulations for $(\gamma_h)_{Swelling}$ and $(\gamma_h)_{Shrinkage}$ are given in the Equation (5-2) and (5-4). These test results are shown in the Table 5-2 and Table 5-3 that these soil samples have significant potential to expand by suction change.

In case of shrinkage the γ_h index as follows

$$(\gamma_h)_{Shrinkage} = \left(\frac{\left(\frac{-Vol_{Wet} + Vol_{Dry}}{Vol_{Wet}} \right)}{pF_{Dry} - pF_{Wet}} \right) \quad (5-3)$$

In case of swelling the γ_h index as follows

$$(\gamma_h)_{Swelling} = \left(\frac{\left(\frac{Vol_{Wet} - Vol_{Dry}}{Vol_{Dry}} \right)}{pF_{Dry} - pF_{Wet}} \right) \quad (5-4)$$

Where: Vol_{Wet} : Wet volume under the lowest pressure, Vol_{Dry} : Dry volume under the highest pressure, pF_{Dry} : Suction at the highest pressure, pF_{Wet} : Suction at the lowest pressure.

Table 5-2: Measured volume data and calculated $(\gamma_h)_{\text{Swelling}}$ and $(\gamma_h)_{\text{Shrinkage}}$ based on the volume change measurement.

Boring No.	Pressure (Bar)	Volume (cm ³)	$(\gamma_h)_{\text{Swelling}}$	$(\gamma_h)_{\text{Shrinkage}}$
B1-11	0.5	50.93	0.0789	0.0707
	15	45.62		
	0.5	50.58		
B1-12	0.5	55.59	0.0682	0.0619
	15	50.50		
	0.5	55.12		
B1-13	0.5	50.72	0.0591	0.0544
	15	46.64		
	0.5	50.33		
B1-14	0.5	44.10	0.0570	0.0526
	15	40.67		
	0.5	44.06		
B1-15	0.5	41.64	0.0242	0.0233
	15	40.21		
	0.5	41.38		
B1-16	0.5	46.66	0.0450	0.0422
	15	43.75		
	0.5	46.55		
B1-17	0.5	45.91	0.0359	0.0341
	15	43.60		
	0.5	45.76		
B1-18	0.5	47.53	0.0433	0.0407
	15	44.67		
	0.5	47.04		
B1-19	0.5	46.01	0.0225	0.0218
	15	44.53		
	0.5	46.09		
B1-20	0.5	46.72	0.0391	0.0370
	15	44.16		
	0.5	46.06		

Table 5-3: Measured volume data and calculated $(\gamma_h)_{\text{Swelling}}$ and $(\gamma_h)_{\text{Shrinkage}}$ based on the volume change measurement.

Boring No.	Pressure (Bar)	Volume (cm ³)	$(\gamma_h)_{\text{Swelling}}$	$(\gamma_h)_{\text{Shrinkage}}$
B2-7	0.5	44.27	0.0359	0.0341
	15	42.04		
	0.5	46.60		
B2-8	0.5	49.38	0.0721	0.0652
	15	44.62		
	0.5	49.15		
B2-9	0.5	47.14	0.0262	0.0252
	15	45.38		
	0.5	49.70		
B2-10	0.5	49.54	0.0600	0.0551
	15	45.51		
	0.5	49.08		
B2-11	0.5	43.60	0.0418	0.0394
	15	41.07		
	0.5	43.43		
B2-12	0.5	43.60	0.0345	0.0329
	15	41.48		
	0.5	43.62		
B2-13	0.5	41.66	0.0575	0.0530
	15	38.39		
	0.5	41.14		
B2-14	0.5	46.84	0.0984	0.0859
	15	40.90		
	0.5	47.14		
B2-15	0.5	44.84	0.0441	0.0414
	15	42.10		
	0.5	44.26		
B2-16	0.5	46.25	0.0385	0.0365
	15	43.76		
	0.5	45.93		

5.5 Soil Water Characteristic Curve Fitting Parameters

The most important reasons for developing the SWCC is to estimate moisture flow in unsaturated porous media. Prediction of the SWCC delineates the soil water retention characteristic of the porous media in which the moisture flows. The SWCC is defined for a soil as the relation between an amount of moisture content in the macro and micro pores of the soil and suction (Fredlund, Xing, Fredlund, & Barbour, 1996). The variations of this relation are defined as gravimetric water content, volumetric water content, or degree of saturation and degree of suction. The SWCC is generally plotted by using these parameters in the mathematical models.

5.6 Optimization Nonlinear Relationship of the Fitting Parameter

The several of the models of SWCC are formulated and defined based on empirical research. Fredlund and Xing (1994) proposed a model that is currently implemented in the Mechanistic Empirical Design Guide (MEPDG). This model is given in Equation (5-5) and (5-6), and it presents the SWCC as an “S” shaped curve. The four fitting parameters a_f , b_f , c_f and h_r are employed in the model. These fitting parameters govern shape of the SWCC with respect to degree of saturation and suction.

$$S = C(\psi) \times \left[\frac{1}{\left\{ \ln \left[e + \left(\frac{h}{a_f} \right)^{b_f} \right] \right\}^{c_f}} \right] \quad (5-5)$$

$$C(\psi) = 1 - \frac{\ln\left(1 + \frac{h}{h_r}\right)}{\ln\left[1 + \left(\frac{1.45 \times 10^5}{h_r}\right)\right]} \quad (5-6)$$

where:

S = Percent degree of saturation,

h = Soil matric suction, in psi

a_f = the air entry value of the soil, in psi and soil fitting parameter

b_f = the rate of water extraction of the soil after exceeding the air entry value and soil fitting parameter

c_f = the residual water content of the soil and soil fitting parameter

h_r = the suction value at which the residual water content occurs, in psi and soil fitting parameter

Optimization of the nonlinear relation by using the SOLVER function in the Microsoft Excel spreadsheet was first proposed by Zapata (2010). This function is used to predict the four fitting parameters of more than 31000 soils.

The maximum suction is set at 100,000 kPa or 145,000 psi in the equation in which minimum moisture content is assumed to be zero moisture. The reason for this is that it eliminates the indeterminate results when the moisture content potential gets close to zero. A set of repeated computations is used to determine the four fitting parameters. The computation required to determine the four parameters for each soil is the solver Function in MS Excel. SOLVER optimizes the nonlinear relation by using the

least sum of squared errors between the available measurements and the estimated moisture content data. The saturated volumetric water content and at least two measured points are available data. A fourth point is the zero moisture content where suction is at 100,000 kPa or 145,000 psi.

5.7 Formulation of the Optimized Fitting Parameter

Four parameters in the Fredlund and Xing (1994) are estimated by using the SOLVER function in MS Excel. Based on the SOLVER data four mathematical equations are developed for each parameter. Each parameter is a function of Percent Fine Content (*pf_c*) which is the ratio of the percent smaller than 2 microns to the percent passing the No. 200 sieve. The *pf_c* is presented in the equation 3 and the *pf_c* data are given in Table 5-4.

$$pf_c = \frac{\% - 2 \text{ micron}}{\% - No.200 \text{ sieve}} \times 100 \quad (5-7)$$

where: *pf_c* = percent fine content, % - 2 micron = percent smaller than 2 microns, % - No.200 sieve = percent passing No. 200 sieve.

Table 5-4: Percent fine content (*pf_c*) values are shown with depth for boring no. 1 and boring no. 2

Boring No.	%- #200	% 2 Micron	Percent Fine Content (<i>pf_c</i>)
B1-11	0.9876	43.34	43.880
B1-12	0.9993	43.76	43.789
B1-13	0.9968	48.72	48.874
B1-14	0.9839	41.24	41.910
B1-15	0.9958	41.59	41.764
B1-16	0.9967	51.27	51.438
B1-17	0.9953	42.41	42.607
B1-18	0.9972	48.19	48.322
B1-19	0.9998	41.32	41.327
B1-20	0.9956	45.43	45.629
B2-7	0.9834	45.07	45.830
B2-8	0.9946	26.06	26.199
B2-9	0.9949	45.79	46.021
B2-10	0.9995	41.97	41.988
B2-11	0.9976	46.99	47.098
B2-12	0.9980	41.16	41.239
B2-13	0.9924	41.18	41.494
B2-14	0.9974	41.18	41.286
B2-15	0.9937	47.79	48.088
B2-16	0.9949	41.54	41.752

The air entry value of soil, a_f , is formulated based on the soil *pf_c* value and given in Equation (5-8). The change in a_f with *pf_c* is given in Figure 5-5. The value of a_f increases by increasing the *pf_c*. The rate of water extraction of the soil after exceeding the air entry value, b_f , is formulated as given in Equation (5-9). The change in b_f with *pf_c* value is shown in Figure 5-6. The b_f decreases as *pf_c* value increases. The mathematical formulation for the residual water content of the soil of c_f is given in

Equation (5-10). The change in c_f with pf_c is shown in Figure 5-7. The c_f value increases by increasing the pf_c . The mathematical formulation for the suction value at which the residual water content occurs, h_r is given in Equation (5-11). The change in h_r with percent passing fine content in pf_c is shown in Figure 5-8. The h_r value increases by increasing the pf_c value.

$$a_f (\text{psi}) = 0.6384e^{0.0369 pf_c} \quad (5-8)$$

$$b_f = 11.748e^{-0.037 pf_c} \quad (5-9)$$

$$c_f = 0.126e^{0.0211 pf_c} \quad (5-10)$$

$$h_r (\text{psi}) = -0.0018 pf_c^2 + 0.5206 pf_c + 2.4305 \quad (5-11)$$

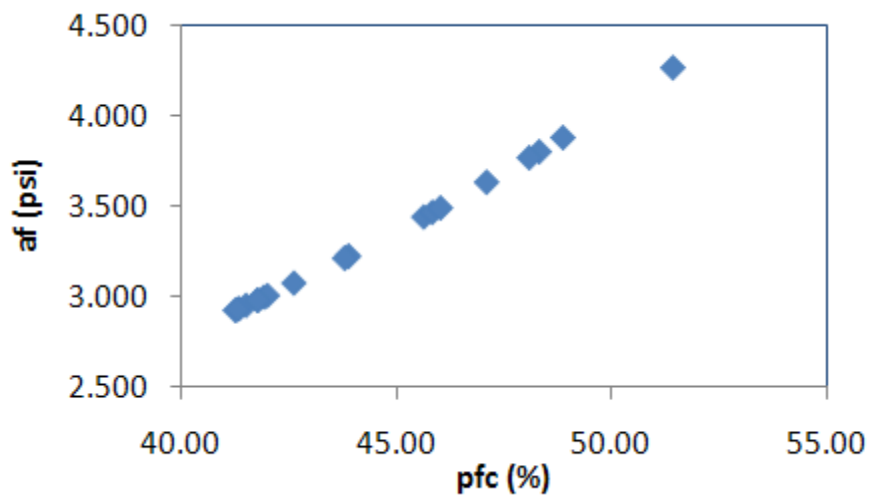


Figure 5-5: Change in a_f with pf_c percent passing fine content.

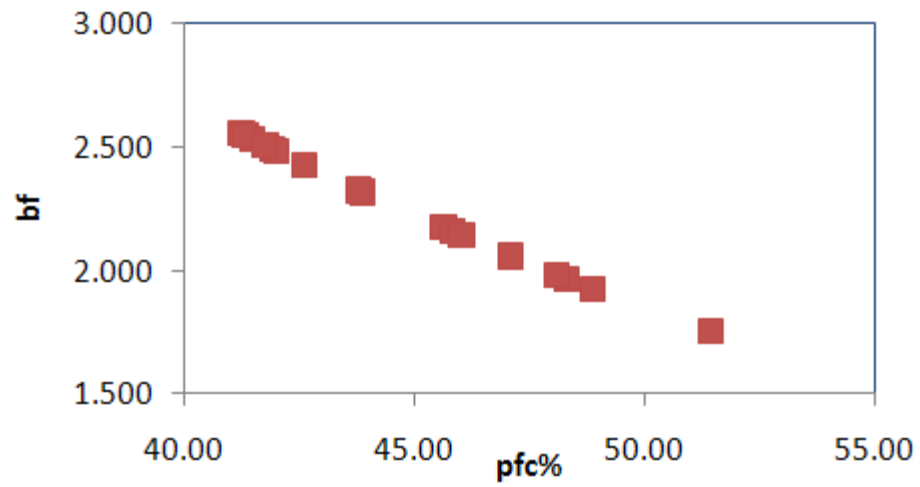


Figure 5-6: Change in b_f with pfc percent passing fine content.

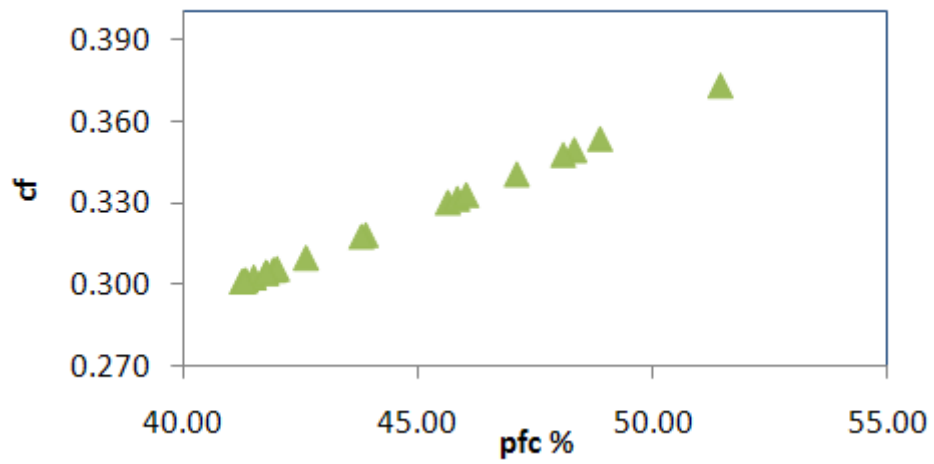


Figure 5-7: Change in c_f with pfc percent passing fine content.

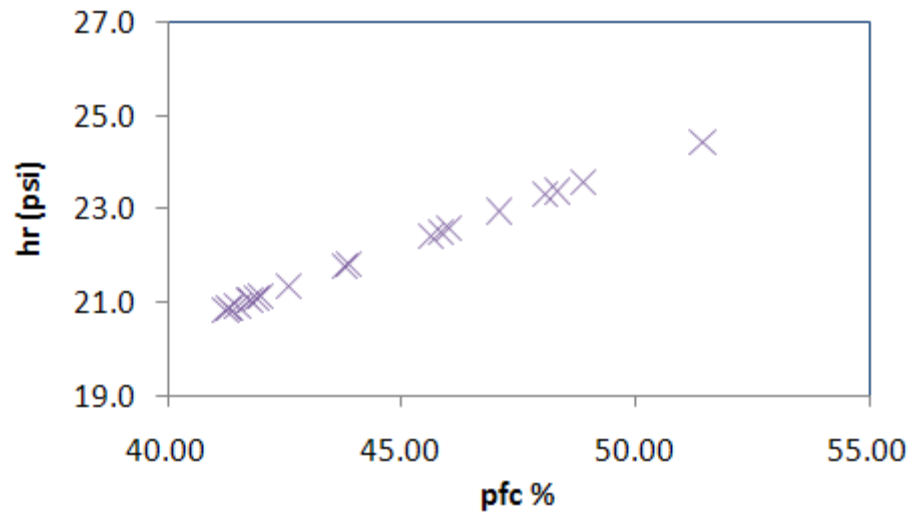


Figure 5-8: Change in h_r with pfc percent passing fine content.

The four figures above illustrate the relation between a_f , b_f , c_f , h_r and the percent fines content pfc . The parameters a_f , b_f , c_f and h_r are increased by increasing the pfc but the parameter of b_f decreases by increasing the pfc . Each data point in each figure corresponds to a soil sample that was taken from different depths. These points in figures are real values for the collected samples.

5.8 Plotting of the Soil Water Characteristic Curves

SWCC curve is generated by using the Fredlund and Xing 1994 formulation. This formulation includes the parameters of a_f , b_f , c_f and h_r that are required to be estimated. By knowing these parameters, the SWCC that is generated is in Figure 5-9.

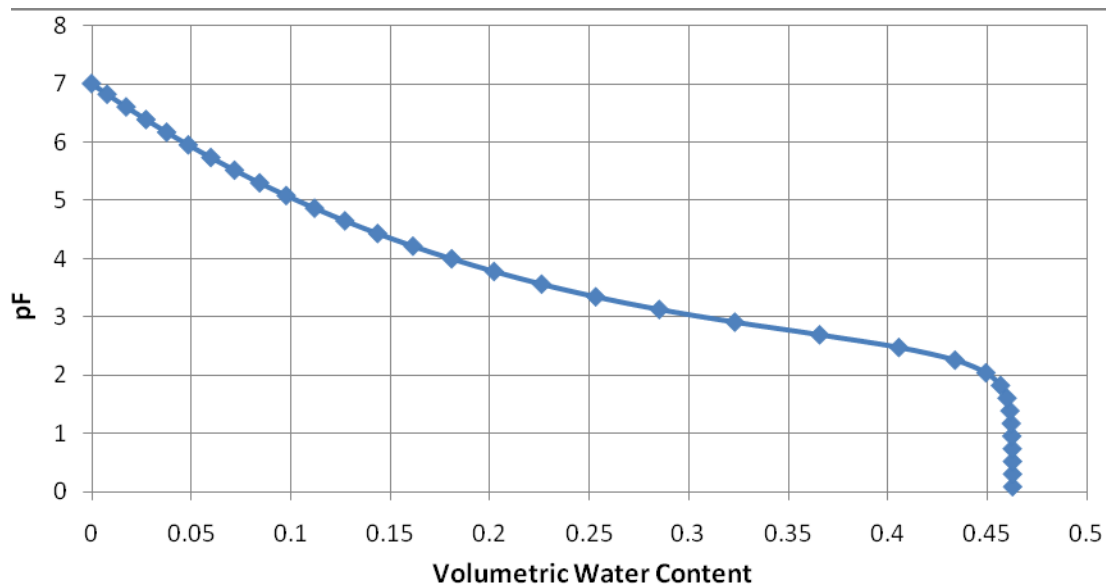


Figure 5-9: A generated Soil Water Characteristic Curve

The SWCC is highly influenced by the amount of percent fines, liquid limit, and plastic limit indexes in the soil (Zapata, 1999). Therefore, the type of the soil affects the shape of the SWCC. The slope of the SWCC significantly changes with the soil fraction of fine content. The change of slope is shown for two of the collected samples in Figure 5-10. The smallest and highest slopes are observed for samples B1-16 and B2-8, respectively. The smallest and highest slopes represent a value between collected samples.

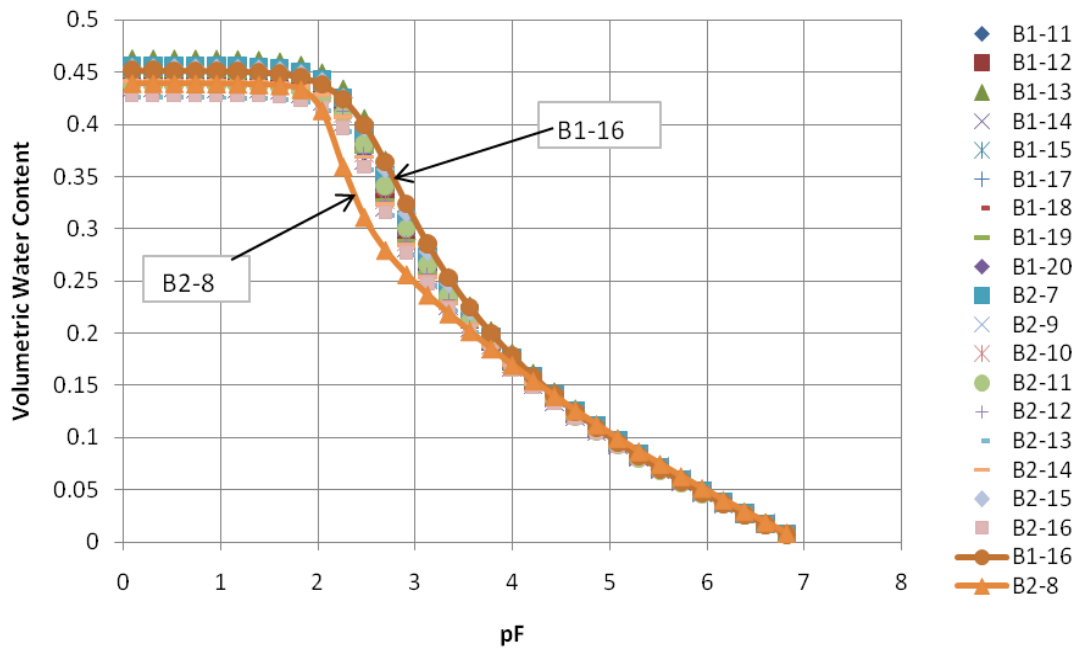


Figure 5-10: Minimum and Maximum slope of SWCC, and change of the slope by pfc .

For the purpose of the control, the parameters, empirical suction values that are determined in the laboratory are used to generate the SWCC. The suction values determined by the filter paper test and the generated SWCC are plotted in Figure 5-11. The SWCC curve and the measured suction points must plot on each other to verify that both of them are precisely determined. To illustrate this concept both the measured suction values and the generated SWCC curve are shown in Figure 5-11. The figure shows a very precise relation between the measured suction and the SWCC curve.

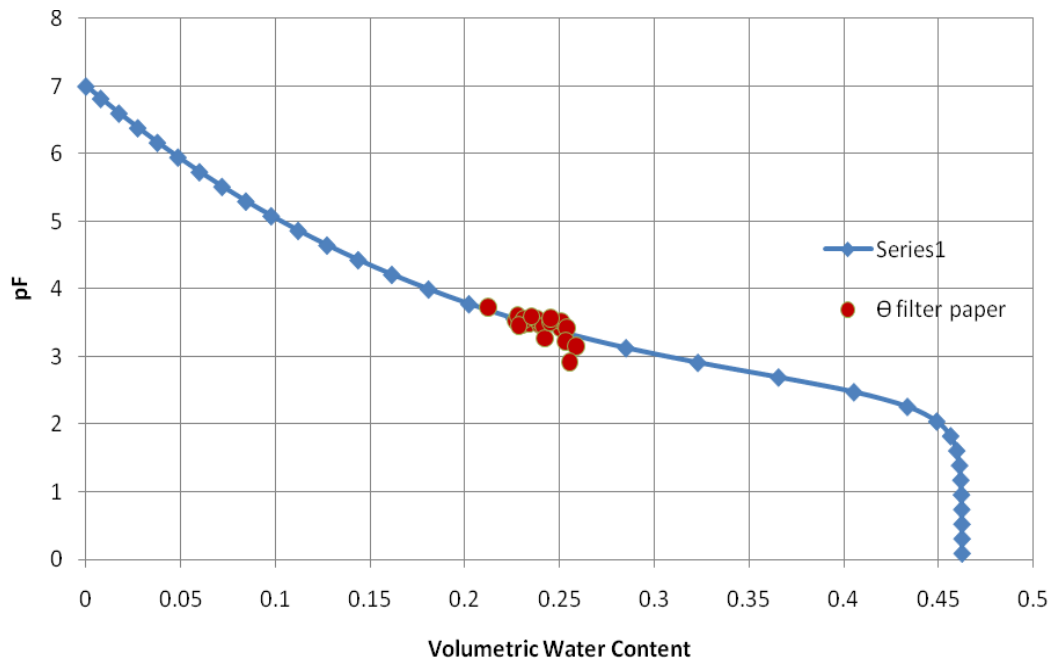


Figure 5-11: Measured suction values are fitting the SWCC

5.9 Matric Suction-Confining Pressure-Shear Strength Curves

To illustrate the relation between matric suction, confining pressure and shear strength, a 3-D plot is generated. The matric suction and shear strength relation; matric suction and confining pressure relation; and confining pressure shear strength relation are given in Figure 5-13. The figure is generated for a soil sample from boring no. 2. The figure presents these relations on a constitutive surface. Laboratory tests of unconfined compression test, filter paper test and Atterberg limit tests are utilized to generate these relations. The relations of the matric suction, shear strength and confining pressure are derived from a failure Mohr's circle in Figure 5-12, and are given in the equations as follows:

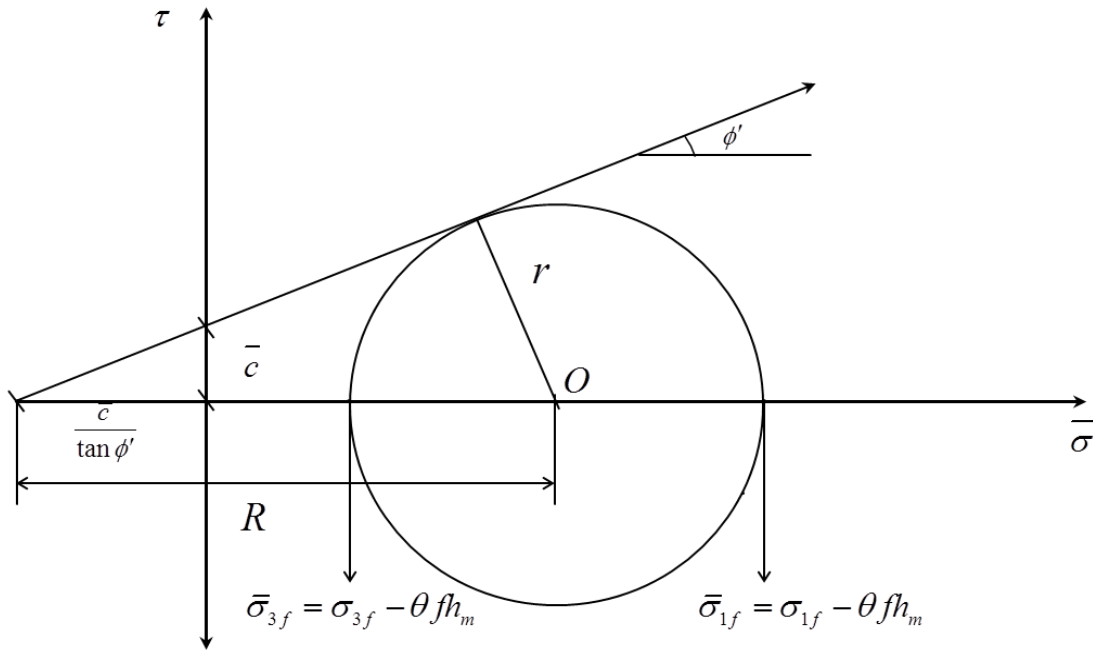


Figure 5-12: Mohr's Failure Circle and Mohr's Envelope are shown with stresses acting on it.

In an unconfined compression test, $\sigma_3 = 0$ and $\sigma_3' = \theta f h_m$

$$\frac{r}{R} = \left(\frac{\frac{\sigma_{1f} - \sigma_{3f}}{2}}{\frac{\bar{c}}{\tan \phi'} + \sigma_{3f} - \theta f h_m + \frac{\sigma_{1f} - \sigma_{3f}}{2}} \right) = \sin \phi' \quad (5-12)$$

$$\left(\frac{\sigma_{1f} - \sigma_{3f}}{2} \right) \times (1 - \sin \phi') = \bar{c} \cos \phi' + \sigma_{3f} \sin \phi' - \theta f h_m \sin \phi' \quad (5-13)$$

$$\left(\frac{\sigma_{1f} - \sigma_{3f}}{2} \right) = \left(\frac{\bar{c} \cos \phi'}{1 - \sin \phi'} \right) + \left(\frac{\sigma_{3f} - \theta f h_m}{1 - \sin \phi'} \right) \times \sin \phi' \quad (5-14)$$

$$f \cong 1 + \frac{Sr - 85}{15} \left(\frac{1}{\theta} - 1 \right) \quad (5-15)$$

If $\sigma_{3f} = 0$ from unconfined compression test

$$\left(\frac{\sigma_{1f}}{2}\right) = \bar{c} \left(\frac{\cos \phi'}{1 - \sin \phi'}\right) - \theta fhm \times \left(\frac{\sin \phi'}{1 - \sin \phi'}\right) \quad (5-16)$$

$$\bar{c} = \left(\frac{\sigma_{1f}}{2}\right) \left(\frac{1 - \sin \phi'}{\cos \phi'}\right) + (\theta fhm) \tan \phi' \quad (5-17)$$

where: \bar{c} = drained cohesive shear strength; σ_{1f} = unconfined compressive strength in the UU test; σ_{3f} = confining pressure at failure; θ = volumetric water content; $hm = -(u_a - u_w)$ $h_m = -(u_a - u_w)$ = Suction (a negative number); f = unsaturated shear strength factor ; ϕ' = effective friction angle; S_r = degree of saturation.

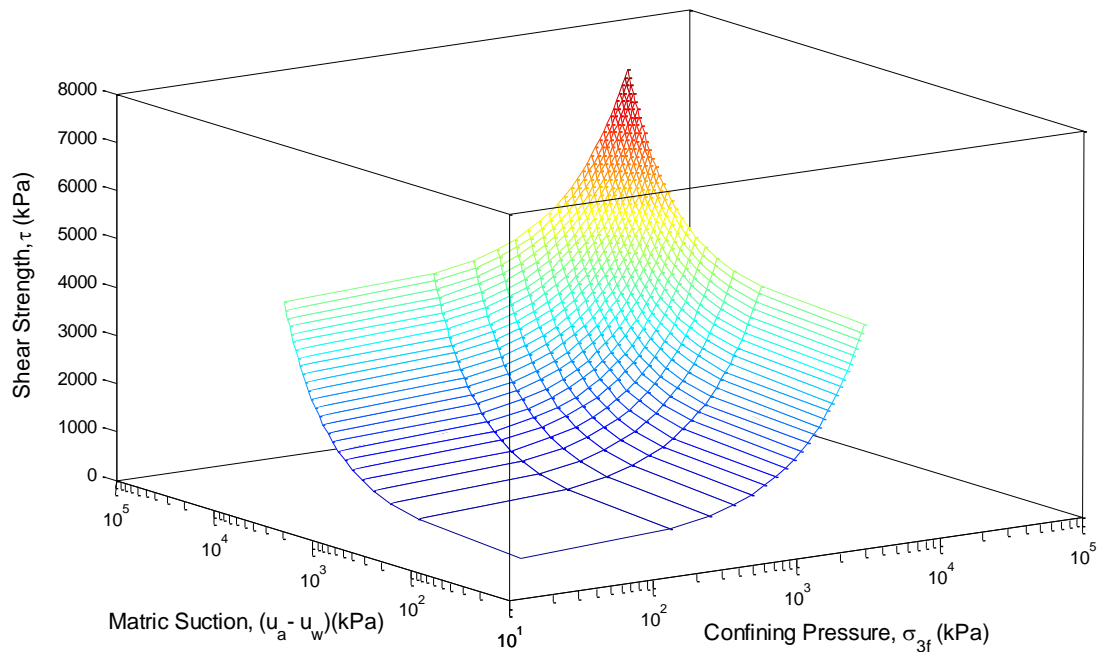


Figure 5-13: Three dimensional matric suction, shear strength and confining pressure constitutive surfaces for a soil sample on boring no.2.

Figure 5-12 shows that there is a non-linear relation for these three parameters. The matric suction and shear strength plane shows a logarithmic increase on the matric suction produces a nonlinear increase in the shear strength. The shear strength and confining pressure plane shows that there is a non-linear increase of shear strength for increasing confining pressure. The figure shows that matric suction has a significant contribution to the engineering strength properties of unsaturated soils.

5.10 Prediction of Lateral Earth Pressure against the Retaining Wall

5.10.1 Moisture Content Variation

Moisture change at the I-35 and Walter Street construction site was monitored for 18 months. To monitor suction in the field, researchers installed psychrometers to different depths in a boring. The seasonal changes in the borings are shown in Figure 5-14. The suction-water content relations that were reported earlier were used to infer the changes in water content that occurred.

Volumetric Water content shows ratio of water in soil mass and defined ratio of volume of water to total volume of a soil sample. The volumetric water content envelope is determined and shown in Figure 5-15.

The amount of seasonal precipitation and very hot and dry, atmospheric conditions directly affected the moisture content at all depths in the high plasticity soil. This seasonal precipitation directly affects the moisture content and volumetric water content. Therefore the soil at the 0 ft depth is exposed to more variation in the atmospheric condition than at deeper depths.

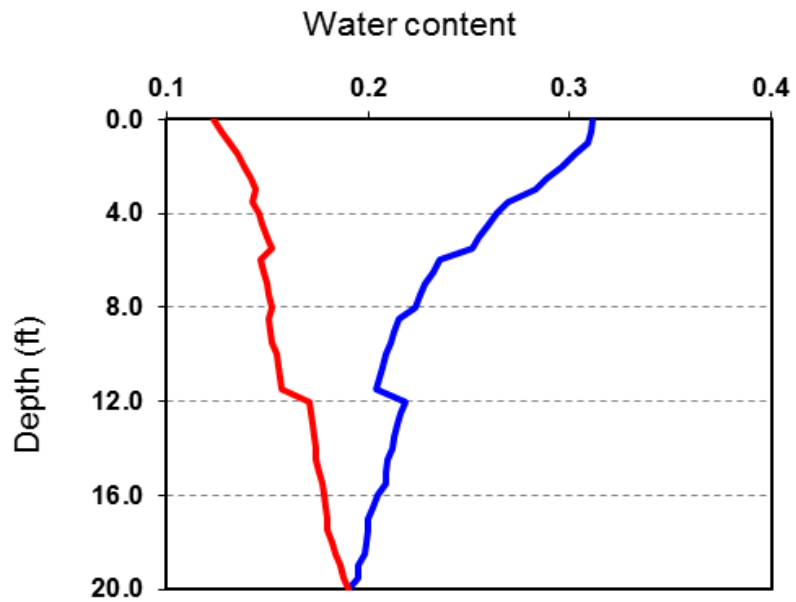


Figure 5-14: Determined moisture content profile change rate with depth

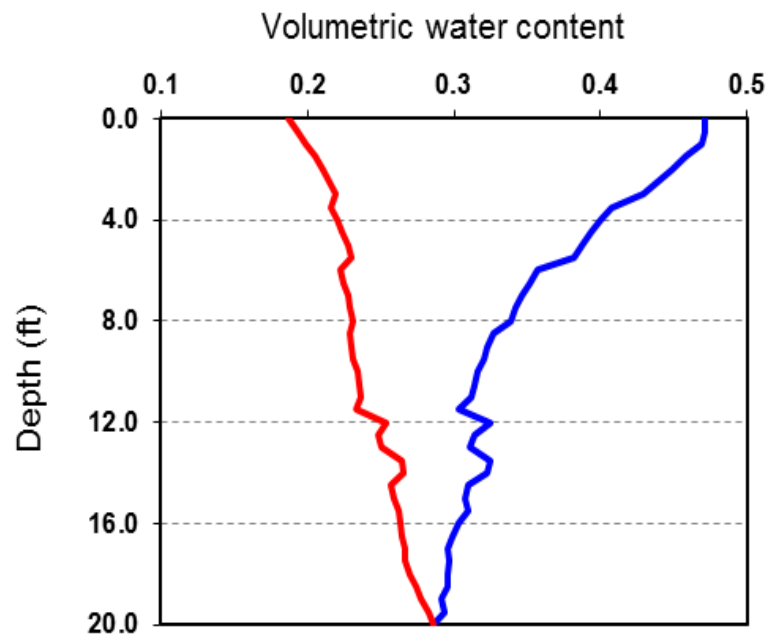


Figure 5-15: Estimated volumetric water content profile based on the moisture content

In other words, the volumetric water content is a volumetric relation between the water volume and total soil volume. Mathematical formulation of volumetric water content is represented as follows:

$$\theta = \frac{V_w}{V_t} \quad (5-18)$$

Where: θ =Volumetric water content, V_w = volume of water, V_t = total volume.

5.10.2 Suction Profile

The suction envelope defines the magnitude of seasonal suction change. The suction envelope is generated by using the data that shows the profile of seasonal moisture content changes in the soil. A generated suction envelope within all depths is shown in Figure 5-16 below.

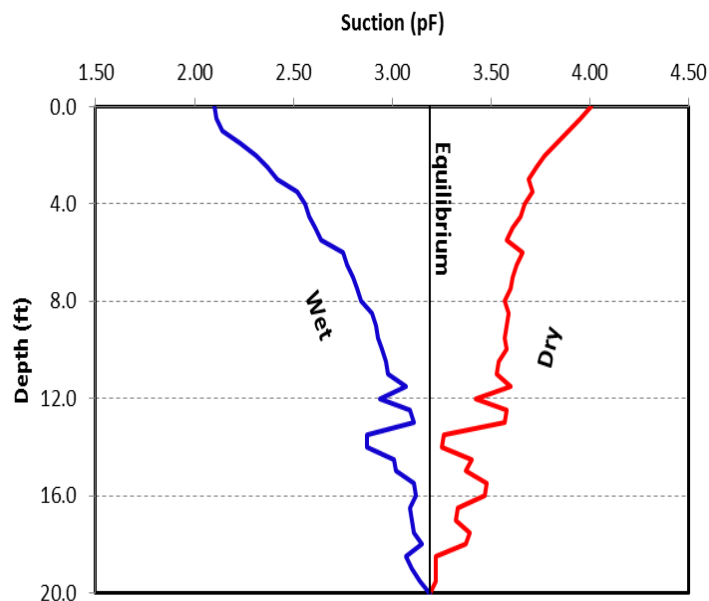


Figure 5-16: Generated suction profile that shows change in suction with depth

The suction values at the ground surface represent field capacity and wilting point. The suction value of pF 2.10 and pF 4.01 pF are field capacity and wilting point respectively. The wet side of the suction envelope defines the lower suction values, and the dry side of the suction envelope defines the higher suction values. An equilibrium suction of 3.19 pF was measured by the filter paper test in the two boreholes in samples at 10-depths.

5.10.3 Horizontal Pressure on the Retaining Wall

Horizontal and vertical stresses are determined on the retaining wall.. The vertical soil stress on the wall is determined by using the classical geotechnical method. The horizontal stress is determined based on suction change in the soil for the three zones of zone I, zone II and zone II. Zone I is the upper zone that is closest to ground the surface in which passive shear failure can occur. Zone II is the zone where passive horizontal swelling pressure occurs due to the suction change in the soil. Zone II is the deepest zone and it is influenced by moisture from water table. The determined horizontal pressure distributions and swelling pressure profile behind the retaining wall is shown in Figure 5-17.

The horizontal pressure distribution in Zone I was determined as the passive earth pressure to cause shear failure Equation (4-10) . The horizontal pressure in Zone II was determined using Equation (4-11) which comes from the change of suction at each depth. The horizontal earth pressure in Zone III is the at-rest earth pressure which is determined from Equation (4-15) using the effective friction angle. The depth at which

the maximum pressure is determined by finding at which the equations for zone I and zone II are both satisfied.

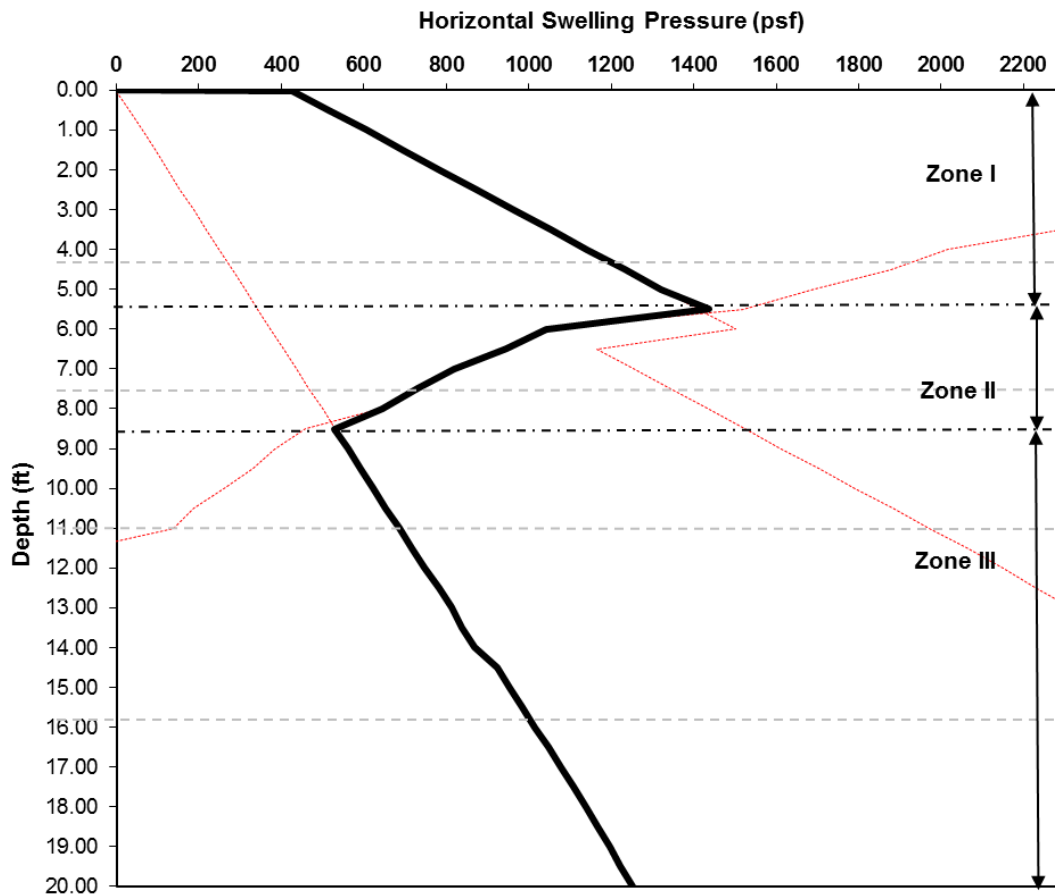


Figure 5-17: Calculated horizontal swelling pressure behind the retaining wall

The vertical stress is a function of the depth and unit weight of the soil. Thus the vertical stress is not affected by the seasonal moisture change. As shown in Figure 5-17, the vertical stress gradually increases with depth and it reaches its maximum value at the

bottom of the retaining wall. The vertical pressure is zero at the ground surface and 1253 psf at the bottom. There is a rapid change on the vertical stress between depths 10-12 ft due to fact that the unit weight of soil varies at these levels.

Horizontal stress is mainly a function of suction and volume change so it is affected by the moisture content variation during the season. The horizontal stress distribution on the wall is separately calculated for Zone I, Zone II and Zone III. It was determined that the zone I is from 0 to 5.3 ft, Zone II is form 5.3 to 8.5 ft and zone III is from 8.5 to 20 ft.

The maximum horizontal pressure exists in zone II where the seasonal change in atmospheric conditions leading to moisture infiltration occurs. The moisture change in Zone II is as shown in figure Figure 5-17, so the moisture causes the volume change and swelling pressure. A result of all these computations, it is concluded that there is strong relation between swelling pressure, horizontal pressure and matric suction changes in highly expansive soil. The relation is well represented by three-zone horizontal pressure model.

6. SUMMARY AND CONCLUSION

The study presented in this thesis includes the determination of the volume change, moisture change, and confining pressure change curve; development a model for the Fredlund and Xing SWCC equation to predict the unknown parameters; development of a new test method to determine volume measurement of soil samples; and refinement the of horizontal earth pressure prediction in three zones for expansive soil. This section summarizes the findings and methodology of the models followed by the conclusions that can be drawn.

The determination of the SWCC curve normally requires lengthy soil testing to be conducted with specialized soil equipment, and a testing program. By using the models that are presented in this study, the SWCC curve is generated in a shorter time. Also, the models utilize two fundamental soil properties that are: % – 2 *micron* (percent smaller than the 2 micron size), and % – *No.200* sieve (percent passing No. 200 sieve). The predicted SWCC curve, and the SWCC prediction models presented are useful for unsaturated soil mechanics testing and design procedures.

There are a number of methods available in the literature to determine the volume of the soil mass. However, most of them have drawbacks in terms of safety, applicability and cost. Therefore, they are not usually used by researchers. The new developed sand displacement method provides to researchers a simple, easy and inexpensive tool. The method determines a relation between the soil mass and the volume of a soil sample. The test method is utilized to determine the soil volume and the

volume change for a soil sample. The volume change curves are generated based on the sand displacement volume measurement method.

The seasonal variation of the moisture change was monitored and this change generates soil volume change pressures against a retaining wall. Volume change in the soil is the result of the soil moisture change during the seasons.

The horizontal earth pressure on a retaining wall due to suction changes is defined for expansive soil by using the three zones. The pressure increases with the depth near the ground surface where a passive shear failure occurs. But at the bottom of the wall, the lateral horizontal pressure is in the at-rest condition which is smaller than in the upper zone. The lateral pressures at depths greater than the upper zone is a function of soil suction change so the horizontal pressure varies by the amount of soil suction change.

This calculated distribution of horizontal pressure is for a retaining wall that is rigid. Any deflection of the wall away from the soil will reduce this pressure the analysis of which requires a soil-structure interaction computation. Therefore the calculated horizontal pressure distribution presented here is the maximum that will occur and as a consequence is useful for design.

REFERENCES

- Aitchison, G.D. (1965). "Soil Properties, Shear Strength and Consolidation," in Proc. 6th International Conference Soil Mechanics Foundation Engineering Montreal, Canada, vol. 3, 1965, pp. 318-321.
- ASTM D1140-00 (2006). Test Method for Amount Finer Than the No. 200 (75 μ m) Sieve, Annual Book of ASTM Standards, Sec. 4, Vol. 04.08, Soil and Rock; American Society for Testing and Materials, 2001.
- ASTM D 5298-94 (2003). Standard Test Method for Measurement of Soil Potential (Suction) Using Filter Paper, West Conshohocken, PA, USA.
- ASTM, D. 2325 (2001). Capillary-Moisture Relationship for Coarse and Medium-Textured Soils by Porous-Plate Apparatus. D2325-68, West Conshohocken, PA.
- ASTM, 3152-72 (2001). Capillary-Moisture Relationship for Fine Textured Soils by Pressure Membrane Apparatus. D3152-72, West Conshohocken, PA.
- ASTM D 2435 (2001). Standard Test Method for One-Dimensional Consolidation Properties of Soils, West Conshohocken, PA, USA.
- ASTM D 4318-00 (2001). Standard Test Methods for Liquid Limit, Plastic Limit, and Plasticity Index of Soils, West Conshohocken, PA, USA.
- ASTM D 422-63(2001). Standard Test Method for Particle -Size Analysis of Soils, West Conshohocken, PA, USA.(Reapproved 1998).
- ASTM D 4546-85 (1990). Standard test methods for one-dimensional swell or settlement potential of cohesive soils. Annual Book of ASTM Standards, vol. 04.08, pp. 846–852.

- ASTM D 2850-95 (1999). Standard Test Methods for Unconsolidated-Unconfined Triaxial Compression Test on Cohesive Soils, West Conshohocken, PA 19428, USA.
- Brackley, I.J.A. and Sanders, P.J. (1992). "In Situ Measurement of Total Natural Horizontal Stresses in an Expansive Clay." *Geotechnique* 42(2), 443-451.
- Bin-Shafique, S., Papagiannakis, A.T., Diaz, M., Lytton, R.L., and Luo, R. (2010). "Design of Cut-Type Retaining Walls in High Plasticity Soils". TxDOT/FHWA reports No 0-6375-1.
- Chen, F. H. and Huang, D. (1987). "Lateral Expansion Pressure on Basement Walls". 6th *International Conference on Expansive Soil*, New Delhi, India pp 55-59.
- Chen, F.H. (1988). *Foundations on Expansive Soils. Development in Geotechnical Engineering*. Elsevier, New York.
- Dhowian, A., Erol, A.O., and Youssef, A. (1987). "Assessment of Oedometer Methods for Heave Prediction." *Proceedings, 6th International Conference of Expansive Soils*, New Delhi, India, 99-103.
- Edlefsen, N.E. and Anderson, A.B.C. (1943). "Thermodynamics of Soil Moisture," *Hilgardia* 15(2), 31-298.
- Erol, A.O. and Ergun, U. (1994). "Lateral Swell Pressures in Expansive Soils", 8th *International Conference on Soil Mechanics and Foundation*, New Delhi, India, pp 1511-1514.
- Ertekin, Y. (1991). "Measurement of Lateral Swell Pressure with Thin Wall Oedometer Technique", MS thesis, Middle East Technical University, Turkey.

- Erzin, Y. and Erol, O. (2004). "Correlations for Quick Prediction of Swell Pressures". The Electronic Journal of Geotechnical Engineering. Available from <http://www.ejge.com/2004/Ppr0476/Ppr0476.htm> accessed May 2010.
- Fourie, A.B. (1989). "Laboratory Evaluation of Lateral Swelling Pressure." *Journal of Geotechnical Engineering, ASCE*, 115(10), 1481-1486.
- Fredlund, D.G. and Rahardjo, H. (1993). *Soil Mechanics for Unsaturated Soils*, John Wiley and Sons, Inc., New York.
- Fredlund, D. G., Xing, A., Fredlund, M. D., and Barbour, S. (1996). "The Relationship of the Unsaturated Soil Shear to The Soil-Water Characteristic Curve." *Canadian Geotechnical Journal*, 33(3), 440-448.
- FWHA (1998). "Manual for Design, Construction Monitoring Soil Nail Walls", FHWA-SA-96-069R, Department of Transportation.
- Holtz, R. D. and Kovacs, W. D. (1981). *An Introduction to Geotechnical Engineering*, Prentice-Hall, Englewood Cliffs, NJ.
- Houston, S. L., Houston, W. N., and Wagner, A. M. (1994). "Laboratory Filter Paper Measurements," *Geotechnical Testing Journal*, GTJODJ, 17(2), 185-194.
- Hong, G. T. (2008) "Earth Pressures and Deformations in Civil Infrastructure in Expansive Soils," PhD Dissertation, Texas A&M University, College Station, TX.
- Hudak, P.F.(1998). "Geologic Controls on Foundation Damage in North Central Texas". *Geojournal* 45, 159–164.
- Johnson, L.D. and Snethen, D.R.(1978). "Prediction of Potential Heave of Swelling Soil". *Geotechnical Testing Journal* 1, 117–124.

- Joshi, R.P. and Katti, R.K. (1980). "Lateral Pressure Development Under Surcharges." *Proceedings of the 4th International Conference on Expansive Soils*, Denver, CO, 227-241.
- Juarez-Badillo, E. (1986). "General Theory of Consolidation for Clays," *Consolidation of Soils: Testing and Evaluation*, ASTM STP 892, R.N. Yong and F.C. Townsend, Eds.
- Juarez-Badillo, E. (1987), "Mechanical Characterization of Mexico City Clay," *Journal.Unknown (Personal Copy)*. pp.65-69.
- Kehew, E.A. (1995). "*Geology for Engineers and Environmental Scientists*", 2nd ed. Prentice Hall Englewood Cliffs, New Jersey.
- Komornik, A. (1962). "The Effect of Swelling Properties of Unsaturated Clay on Pile Foundations." D.Sc. Thesis, Israel Institute of Technology, Technion.
- Komornik, A. and Zeitlen, J.G. (1973). "Effect of Swelling Clay on Piles." *Proceedings of the Eight International Conference on Soil Mechanics and Foundation Engineering*, Moscow, USSR, 123-128.
- Lee, H. C. (1991). "An Evaluation of Instruments to Measure Soil Moisture Condition," M.Sc. Thesis, Texas Tech University, Lubbock, Texas.
- Lu, N. and Likos, W.J.(2004). *Unsaturated Soil Mechanics*, John Wiley & Sons, Inc., New York.
- Lytton, R.L. (1977). "The Characterization of Expansive Soils in Engineering." *Presentation at the Symposium on Water Movement and Equilibria in Swelling Soils*, American Geophysical Union, San Francisco, CA.

- Lytton, R.L. (1995). "Foundations and Pavements on Unsaturated Soils." *Proceedings of the 1st International Conference on Unsaturated Soils*, Paris, France, 3, 1201-1220.
- Lytton, R.L., (1994). "Prediction of Movement in Expansive Clay." *Geotechnical Special Publication*, No. 40, ASCE, NY, 2, 1827-1845.
- Lytton, R., Aubeny, C., and Bulut, R. (2004). "Design Procedure for Pavement on Expansive Soils", Volume 1, Report No. FHWA/TX-05/0-4518-1.
- Lytton, R., Aubeny, C., and Bulut, R. (2004). "Design Procedure for Pavement on Expansive Soils", Volume 2, Report No. FHWA/TX-05/0-4518-1.
- Mason, J.G., Ollayos, C.W., Guymo, G.L., and Berg, R.L. (1986). "User's Guide for the Mathematical Model of Frost Heave and Thaw Settlement in Pavements." US Army Cold Region Research and Engineering Laboratory, Hanover, NH.
- Mitchell, J.K. (1993). *Fundamentals of Soil Behavior*, 2nd edition. Wiley Press, New York.
- Nelson, J.D. and Miller, J. D. (1992). *Expansive Soils, Problems and Practice in Foundation and Pavement Engineering*. Wiley Press, New York.
- New Mexico State University, Pressure Plate, web online source date as of on June 2010
http://weather.nmsu.edu/teaching_material/soil698/Student_Material/pressureplate/Performance.htm
- Ofer, Z. (1980). "Instruments for Laboratory and In-Situ Measurements of Lateral Swelling Pressure of Expansive Clays," *Proceedings of the 4th International Conference on Expansive Soils*, Denver, pp 45-53

- Perera, Y.Y., Zapata, C.E., Houston, W.N., Houston, S.L. (2005). "Prediction of the Soil-Water Characteristic Curve Based on Grain-Size-Distribution and Index Properties." *Proceeding of Geo-Frontiers 2005*, Austin, Texas, January 24-26.
- Ruwaih, I.A., (1987). "Experiences with expansive soils in Saudi Arabia." *Proceedings of the 6th International Conference on Expansive Soils*, New Delhi, India, pp. 317–322.
- Thakur, B. A. (2005). "Determination of Diffusion Coefficient Through Laboratory Tests and Analytically Validating It Using Empirical Relations for Unsaturated Soils," MS Thesis, Texas A&M University, College Station, TX, August 2005.
- Sapaz, B. (2004). "Lateral vs. Vertical Swell Pressure in Expansive Soils," MS thesis, Middle East Technical University, Turkey.
- Snethen, D.R., (1980). "Characterization of Expansive Soils Using Soil Suction Data," *Proceedings of the 4th International Conference on Expansive Soils, Boulder, Colorado*, pp. 18–23.
- Schofield, R. K. (1935). "The pF of the Water in Soil," *Transactions, 3rd International Congress of Soil Science*, 2, 37-48.
- Sillers, W.S., Fredlund, D.G. and Zakerzadeh, N. (2001). "Mathematical attributes of Some Soil–Water Characteristic Curve Models." *Geotechnical and Geological Engineering* 19 (3–4), 243–283.
- Soil Moisture Equipment Corporation: 15 Bar Pressure Plate Extractor Operating Instructor, Soil Moisture Equipment Corporation, Santa Barbara California, USA..<http://www.personal.psu.edu/users/s/z/szw138/Soil%20mechanics%20Lab/Lab%203.pdf> .in June 2009(a).

Soil Moisture Equipment Corporation; Pressure Plate Extractor Operating Instructor, Soil Moisture Equipment Corporation, Santa Barbara California, USA. Electronic source: <http://www.soilmoisture.com/pdf/1500F1.pdf> in June 2009(b).

Soil Moisture Equipment Corporation; Pressure Plate Set Up in the Laboratory, Soil Moisture Equipment Corporation, Santa Barbara California, USA. Electronic source: <http://www.soilmoisture.com/PDF%20Files/Lab023setup.pdf> in June 2009(c).

TxDOT (2001). "Bridge Design Manual," Texas Department of Transportation (TxDOT)

TxDOT (2006). "Geotechnical Manual," Texas Department of Transportation (TxDOT)

Vanapalli, S., Fredlund, D., Pufahl, D. and Clifton, A. (1996). "Model for the Prediction of Shear Strength with Respect to Soil Suction." *Canadian Geotechnical Journal*, 33(3), 379-392.

Yeager, M.S. and Slowey, N.C. (1996). "A New Method for Measuring the Bulk Volume of Small Rock Samples for Determinations of Porosity and Mass Accumulation Rates". *Journal of Sedimentary Research, Section A: Sedimentary Petrology and Processes* 66 (5), 1036-1039.

Zapata, C. E. (1999). "Uncertainty in Soil-Water-Characteristic Curve and Impacts on Unsaturated Shear Strength Predictions." Ph.D. Dissertation, Arizona State University, Tempe, AZ.

Zapata, C. E. (2010). "A National Catalog of Subgrade Soil-Water Characteristic Curve (SWCC) Default Inputs for Use with the MEPDG," The National Cooperative Highway Research Program (NCHRP), NCHRP Report 9-23A, Arizona State University, Temple, AZ.

Windal, T. and Shahrour, I. (2002). "Study of the Swelling Behavior of a Compacted Soil Using Flexible Odometer." *Mechanics Research Communications*, 29(5), 375-382.

APPENDIX

1. Liquid Limit Test

A brass cup drops onto a base surface from a height of 1.0 cm by operating a crank. For the liquid limit test, a soil is placed in the cup, and then the soil is cut in half by a standard grooving tool. Next, the crank is turned and the cup is lifted and dropped from a height of 10 mm until the soil groove is closed and each side of the soil touches 12.7 mm along the bottom of the cup. The moisture content at the 25th drop is defined as the liquid limit. The details of the liquid limit test procedure are given in the ASTM D 4318-00.

1.1. Test Apparatus

Liquid limit test devices tools that are used for the experiment are described below.

1. Liquid Limit Device: A mechanical device consisting of a brass cup suspended from a carriage designed to control its drops onto a hard rubber base. The device is operated by a hand crank.
2. Base: A hard rubber base having a Type D Durometer hardness of 80 to 90, and a resilience rebound of at least 77% but, no more than 90%.
3. Rubber Feet: Supporting the base, designed to provide isolation of the base from the surface and having a Type A Durometer hardness no greater than 60 as measured on the finished feet attached to the base.

4. Cam: Designed to raise the cup smoothly and continuously to its maximum height, over a distance of at least 180° of cam rotation, without developing an upward or downward velocity of the cup when the cam follower leaves the cam.
5. Carriage: Constructed in a way that allows a convenient but secure adjustment of the height-of-drop of the cup to 10 mm (0.394 in.), and designed such in a way that the cup and hanger assembly is only attached to the carriage by means of a removable pin.
6. Flat Grooving Tool: A tool made of plastic or non-corroding-metal having the dimensions. And the design of the tool may vary.
7. Gage: A metal gage blocks for the adjustment of the height-of-drop of the cup. The design of the tool may vary. Providing the gage will allow to test securely on the base without being susceptible for rocking. The edge which contacts the cup during adjustments should be straight at least 10 mm (3/8 in.) wide, without a bevel or radius.
8. Water Content Containers: Small corrosion-resistant containers with snug-fitting lids for water content specimens. Aluminum or stainless steel cans with the measurements of 2.5 cm (1 in.) high by 5 cm (2 in.) in diameter are sufficient.
9. Mixing and Storage Container: A container to mix the soil specimen (material) and to store the prepared material. During the time of the mixing and storage, the container shall not contaminate the material in any way, and

should prevent moisture loss during the time of storage. A porcelain, glass, or plastic dish about 11.4 cm (4 ½ in.) in diameter and a plastic bag large enough to enclose the dish should be folded over the dish adequately.

1.2. Test Procedure

1. Mix the soil thoroughly with distilled water which is almost the same texture as peanut butter. It is easy to add water to the mixture rather than taking it out, so it should be better to start the test from the hardness soil mix rather than the loose soil mix.
2. Take a portion of the soil from the mix with a spatula, and spread it into the liquid limit bowl. The maximum thickness of the soils layer must be 10 mm in the bowl.
3. Eliminate the air bubbles on the soils layer and remove the excess soil particles from the inside or from the top of the soils surface.
4. Make a groove path like letter “V” by using the flat grooving tool. When the path is opening from one side to the opposite side, the grooving tool must be held perpendicularly to the liquid limit bowl.
5. Drop the bowl from a height of 1 cm by operating the crank. The bowl must be dropped on the base surface rate with an estimation of two drops per second.
6. Drop the bowl until the two sides are closed and touching each other along the side of 1.27 cm (½ inch).
7. Record the number of drop as the grove is closed by the drops.

8. Remove a portion of the soil where the groove is closed. Put it into a can and weigh them as a wet sample plus can.
9. Eliminate the liquid limit device bowl and clean the inside of it.
10. Increase the water content of the mixed soil by adding more distilled water in it, and then remix it once again.
11. Repeat the step 2 to 7 times, since the water ratio is higher in the new soil mix, the number of drops must be less. In other words, the amount of water in the mixer and the number of bowl drops have an opposite ratio.
12. Repeat this process, the number of drops must be between 15 to 35. One for closure between 20 and 30, another closure requires 15 to 25.
13. Put the sample into a thermostatically controlled oven and keep them in there approximately for 12 hours to obtain the weight of a dry sample and the water content of the soil.

The calculation of the Plasticity Index is given as

$$PI = LL - PL \quad (1)$$

where;

LL, Liquid limit (a water content percentage value)

PL, Plastic limit (a water content percentage value)

1.3. Test Results

Table A-1: Liquid Limit Test Results for boring no 1.

Boring no.	Depth (ft)	Liquid limit (%)
B1-11	10-11	57.68
B1-12	11-12	59.46
B1-13	12-13	62.47
B1-14	13-14	55.41
B1-15	14-15	58.35
B1-16	15-16	59.19
B1-17	16-17	58.66
B1-18	17-18	58.84
B1-19	18-19	57.84
B1-20	19-20	56.48

Table A-2: Liquid Limit Test Results for boring no 2.

Boring no.	Depth (ft)	Liquid limit (%)
B2-7	10-11	60.75
B2-8	11-12	54.98
B2-9	12-13	57.88
B2-10	13-14	57.14
B2-11	14-15	55.54
B2-12	15-16	56.75
B2-13	16-17	53.49
B2-14	17-18	55.14
B2-15	18-19	60.03
B2-16	19-20	51.88

2. Plastic Limit Test

2.1. Test Apparatus

Plastic limit test devices tools that are used for the experiment are described below.

1. Ground Glass Plate: A ground glass plate at least 30 cm (12 in.) square by 1 cm (3/8 in.) thick for the rolling of plastic limit threads.
2. Spatula: A spatula or pill knife having a blade about 2 cm (3/4 in.) wide, and about 10 to 13 cm (3 to 4 in.) long.
3. Sieve(s): A 200-mm (8 in.) diameter, 425- μm (No. 40) sieve conforming to the requirements of Specification E11 and having a rim at least 5 cm (2 in.) above the mesh. A 2.00-mm (No. 10) sieve that meets the same requirements may also be needed.
4. Wash Bottle or a similar container for adding controlled amounts of water to the soil and washing fines from the coarse particles.
5. Drying oven, thermostatically controlled, preferably of the forced-draft type, capable of a continuous] temperature of $110 \pm 5^{\circ}\text{C}$ ($230 \pm 9^{\circ}\text{F}$) throughout the drying chamber.
6. Washing pan round, flat-bottomed, at least 7.6 cm (3 in.) deep and slightly larger at the bottom than a 20.3-cm (8-in.) diameter sieve.
7. Pure water, where distilled water is referred to in this test method, either distilled or demineralized water may be used.

2.2. Test Procedure

1. Take a portion of around 20 g of the prepared sample for the liquid limit test.
2. Reduce to the water content of the sample. To reduce the water content do not put the samples into an oven or microwave. If soil is not sticking to ones hand, it is ready for the plastic limit test.
3. Take a sample portion of 1.5 to 2.0 g and make a round (ball) shape.
4. Roll the round shape samples between the palm or finger and the ground glass plate in order to make the same diameter along the sample thread.
5. Keep rolling the soil thread until it reaches to 3 mm in diameter.
6. If the soil threads brake before the diameter reaches 3 mm , 3.3 mm or 3.5 mm, you need to make a ball round shape again.
7. When the soil thread reaches 3 mm in diameter, it should break in to small pieces.
8. During the rolling process, you should apply the same pressure on the soil thread. The cause of the breakings into small pieces must be the lower water content not hand pressure.
9. Collect the small pieces of soil and put them into a can
10. Repeat the steps 3 to 9 times to get at least 6 g of soil. Record the weight as the mass of the wet sample plus can.
11. Put the sample into a thermostatically controlled oven. Keep them in there for about 12 hours to obtain the dry sample and then the water content of the soil.

2.3. Test Results

Table A-3: Plastic Limit, Liquid Limit, Plasticity Index and Related Test Results for boring no 1.

Boring no	Depth (ft) (ft)	LL (%)	PL (%)	PI (%)	Φ' Degree	γ^t kN/m ³	Water Content (%)	Ssat (%)	Qsat
B1-11	10-11	57.68	22.61	35.07	27.58	18.44	23.99	83.78	0.4908
B1-12	11-12	59.46	21.83	37.63	27.10	18.25	25.10	83.85	0.5007
B1-13	12-13	62.47	20.85	41.62	26.41	18.01	26.56	83.93	0.5131
B1-14	13-14	55.41	21.02	34.39	27.71	18.50	23.69	83.76	0.4880
B1-15	14-15	58.35	19.16	39.19	26.83	18.16	25.63	83.88	0.5053
B1-16	15-16	59.19	20.65	38.54	26.94	18.20	25.40	83.87	0.5033
B1-17	16-17	58.66	20.09	38.57	26.94	18.20	25.39	83.87	0.5032
B1-18	17-18	58.84	20.78	38.06	27.03	18.23	25.23	83.86	0.5018
B1-19	18-19	57.84	20.72	37.12	27.20	18.28	24.92	83.84	0.4991
B1-20	19-20	56.48	20.32	36.16	27.38	18.36	24.50	83.81	0.4954

Table A-4: Plastic Limit, Liquid Limit, Plasticity Index and Related Test Results for boring no 2.

Boring no	Depth (ft) (ft)	LL (%)	PL (%)	PI (%)	Φ' Degree	γ_t kN/m ³	Water Content	Ssat (%)	Qsat
B2-7	10-11	60.75	20.5	40.25	23.760	21.5	25.840	83.89	0.5071
B2-8	11-12	54.98	19.69	35.29	24.435	22.25	24.161	83.79	0.4923
B2-9	12-13	57.88	20.8	37.08	24.083	22.19	24.832	83.83	0.4983
B2-10	13-14	57.14	20.85	36.29	24.170	21.56	24.600	83.82	0.4963
B2-11	14-15	55.54	20.74	34.8	24.365	21.05	24.017	83.78	0.4910
B2-12	15-16	56.75	19.84	36.91	24.217	22.15	24.812	83.83	0.4982
B2-13	16-17	53.49	21.74	31.75	24.627	23.64	22.813	83.70	0.4799
B2-14	17-18	55.14	19.49	35.65	24.415	22.22	24.332	83.80	0.4939
B2-15	18-19	60.03	20.43	39.6	23.839	21.39	25.755	83.89	0.5064
B2-16	19-20	51.88	19.49	32.39	24.842	22.66	23.082	83.72	0.4824

3. Hydrometer Analysis Test

3.1. Test Apparatus

1. Oven: A thermostatically controlled oven capable of maintaining a temperature of 230 ± 9 ° F (110 ± 5 °C) for drying the hydrometer analysis samples.
2. Balances: A balance sensitive to 0.01 g for weighing the material passing a No. 10 (2.00 mm) sieve, and a balance sensitive to 0.1% of the mass of the sample to be weighed for weighing the material retained on a No. 10 sieve.
3. Stirring apparatus: A mechanical operated stirring apparatus for mixing the soil slurry. The stirring apparatus consists of an electric motor capable of turning a vertical shaft with speed of no less than 10, 00 rpm without load.
4. Hydrometer: An ASTM hydrometer, graduated to read in either specific gravity of the suspension or grams per liter of suspension, and conforming to the requirements of hydrometer 152H in specifications E 100.
5. Sedimentation cylinder: A glass cylinder essentially 18 in. (457 mm) in height and $2 \frac{1}{2}$ in. (63.5) in diameter, and marked for a volume of 1000-mL marks is 36 ± 2 cm from the bottom on the inside.
6. Thermometer: A thermometer accurate to 0.5 ° C.
8. Sieve: A series of sieves as given in Table A-5 of square-mesh woven-wire cloth, conforming to the requirements of specification 11.

Table A-5: A full set of sieves includes the following sieves

Sieve Number and Opening (mm)	Sieve Number and Opening (mm)
3-in. (75-mm)	No.16 (1.18-mm)
1 ½ - in. (37.5-mm)	No.16 (1.18-mm)
¾ - in. (19.0-mm)	No.30(600-µm)
3/8-in. (9.5-mm)	No.50 (300- µm)
No. 4 (4.75-mm)	No. 100 (150- µm)
No.8 (2.36-mm)	No. 200 (75- µm)

9. Water bath: A water bath for maintaining the soil suspension at a constant temperature during the hydrometer analysis. A satisfactory water tank is an insulated tank that maintains temperature of the suspension at a convenient constant temperature at or near 68° F (20°C).

10. Beaker and watch glass: Capacity of 0.5 pt. (=250 mL) beaker and a watch glass large enough to cover over the beaker.

13. Distilled water: A supply of approximately 1.1 qt (1L) of distilled water per sample to be tested.

14. Water dispenser: A dispenser for distilled water to wash the container when transferring the hydrometer analysis sample from one container to another.

15. Container: A sealable container for storing distilled water at room temperature.

16. Sodium hexametaphosphate crystals (NaPO₃)₆: A supply of purified sodium hexametaphosphate for preparing the dispersing agent.

17. Magnetic Stirring Apparatus: A stirring apparatus for mixing the dispersing agent.

18. Beaker: A beaker in which to mix the dispersing agent.

19. Storage Container: A large, sealable glass container for storing the dispersing agent.

3.2. Test Procedure

This procedure describes that more than 90 percent fine soil is passed from sieve No. 200.

1. Take out nearly 50 g. of the oven dry sample out of the oven.
2. Weigh 40 g of sodium hexametaphosphate as a deflocculating agent that is usually 4% of the 1000 cc distilled water, and mix them thoroughly.
3. Take a beaker and place the dry sample (step 1) and 125 cc prepared mixture (step 2). Leave the beaker sitting for about 8 to 12 hours to soak.
4. Take a 1000 cc cylinder first; pour the mixture (in step 3) into the cylinder and then fill up the rest of the cylinder with 875 cc of distilled water.
5. Record the temperature of the cylinder water-solution.
6. Put the hydrometer in the cylinder and record the readings. The readings should be taken from the top of the meniscus.
7. Mix the solution prepared (in Step 3) by using a spatula because the soil particles can stick to each other.
8. Pour the solution into a mixer cup and fill 2/3 of it with distilled water. Mix the solution thoroughly by means of a mixture within 2 minutes.

9. Pour the mixed solution into a 1000 cc cylinder. If there is some soil inside of the mixtures cup, then wash the inside of it well and pour it back into the cylinder.
10. Close the cylinder top by hand and mix the soil-water solution for 1 minute by turning it upside down
11. After mixing the solution, record the time immediately. This cumulative time is $t=0$. At this time insert the hydrometer in the soil-water suspension.
12. Take readings at 0.25, 1, 1.5, and 2, minutes from the top of the meniscus. During the 2 minutes let the hydrometer hold in the suspension.
13. After two minutes, take the hydrometer from the solution and leave it in the water bath (in step 5).
14. Take the hydrometer from the water bath and take readings for 5, 15, 30, 60, 250, and 1440 minutes. The readings should always be taken from the top of the meniscus.
15. After the readings are taken, put the hydrometer in the water bath.

3.3. Test Results

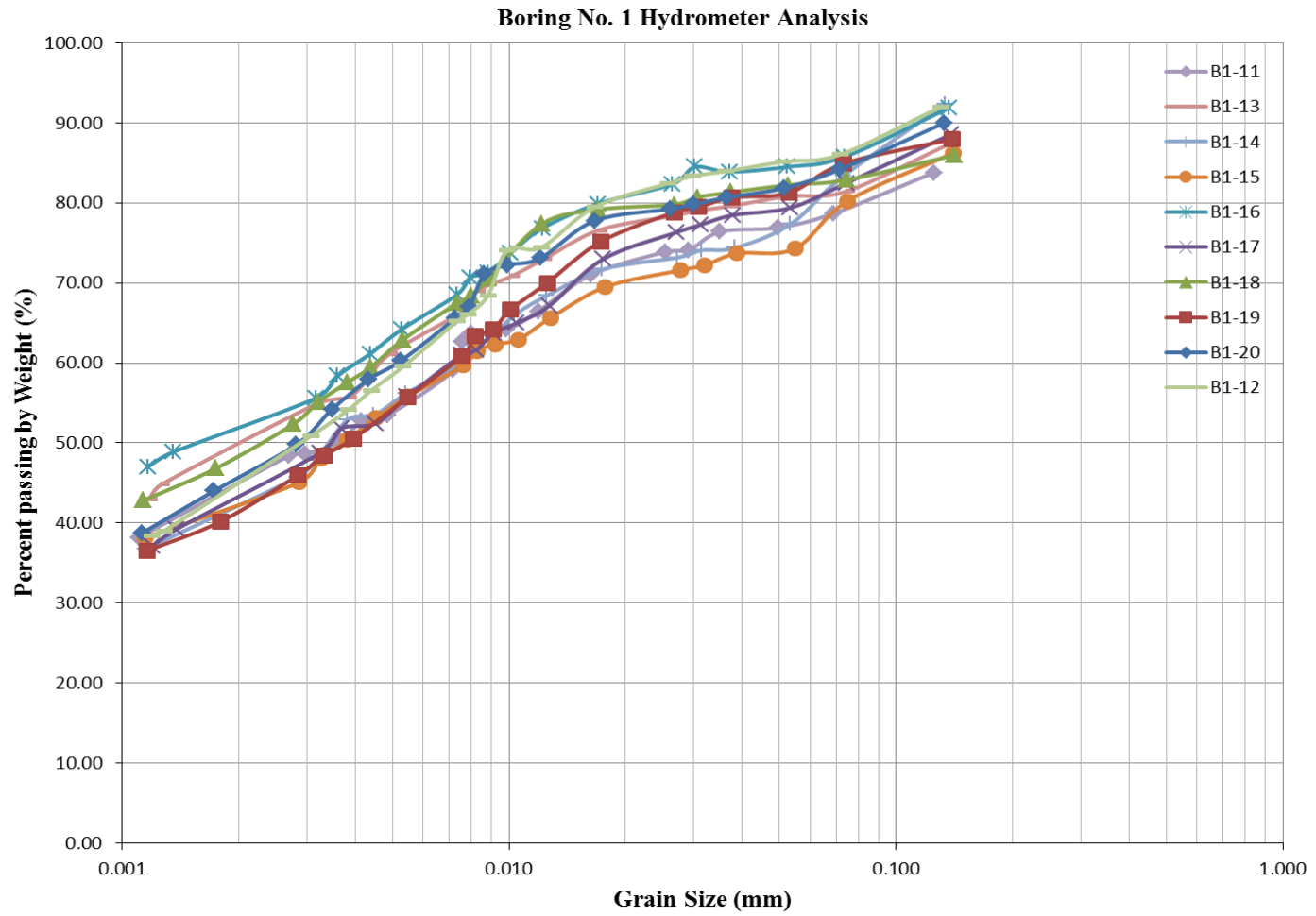


Figure A-1 Hydrometer test results of boring no1 all depths are together

Hydrometer Analysis Boring # 2

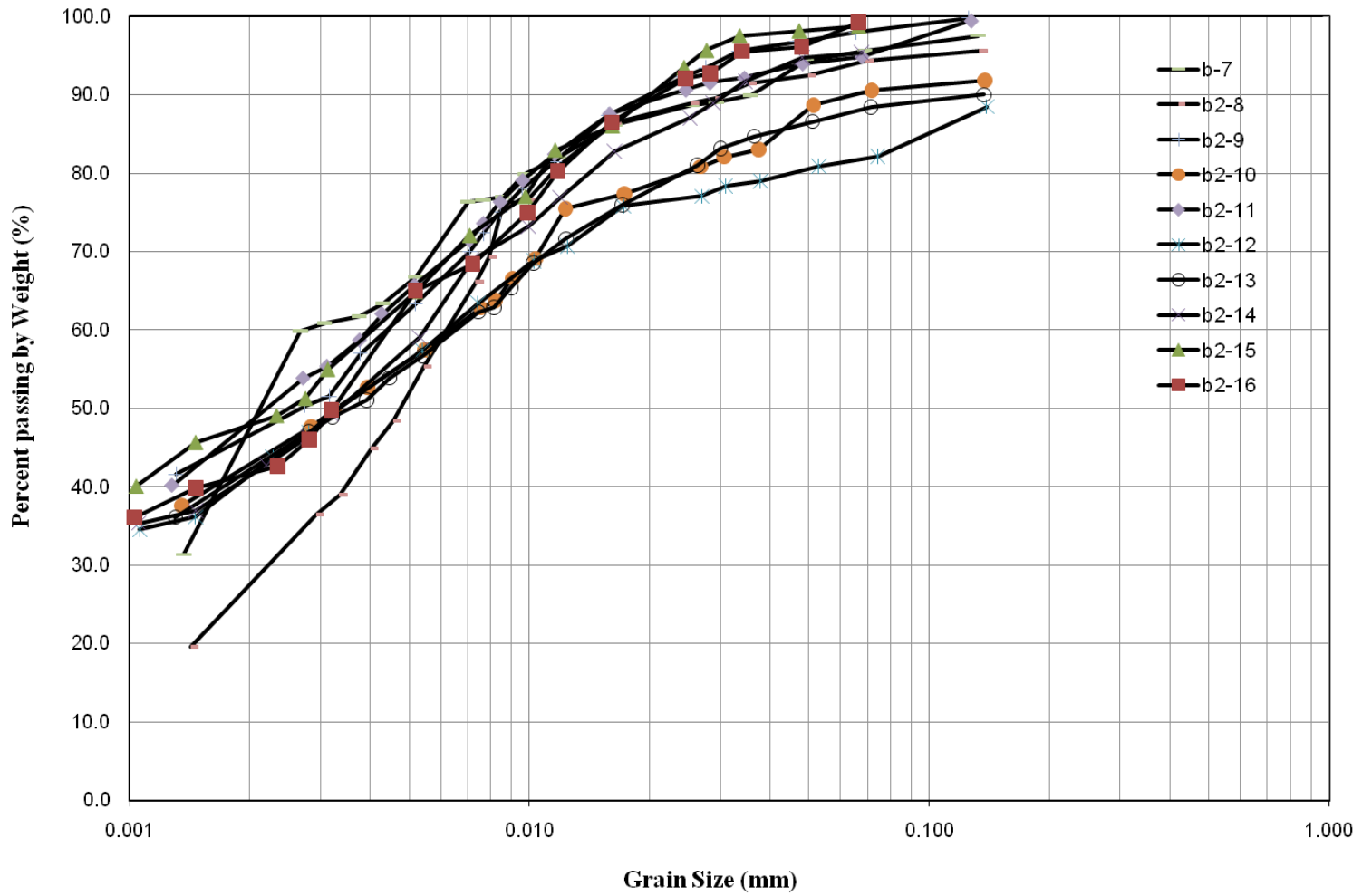


Figure A-2: Hydrometer test results of boring no 2 all depths are together

4. Wet Sieve Analysis Test

4.1. Test Apparatus

1. Balance: A balance or scale conforming to the requirements readable to 0.1 % of the test mass, are more accurate.
2. Sieves: A nest of six sieves are used, the lower was a 75- μm (No. 200) sieve and the upper five are (No. 80), 425- μm (No. 40), a (No. 20), a (No. 10), and a (No. 4). A stainless sieve mesh is preferred, as it is less prone to damage or wear out from the 75- μm sieve and other sieves as well.
3. Oven: An oven that maintains a uniform temperature of $100 \pm 5^\circ\text{C}$ ($230 \pm 9^\circ\text{F}$) capable enough for the heat for the sieves.
4. Deflocculating Agent: A Sodium Hexametaphosphate solution, which causes particle separation with an amount of 40 g per 1000 mL of water.
5. Glass Jar: Volume sizes are nearly 500 ml, which are capable of holding enough solution and samples.
6. Stirring Apparatus: An apparatus that mixes the soil sample and the deflocculating agent solution thoroughly and mechanically that operates by turning a vertical shaft.

4.2. Test Procedure

1. Take out approximately 50 g. of the sample which is the natural water content. Determine the mass of the sample nearest to 0.1 g.

2. Prepare the deflocculating agent solution with an amount of 40 g. per 1000 ml.
3. Place the sample into a jar after recording its mass to the data sheet.
4. Add the sample to the deflocculating agent solution of an amount of 250 ml.
5. Allow the sample to stay in the solution for a minimum of 12 hours before mixing.
6. Mix the solution after 12 hours by using the stirring apparatus with a medium speed for one minute to disperse adhered soil particles. It should turn out to be a slurry mixture.
7. Weigh and record a set of dry sieves No. 4, No. 10, No.20, No. 40, No. 80, and No. 200.
8. Nest the sieves in order of decreasing size No. 4, No. 10, No.20, No. 40, No. 80, and No. 200. The smallest size would be at the bottom and the biggest size would be at the top.
9. Place the sieve in a sink, and then dip the slurry mixture solution very carefully into the sieve.
10. Wash the slurry solution by means of slow median temperature stream water, and during this process be careful to not lose any of the retaining soil. Also by lightly manipulating the soil by hand may help the water pass through the sieve, however do not push the sample downwards.
11. The washing process should continue until the water color turns clear.

12. Place each sieve in to the oven at a temperature of $100 \pm 5^{\circ}\text{C}$. Keep them in the oven for a minimum of 10 hours.
13. Take out the sieve and determine the weight of each sieve, but before doing so, allow the sieve to cool down until a uniform temperature. At this weighing process make sure to not lose any material from the sieve.

4.3. Test Results

Table A-6: A set of wet sieves analysis results for boring no 1

Sieve No.	Boring No.									
	B1-11	B1-12	B1-13	B1-14	B1-15	B1-16	B1-17	B1-18	B1-19	B1-20
4	100	100	100	100	100	100	100	100	100	100
10	100	100	98.82	98.74	100	100	100	100	100	100
20	99.95	100	98.44	98.05	99.92	99.99	98.86	100	100	99.96
40	99.89	100	98.18	97.88	99.86	99.99	98.69	99.94	100	99.9
80	99.82	99.81	98.03	97.69	99.77	99.98	98.51	99.88	100	99.84
200	99.63	99.56	97.79	97.08	99.69	99.93	98.18	99.78	99.84	99.75

Note: Table is organized based on Percentage Passing by Weight

Table A-7: A set of wet sieves analysis results for boring no2

Sieve No.	Boring No.									
	B2-7	B2-8	B2-9	B2-10	B2-11	B2-12	B2-13	B2-14	B2-15	B2-16
4	100	100	100	100	100	100	100	100	100	100
10	100	100	100	100	100	100	100	100	100	100
20	94.71	99.98	99.97	98.46	99.88	100	99.95	99.85	99.94	99.78
40	94.56	99.93	99.94	98.3	99.75	99.94	99.77	99.78	99.91	99.75
80	94.37	99.83	99.86	98.06	99.55	99.77	99.67	99.62	99.76	99.56
200	94.04	99.28	99.54	97.47	98.22	99.41	98.88	99.2	99.51	99.24

Note: Table is organized based on Percentage Passing by weight

5. One Dimensional Consolidation Test

5.1. Test Apparatus

1. Load Device: A suitable device for applying vertical loads or total stresses to the specimen. The device shall be capable of maintaining specified loads for long periods of time with a precision of $\pm 0.5\%$ of the applied load and shall permit quick applications of a given load increment without significant impact.
2. Consolidatiometer: A device to hold the specimen in a ring that is either fixed to the base or floating with porous disks on each face of the specimen. The inner diameter of the ring shall be determined of a tolerance of 0.0075mm (0.03 in.) The consolidometer shall also provide a means of submerging the specimen, for transmitting the concentric vertical load to the porous disks, and for measuring the change in height of the specimen, for transmitting the concentric vertical load to the porous disks, and for measuring the change in height of the specimen.
3. Minimum Specimen Diameter: The minimum specimen diameter shall be 50 mm (2.00 in.).
4. Specimen Ring Rigidity: The rigidity of the ring shall be such that, under hydrostatic stress conditions in the specimen and the change in the diameter of the ring will not exceed 0.03 % of the diameter under the greatest load applied.

5. Specimen Ring Material: The ring shall be made of a material that is noncorrosive in relation to the tested soil. The inner surface shall be highly polished or shall be coated with low-friction material.
6. Porous Disks: The porous disks shall be of silicon carbide, aluminum oxide, or similar to noncorrosive material. The grade of the disks shall be fine enough to prevent intrusion to inside the pores.
7. Specimen Trimming Device: A trimming turntable or a cylindrical cutting ring may be used for trimming the sample down to the inner diameter of the consolidometer ring with minimum disturbance. A cutter having the same inner diameter as the specimen ring shall be attached to or be integral with the specimen ring. The cutter shall have a sharp edge, a highly polished surface and coated with low-friction material.
8. Deformation Indicator: To measure change in the specimens' height, with a readability of 0.0025 mm (0.0001 in.).
9. Miscellaneous Equipment: Including a timing device with a readability of 1 s, distilled or demineralized water, spatulas, knives, and wire saws, are used in preparing the specimen.
10. Balance: Balance is with 0.01 grams of accuracy.
11. Drying Oven: Thermostatically controlled, preferably of the forced-draft type, capable of continuously maintaining a temperature of $110 \pm 5^{\circ}\text{C}$ ($230 \pm 9^{\circ}\text{F}$) throughout the drying chamber.

12. Water Content Containers: Small corrosion-resistant containers with snug-fitting lids for water content specimens. Aluminum or stainless steel cans of 2.5 cm (1 in.) high by 5 cm (2 in.) in diameter are appropriate.
13. Environment: Tests shall be performed in an environment where temperature fluctuations are less than $\pm 4^{\circ}\text{C}$ ($\pm 7^{\circ}\text{F}$) and where there is no direct exposure to sunlight.

5.2. Test Procedure

The procedure given below is for the mechanical loading consolidation test frame.

1. Weigh the consolidation ring before the test is started.
2. Measure the height and dimension of the ring.
3. Submerge the porous stones in a bowl to observe an adequate amount of water.
4. Keep the soils samples until test time in an environmental room which is 25°C and 100% humid.
5. Cut the sample in an appropriate way, but do not slam the ring down to the soil. First use a thin wire to trim the sample, next place the sample in the ring gently and then rotate the ring and pare off excess soil by using a cutting tool or wire. Get a smooth and flat soil surface.
6. Moisture content of the soil is obtained by using trimmed soils. Basically, put enough amount of the soil in a lid can, then place the cans in an oven for 18 hours, and then take out and weigh the cans.

7. Weigh the soil specimen and the ring together.
8. Place, first, the porous stone, then consolidation ring on it, and then another porous stone on the ring.
9. Tight three nuts
10. Adjust the dial gauge to zero
11. Place the load first, which is usually called the seating load, on the arm
12. Record the change in the dial gauge in a prepared data sheet.
13. Wait for 24 hours.
14. Increase by doubling the load and load it.
15. Repeat 10, 11, 12, and 13 until desired loading.
16. Decrease the loading by dividing the four.
17. Until you reach the seating load decrease the loading.
18. After the last loading remove the sample from the consolidation ring and weigh it before the loose soil, and place the sample in an oven for 12 to 18 hours.
19. Take the sample from the oven, wait until it cools and weigh the dry sample.

5.3. Test Results

Table A-8: Consolidation test results of void ratio, Compression index, Recompression index and Volume compression index for boring no1.

Boring no	Depth (ft)	e_o	C_c	C_r	Volume Compression Index γ_σ
B1-11	10-11	0.8100	0.2200	0.1300	0.0718
B1-12	11-12	0.8000	0.2008	0.1100	0.0611
B1-13	12-13	0.8800	0.2750	0.1250	0.0665
B1-14	13-14	0.9000	0.2345	0.1373	0.0723
B1-15	14-15	0.9400	0.2006	0.1089	0.0562
B1-16	15-16	0.8400	0.2917	0.1599	0.0869
B1-17	16-17	0.7600	0.2400	0.1316	0.0748
B1-18	17-18	0.8500	0.2414	0.1224	0.0662
B1-19	18-19	0.7900	0.2289	0.1114	0.0622
B1-20	19-20	0.7200	0.1717	0.0920	0.0535

Table A-9: Consolidation test results of void ratio, Compression index, Recompression index and Volume compression index for boring no 2.

Boring no.	Depth (ft)	e_o	C_c	C_r	Volume Compression Index γ_σ
B2-7	10-11	0.7783	0.2677	0.1173	0.066
B2-8	11-12	0.6006	0.2003	0.1001	0.063
B2-9	12-13	0.6593	0.2146	0.1260	0.076
B2-10	13-14	0.6702	0.2295	0.1118	0.067
B2-11	14-15	0.8163	0.1912	0.1118	0.062
B2-12	15-16	0.6194	0.2146	0.1200	0.074
B2-13	16-17	0.6783	0.2432	0.1295	0.077
B2-14	17-18	0.6058	0.2146	0.1130	0.070
B2-15	18-19	0.6647	0.2432	0.1260	0.076
B2-16	19-20	0.6728	0.2289	0.1299	0.078

6. Filter Paper Test Method

6.1. Test Apparatus

The tools used for the experiment are shown in Figure 3-10 and described below.

1. Filter paper: The paper used must be ash-free quantitative Type II filter paper *Schleicher and Schuell No. 589*. A suitable diameter is 5.5 cm (2.2 in.)
2. Specimen Container: 120 to 240 mL (4 to 8 oz.) of capacity metal or glass (rust free) container and a lid that contains the specimen and filter papers.
3. Filter Paper Container: This container holds filter paper following the equilibration of suction and removal from the specimen container.
4. Metal Container Alternate: Two nominal 70 mL (2 oz.) capacity metal moisture containers (aluminum or stainless) with lids to dry the filter paper. The containers should be numbered by imprinting with a metal stamp. The containers should not be written on with any type of marker or labeled in any manner.
5. Throw –away vinyl surgical non-powered or similar gloves should be used anytime the small containers designated for filter paper measurements are handled to prevent body oils from influencing any mass measurements made prior to handling.
6. Plastic Bag Alternate: A plastic bag large enough to accommodate the filter paper disks and capable of an airtight seal.
7. Insulated Chest: A box of approximately 0.03 m³ capacity insulated with foamed polystyrene or other material capable of an airtight seal.

8. Balance: A balance or scale having a minimum capacity of 100 g and with 0.0001 grams of accuracy.
9. Drying Oven: Thermostatically –controlled, preferably of the forced the forced-draft type, and capable of maintaining a uniform temperature of 110 ± 5 °C throughout the drying chamber.
10. Metal Block: A metal bock > 500 g mass with a flat surface to hasten cooling of the metal containers with filter paper.
11. Thermometer: An instrument to determine the temperature of the tested soil to an accuracy of ± 1 °C
12. Miscellaneous Equipment: Tweezers, trimming knife, flexible plastic electrical tape, O-rings, screen wire, brass discs.
13. Desiccator: A desiccator jar of suitable size containing silica gel or anhydrous calcium sulfate.

6.2. Test Procedure

In the following steps Total and Matric suction procedures are given together.

1. Prepare two cylindrical samples by trimming with minimal disturbance and cut half-half piece to get two cylindrical samples.
2. The samples must fit into a glass jar and the total sample volume must fill at least 75 percent of the glass jars volume.
3. The sample surface should be smooth and flat for an intimate connection to get accurate results.

4. A sandwich *Schleicher and Schuell No. 589 WH 5.5 cm* filter paper is placed between two larger diameter protective filter papers.
5. Bring two halve cylinder samples together, and seal them by using electrical type.
6. Steps 3 through 5 are given to obtain the Matric suction measurement.
7. Insert the whole sample into the glass jar. At this point the volume of the cylindrical samples must fill a minimum of 75 percent of the total jar volume.
8. Put the plastic “O” ring on top of the cylinder. The ring will keep the paper above from the sample in other words the filter paper is not able to touch the sample.
9. Place two *Schleicher and Schuell No. 589-WH* filter paper on top of the ring. The two papers should not make contact with the sample in any way.
10. Close the glass jar lid and seal it well.
11. Steps 6 through 10 are given to obtain the Total suction measurement.
12. Carry the glass jar very carefully and place it into an ice chest.
13. The Glass jar in the ice chest should stay about one week to reach the equilibrium. At this point a minimum equilibrium period of seven days (ASTM D 5298 and Houston et al., 1994, Lee, 1991). Once the seven days are over for the equilibrium then the test can be continued with the following steps.
14. Weigh the aluminum cans with a scale of 0.0001 g. of accuracy and record them in a spreadsheet.

15. Take the glass jar from the ice chest, and bring it near the scale.
16. In this step two people are needed. One person opens the sealed glass jar's lid; the other person takes the filter from the top of the plastic 'O' ring by using two tweezers and puts the paper into the can. In order to avoid evaporation of water from the paper, this must be carried out in a few seconds.
17. Weigh each of the cans with the 0.0001 scale and record them.
18. Switch on the thermostatically-controlled oven and let it heat up.
19. Place all of the cans into the oven and keep the lid half-open to allow evaporation.
20. All cans are kept inside the oven at $110 \pm 5^{\circ}\text{C}$ at least 10 hours for evaporation of water.
21. Before taking out the sample close the lids and let the cans wait for about 5 minutes in the oven for equilibration.
22. Take one can and put it on top of the aluminum block and let it sit for 20 seconds for cooling down. The purpose of using the block is to absorb the heat and expedite the cooling time.
23. Very quickly weigh the can with dried filter paper inside and record it.
24. Again very quickly take dried filter paper from the can, and weigh the can alone and then record it.
25. Steps of taking it out are shown above from 22 to 24 and these steps are repeated for every can.

The determination of matric and total suction through water content of filter paper is given below with the equations (Bulut et al., 2001).

$$M_f = M_2 - T_h \quad (2)$$

$$M_w = M_1 - M_2 - T_c + T_h \quad (3)$$

$$W_f = M_w / M_f \quad (4)$$

where:

M_f : Mass of dry filter paper; M_w : Mass of water in filter paper; W_f : Filter paper water content; T_h : Hot tare mass; T_c : Cold tare mass; M_2 : Mass of dry filter paper and hot tare mass; M_1 : Mass of wet filter paper and cold tare mass.

6.3. Test Results

Table A-10: Matric, Total and Osmotic Suction are estimated by the filter paper test for boring no 1.

Boring no	Depth (ft)	Total Suction pF	Matric Suction pF	Osmotic Suction pF
B1-11	10-11	3.86	3.42	3.66
B1-12	11-12	3.91	3.47	3.71
B1-13	12-13	3.96	3.52	3.76
B1-14	13-14	3.82	3.49	3.55
B1-15	14-15	3.79	3.47	3.51
B1-16	15-16	3.80	3.53	3.47
B1-17	16-17	3.74	3.55	3.29
B1-18	17-18	3.65	3.61	2.59
B1-19	18-19	3.65	3.45	3.22
B1-20	19-20	3.48	3.42	2.59

Table A-11: Matric, Total and Osmotic Suction are estimated by the filter paper test for boring no 2.

Boring no	Depth (ft)	Total Suction pF	Matric Suction pF	Osmotic Suction pF
B2-7	10-11	3.78	3.22	3.64
B2-8	11-12	3.89	3.15	3.8
B2-9	12-13	3.86	3.27	3.73
B2-10	13-14	3.9	2.92	3.85
B2-11	14-15	3.86	3.51	3.6
B2-12	15-16	4.02	3.55	3.84
B2-13	16-17	4.23	3.57	4.12
B2-14	17-18	3.73	3.46	3.4
B2-15	18-19	3.87	3.59	3.55
B2-16	19-20	3.84	3.73	3.19

7. Pressure Plate Test

7.1. Test Apparatus

1. Pressure Vessel (Chamber or Extractor); it is a rounded metal slender with a weight of 85 lb and a capacity of 15 liters. 1500 F1 15 Bar Pressure Plate Extractor with attached PM hinge is used in the laboratory.
2. Ceramic plate; it is a porous ceramic plate supported with mesh to drain excess water from the samples, and then provides an out flow of excess water to the outside. It should be submerged inside an ice chest within 24 hours to absorb water each time before the test is started.

3. “O” ring seal; it is a rubber seal placed inside of the groove of the pressure extractor tank to avoid leaking between the extractor tank and lid. Thus, before the test is started it should be checked for any kind of damages and scratches.
4. Triangular support; the duty of triangular support is to keep the lower ceramic plate cell from the bottom of the pressure plate extractor. To avoid the ceramic plate from breaking, make sure the triangular support is in place.
5. Air compressor; it provides a constant air source to increase pressure at any level within the test and helps keep the air pressure in a certain level. The electrical compressor includes a tank which has a maximum limit of 20,000 kPa.
6. Pressure regulator; its primary task is to monitor the gas pressure in the whole system. The air pressure increases and decreases by the amount of desired air pressure in the extractor.
7. Scale; it has a capacity of 200 g and a sensitivity of 0.01 g. Sometimes the air circulation in a laboratory can have a negative effect on the accuracy of the test result, so it might give more reliable readings if the scale is protected from air circulation during the reading time.
8. Grease; it is used between the “O” ring seal and the lid to prevent any level of air leaking, and the grease should be used on nuts which has a very fine coat and hence grease helps tighten the wing nuts.
9. Oven; it has a thermostatic control with the capacity of $110 \pm 5^{\circ}\text{C}$

10. Ice chest; it is a box filled with adequate distilled water which can cover the surface of the ceramic plate within at least 7 hours to thoroughly wet the plate. Each plate needs to absorb around 150 ml of water.
11. Trimmer; it is a tool that can help trim samples. This is a very essential tool to get an ideal sample size and shape from.
12. Wrench; it is a tool that is used to provide torque to loosen and tighten wing nuts around the lid.
13. Container; A small container with a volume of approximately 300 ml- 500 ml to hold water that comes from the pressure plate vessel. It can be made by plastic or glass.
14. Tubing; a small flexible tube nearly 3 mm in diameter that carries out water from the ceramic plate into the container. It usually has a short length since the container is located next to the pressure chamber.
15. Specimen cutter; a tool is needed to cut the sample which has a cylindrical shape with a diameter of 3 inches. In this case a saw was used to cut the sample into around 1 cm in height.
16. Desiccator; a big enough volume capacity desiccator to hold the sample for a short time of period after taking out the sample from the pressure chamber.
17. Plastic rings; made out of PVC plastic with a diameter of larger than 3 inches and a height of nearly 1 inch.

7.2. *Sample Preparation*

Test samples area taken from two different borings that are located to the same construction site by using a Shelby tube and the undisturbed samples are carried and stored until the test has been implicated. The following process states the preparation of the samples.

1. Samples are extracted out from the Shelby tube, which is nearly 3 inches in diameter, and are stored in a moisture controlled environment room.
2. Cut the sample in length to nearly 1 inch by using a specimen cutter which is usually a thin saw. Since samples are very stiff to cut, rotating the samples while cutting them can make an easier process.
3. A 1 cm high soil sample is needed for the pressure plate test, but more than 1 cm of the sample needs to be sliced high because generally samples break down a little bit differently than the ones sawed, so it is better to saw it a little wider than 1 cm.
4. Trim out the sample surface until the final product gets a very smooth surface. During the process; first choose the side that is not smooth and slice the surface side of the sample and trim that side. Once you get a smooth surface on there, flip the sample over and then trim the other side of the sample.
5. Once you trim the sample near to the length of 1 cm, take the soft brush and clean the small soil particles from the sample.

6. Weigh the mass of the sample and record it as an initial or as the first sample weight.
7. If more than one sample is prepared for the pressure plates test, store the sample in a desiccators until all of the samples are ready.

7.3. Test Procedure

1. Ahead of time, submerge the ceramic porous stone, which is absorbed with clean distilled water which sat inside the ice chest for a minimum amount of required time within 24 hours.
2. Clean the inside of the pressure plate chamber for any small soil particles, or other particles that are retained from previous tests.
3. In order to avoid leaking in the system, obey safety regulations; check the pipe system, including the gas tank, gas regulator, gas control panel, and compressor by applying little pressure to the whole pipe system.
4. Number 1, 2, and 3 are the steps that might be done before starting the test, and number 2 and 3 concern safety.
5. After this time, keep the gas supply closed using a gas regulator valve and do not operate the compressor.
6. Place the triangular support to the bottom of the pressure chamber and make sure it does not swing.
7. Place the ceramic plate into the pressure chamber on top of the triangular support. Also arrange the plate on the triangular support because the tube

hose on the plate needs to stay at the closest position to the exit hose, which transfers water to the outside container, on the pressure plate chamber.

8. An internal connection between the ceramic plate and extractor a tube is placed, which is around the length of 5 inches, to transfer the excess pore water outside of the extractor.
9. Before setting the sample on the ceramic plate, due to the plate being wet, clean the surface of the plate only in a very gentle manner. Do not try to dry out the surface because a dried surface is not the purpose of this step.
10. Properly prepared and trimmed (height of 1 cm and diameter of 5 ½ cm) soil samples are placed slowly on the ceramic plate inside of the extractor.
11. Make sure, the trimmed soil samples have a smooth and clean surface to get an intimate connection between the ceramic plate and the samples on the bottom. The samples should stay exactly on the surface of the plate and inside of the plate surface boundaries.
12. The plastic rings are placed on the porous ceramic plate. In order to indent the samples, plastic rings are marked and the samples can be distinguished easily. Also the rings avoid intermixing in soils due to the lack of space, however if you are testing a few samples this is not the direct purpose of the rings.
13. The “O” ring is placed inside the groove in the extractor; make sure the groove and the “O” ring are completely greased in order to prevent the gas from leaking.

14. Close the extractor lid properly and screw the opposite nuts to each other enough with hand power. Once all nuts are placed and screwed, all nuts can be tightened by a wrench one more time.
15. The air tank should be filled with an adequate amount of air by using the electrical air compressor ahead of time before the test starts running.
16. The valve of the tank is opened in order to fill in the extractor by 1/3 of bar pressure, during the next couple of hours air leaking can be checked.
17. After 1/3 bar applying pressure increases to 1/5 of pressure, becomes the first pressure point.
18. The first applied pressure inside the extractor holds in the same amount until the water moisture reaches the equilibrium and the outflow of water is ceased.
19. After the soil reaches the equilibrium, let the gas inside the chamber release by switching off the knob next to the dialed gauge. If the lid is opened before the gas inside the chamber is released completely, either the lid can be damaged or a serious injury can occur.
20. While either taking samples from the extractor or placing samples in the extractor, and due to the lid and "O" ring seals being greasy, samples should not touch the grease. Because it may slow down the equilibrium time and results.

21. Individually select the samples from the extractor and carefully weigh them to an accuracy of 0.01g, without losing any of the samples mass during the process.
22. After weighing each sample, write down the samples weight on a prepared excel spread sheet.
23. The pressure plate lid needs to be closed properly and then the nuts should be installed and tightened as in a similar way explained as before.
24. The gas valve needs to be opened, the desired air applied to the chamber and the amount of gas can be monitored through the dial gauge.
25. The procedures of 16 to 22 needs to be applied by increasing the pressure values 1/3, 1/2, 1, 5, 10, 15 and 1 bar respectively.
26. One concern should be taken into account of that the soil samples reach the equilibrium points in a different time for each applied pressure according to ASTM D 2325 (2001 d) and ASTM D 3152-72 (2001 e). Therefore, keeping the time of the soil in the pressure chamber may vary from 24 hours to 96 hours based on the applied pressure.
27. The volume of the samples are measured accordingly by using Ottawa sand, and is measured after the first 1/2 bar, 15 bars and last 1/2 bar. With more detailed information the test processer and method are given in this chapter.
28. After a minimum air pressure of 1/2 bars is reapplied. First, the samples will be weighed and then will be placed in a thermostatically controlled oven at $110 \pm 5^{\circ}\text{C}$ for a day to let dry.

29. After a minimum period of 24 hours, the samples will be taken from the oven and let cool for a while. Because the weight of the hot samples are different than then the cooled samples weights, in order to get more accurate weight results, wait until samples cool down enough.
30. The cooled samples are weighed and the mass of the dry samples are obtained, the value is written down on the prepared form.
31. At the end of the test, there will be data which are; the water content of each pressure, and a dry sample weight and also an initial (wet or saturated) sample weight. And hence the physical characteristic relationship between the soil moisture and the matric suction would be estimated and demonstrated.

7.4. Test Results

Table A-12: Pressure Plate is used to determine soil sample suction change. An example pressure plate spreadsheet is given for boring no 2, depth of 17-18 ft.

Tested by:		Sahin, Hakan		Test date:		11/6/2009
Sample Description:		Tan color		Project No.:		0-6375
Sample Location:		San Atonio, Texas, USA		Boring No.:		B2-14
Weight of Sample initial, Mi, g:		95.21		Depth (ft):		17-18
Weight of Dry Sample, Mdry, g:		81.02		Sample No.:		8
Water content, w, % :		0.175				
Pressure	Pressure	Suction	Suction	Mass	water	Mwater
Bar	kPa	Log kPa	PF	g	%	g
0.5	50.00	1.70	2.71	95.76	0.182	14.74
1	100.00	2.00	3.01	95.38	0.177	14.36
5	499.98	2.70	3.71	95.30	0.176	14.28
10	999.95	3.00	4.01	94.95	0.172	13.93
15	1499.93	3.18	4.19	94.03	0.161	13.01
0.5	50.00	1.70	2.71	95.66	0.181	14.64

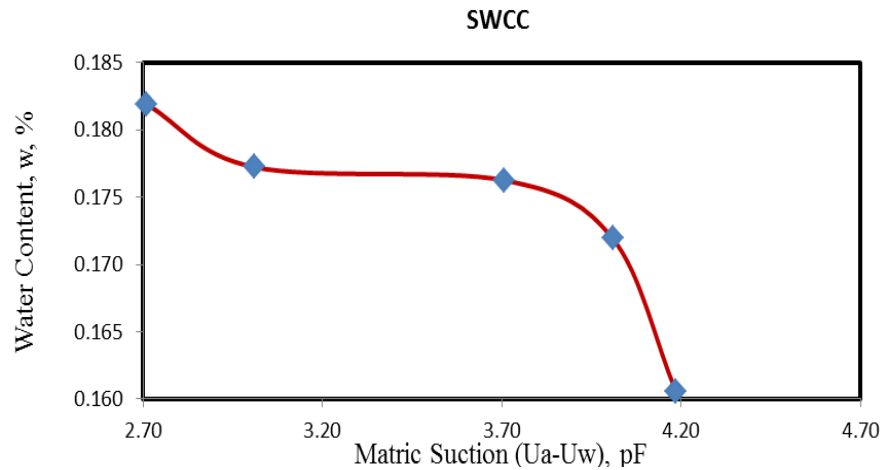


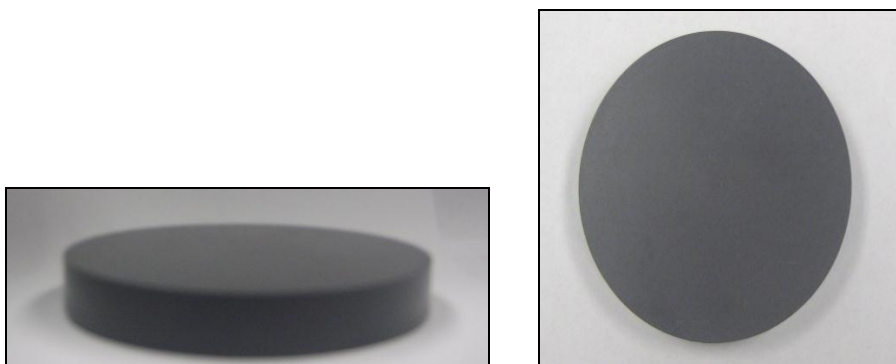
Figure A-3: An determined SWCC curve by using the Pressure Plate Extractor

8. New Volume Measurement Method

8.1. Test Calibration Procedure

To calibrate the equipment for the volume measurement method the following steps are completed and list of steps are given as follows;

1. A cylindrical PVC block is cut in 0.7 cm, 1.0 cm and 1.5 cm in height . A machine shop is used to obtain very smooth surfaces on PVC cylinders. Three PVC samples of (0.7 cm x 2.9"), (1 cm x 2.9") and (1.5 cm x 2.9") are prepared and shown in Figure A-4.
2. Dimensions of the PVC samples are measured at three points and an average dimension is determined.



(a) Side of the PVC cylinders (b) Surface of the PVC cylinders

Figure A-4: Shows pictures of PVC cylinders that used for calibration.

- The PVC samples are weight by using a 0.0001 gr sensitive scale and recorded.

Table A-13: Weight and Dimension of the PVC samples

Dimension of PVCs	0.7 cm x 2.9"	1 cm x 2.9"	1.5 cm x2.9"
Weight of PVCs (g)	41.4286	58.5682	88.4540

- A plastic jar is filled by only Ottawa sand and weigh. This process is repeated 10 times and recorded as Trials in Table.
- The plastic jar, Ottawa sand and a PVC cylinder are weight 10 times with an accuracy of 0.01 g. This is done for all three PVC samples and recorded in Table A-14.

6. The determined weights are sorted from the smaller value to the larger value in Table A-14.
7. The term “*Trim Med Average*” is an average value of eight readings. *Trim Med Average* excludes minimum and maximum measured weights.
8. The standard deviation is determined based on the *Trim Med Average* value. Thus minimum and maximum readings are not included here as well. This is recorded in spread sheet as the *Trim Med Standard Deviation*.

Table A-14: Measured weights of Jar & Ottawa sand and Jar, PVC sample & Ottawa sand are shown for each PVC samples.

Sorted Trials	Jar	0.7 cmx2.9"	1 cm x2.9"	1.5 cm x2.9"
1	1514.19	1543.23	1534.53	1525.32
2	1515.06	1546.84	1537.37	1530.98
3	1517.90	1547.02	1542.36	1531.10
4	1517.94	1548.25	1542.78	1534.98
5	1518.18	1548.46	1542.89	1537.09
6	1518.92	1549.40	1543.93	1539.14
7	1522.17	1550.97	1548.99	1539.88
8	1524.99	1553.06	1549.10	1540.37
9	1525.13	1554.17	1549.71	1540.48
10	1525.74	1557.29	1550.74	1543.10
Trimmed Average	1520.04	1549.77	1544.64	1536.75
Trimmed Med Standard Deviation	3.65	2.72	4.30	3.98

9. “ Δ mass” is the mass of Ottawa sand that fills the volume of a PVC sample. “ Δ mass” is determined as follows:

$$\Delta \text{ mass} = \text{Jar mass} - (\text{Trim Med Average} - \text{Mass of the PVC}) \quad (5)$$

Where the Jar mass is average value of the jar filled with Ottawa sand. The data are presented in Table.

10. Density of the PVC block is determined by utilizing a pycnometer device that allows measuring smaller size volumes. To determine the density of PVC a small mass of PVC which is less than 2" in dimension and height is prepared in the machine shop to fit into the pycnometer. The volume of the small PVC mass is estimated and the density of the small PVC was obtained by utilizing 0.0001 g sensitive scale. Then the density is estimated for the PVC.

11. The volumes are determined for each PVC cylinder by using the determined density.

Table A-15: Determined volume is shown for each cylinder PVC

Shapes	Mass PVC (g)	Trimmed Average (g)	Δ Mass (g)	Measured density (g/cm³)	Volume (mass/density) (cm³)
0.7 cmx2.9"	41.43	1549.77	11.69	1.38	29.99
1 cm x2.9"	58.57	1544.64	33.96	1.38	42.40
1.5 cm x2.9"	88.45	1536.75	71.74	1.38	64.03

12. Table A-15 represents the relation between the volume of the PVC cylinders and of the $\Delta Mass$ of the Ottawa sand. The relation between the volume and the mass of the Ottawa sand are plotted in Figure A-5. Also this relation is given in a mathematical formulation. The equation has an R value of 0.99997 and the equation is given as follows:

$$\text{Volume (cm}^3\text{)} = 23.266 + 0.56747 * \text{Change mass} \quad (6)$$

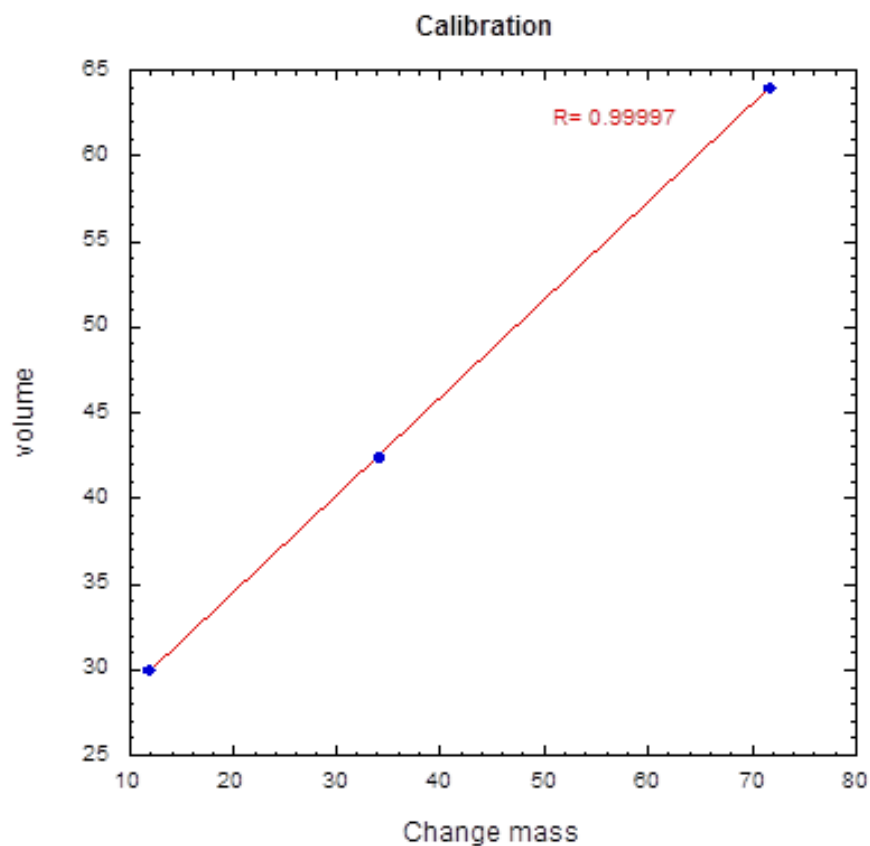


Figure A-5: Relation change in mass and volume is shown.

9. Unconfined Compression Test

9.1. Test Apparatus:

1. Soil sample
2. Knife
3. Sample holder; trimming tools
4. Calipers
5. Pressure chamber
6. Porous stones
7. Transducers - force and displacement
8. Computer - Geotech Data Logger Program which is available to use in Geotech-Graduate laboratory.
9. Digital Voltmeter
10. Scale reading from 1 g and to 0.01 g.

9.2. Test Procedure

Standard test method for unconsolidated unconfined triaxial compression test on cohesive soils ASTM D 2850-95 is followed.

1. To trim the sample, place the sample in holder that sides are designed to trim the sample in two different diameters.
2. Trim the sample very carefully with the knife so that it gets a cylindrical product.

3. Take the sample and measure the diameter of the sample from several points by means of caliper. Then cut an excess length of the sample as in the ratio of L/D between 2 and 3.
4. Record the dimensions three times and the heights of the sample in order to estimate the average values. Prepare the compression test chamber by disassembling it.
5. Place one porous stone on the bottom of the sample and place the other one on top of the sample. Then re-assemble the compression chamber.
6. Place the compression chamber in to the loading frame of the instrumental. Then adjust the plunger in the center by hand so that the sample would have just contacted with the plate and plunger.
7. Turn on the compute and prepare the Geotech Data Logger Program data acquisition system.
8. Apply the load to a rate of 1/2 to 2 percent per minute, and allow the computer to take the readings.
9. Apply the load until the sample reaches the failure state and then save the data on the computer.
10. Take out the sample from the chamber immediately and measure the water content of the sample.
11. Plot the graphs by using the results and get the q_u .

9.3. Test Results

Table A-16: Unconfined compression strength and effective cohesion are determined for boring no 1.

Boring no	Depth (ft)	Unconfined compression strength, σ_f kPa	Effective cohesion, \bar{c} kPa
B1-11	10-11	175.66	55.62
B1-12	11-12	174.66	49.42
B1-13	12-13	-	-
B1-14	13-14	-	-
B1-15	14-15	151.25	31.96
B1-16	15-16	-	-
B1-17	16-17	-	-
B1-18	17-18	-	-
B1-19	18-19	-	-
B1-20	19-20	-	-

Table A-17: Unconfined compression strength and effective cohesion are determined for boring no 2.

Boring no	Depth (ft)	Unconfined compression strength, σ_f kPa	Effective cohesion, \bar{c} kPa
B2-7	10-11	-	-
B2-8	11-12	80.15	22.39
B2-9	12-13	-	-
B2-10	13-14	-	-
B2-11	14-15	126.26	18.47
B2-12	15-16	-	-
B2-13	16-17	-	-
B2-14	17-18	-	-
B2-15	18-19	-	-
B2-16	19-20	-	-

VITA

Hakan Sahin received his Bachelor of Science degree in civil engineering from Nigde University in May 2006. Then he enrolled in the geotechnical engineering program at the Zachry Department of Civil Engineering, Texas A&M University, in August 2008, and obtained his Masters of Science degree in December 2011.

Hakan Sahin may be reached at Zachry Department of Civil Engineering, 3136 TAMU, College Station, TX 77843. His e-mail address is shnhakan@neo.tamu.edu